45

AD

USAAVLABS TECHNICAL REPORT 67-57

FLEXIBLE WING TOWED UNIVERSAL GLIDER

October 1967

U. S. ARMY AVIATION MATERIEL LABORATORIES
FORT EUSTIS, VIRGINIA

CONTRACT DA 44-177-AMC-179(T)
RYAN AERONAUTICAL COMPANY
SAN DIEGO, CALIFORNIA

SPONSORED BY:
ADVANCED RESEARCH
PROJECTS AGENCY

151

DEPARTMENT OF THE ARMY
U. S. ARMY AVIATION MATERIEL LABORATORIES
FORT EUSTIS, VIRGINIA 23604

The work described in this report was accomplished by the Ryan Aeronautical Company under the terms of Contract DA 44-177-AMC-179(T) and was sponsored by the Advanced Research Projects Agency (ARPA). The report covers the design, fabrication, and testing of the Flexible Wing Towed Universal Glider (TUG).

This command concurs with the conclusions made by the contractor.

Based on the results of this program, this command does not feel that the TUG requires further evaluation at this time, since the basic concept has been proven. Further refinements are required to bring the glider to a condition where it can be employed with maximum effectiveness.

Task 1F121401A 14172
Contract DA 44-177-AMC-179(T)
USAAVLABS Technical Report 67-57
October 1967

FLEXIBLE WING TOWED UNIVERSAL GLIDER

RYAN REPORT NUMBER 29267-1

This research was sponsored by the Advanced Research Projects Agency of the Department of Defense under ARPA No. 294, Amendments 13 and 19, and was monitored by the U. S. Army Aviation Materiel Laboratories (USAAVLABS) under Contract DA 44-177-AMC-179(T).

Prepared By

Ryan Aeronautical Company
San Diego, California

For

U.S. ARMY AVIATION MATERIEL LABORATORIES
FORT EUSTIS, VIRGINIA

SUMMARY

This report is the final report on the design, fabrication, and test of a Flexible Wing Towed Universal Glider. The work was accomplished under Contract No. DA 44-177-AMC-179(T) by the Ryan Aeronautical Company, San Diego, California. The purpose of the glider design was to develop an unpowered roadable winged vehicle which could carry up to 4000 pounds of payload on an open bed which would put minimum restrictions on cargo volume and shape. The vehicle, towed by a helicopter, would extend the normal helicopter internal load and sling load capacity as well as place hazardous cargo remote from the helicopter and crew.

The report describes the vehicle, presents the technical engineering analysis, and summarizes the results of the flight tests which were conducted.

The results confirmed that the vehicle was feasible and would operate as expected. A family of successful operating parameters of weight, airspeed, and wing incidence angles was established along with related tow cable forces and operating limits. Flight tests were concluded after reaching a 2820-pound payload weight due to accumulated vehicle operational damage for which no funds were available for repairs. Successful operations up to the design gross weight were otherwise anticipated and indicated by flight test results.

All flight testing was conducted at the U.S. Army Yuma Proving Ground, Yuma, Arizona.

BLANK PAGE

CONTENTS

ILLUSTRATIONS

ILLUSTRATIONS (CONT)

ILLUSTRATIONS (CONT)

ILLUSTRATIONS (CONT)

SYMBOLS

A	Total wing axial force (LB)
a	dv/dt = longitudinal acceleration
ac	Aerodynamic center
A_K	Keel axial force (LB)
$(A_A)_K$	Keel axial force at the apex (LB)
A_{F_K}	Keel axial force at the actuator fitting (LB)
A_{LE}	Leading-edge axial force (LB)
$(A_A)_{LE}$	Leading-edge axial force at the apex (LB)
A_{R_K}	Keel axial force at the aft keel fitting (LB)
$(A_{SB})_K$	Keel axial force at the spreader-bar joint (LB)
$(A_{SB})_{LE}$	Leading-edge axial force at the spreader-bar joint (LB)
b	Wing span (FT)
c	Local chord length (FT)
C_A	Wing axial force coefficient, $\frac{A}{qS}$
$(C_{AX})_{LE}$	A coefficient which when multiplied by qS gives the forward component of load applied to the leading edge (LB)
C_{D_O}	Profile drag coefficient
C_{D_S}	Drag coefficient of struts
C_{H_H}	Apex horizontal hinge-moment coefficient = (Apex horizontal hinge moment)/qS c_{root}

SYMBOLS (CONT)

C_{H_V}	Apex vertical hinge-moment coefficient = (Apex vertical hinge moment)/ qSc_{root}
C_K	Length of keel (FT)
C_L	Lift coefficient, $\frac{L}{qS}$
C_{ℓ_β}	$\partial C_\ell / \partial \beta$ = rate of change of rolling moment coefficient with sideslip angle
$C_{m_{cg}}$	Pitching moment coefficient about center of gravity
$C_{m_{o_w}}$	Zero lift pitching moment coefficient of wing
$C_{m_{C_L}}$	$\partial C_m / \partial C_L$ = rate of change of pitching moment coefficient with lift coefficient
$C_{m_{\alpha_B}}$	$\partial C_m / \partial_{\alpha B}$ = rate of change of pitching moment coefficient with body angle of attack
C_N	Wing normal force coefficient, $\frac{N}{qS}$
C_n	Wing local normal force coefficient, $\frac{\text{local normal force}}{qS}$
C_{N_β}	$\partial C_\ell / \partial \beta$ = rate of change of yawing moment coefficient with sideslip angle
c_p	Pressure coefficient
c_{root}	Wing root chord length (FT)

SYMBOLS (CONT)

C_{y_β}	$\partial C_{y/\partial \beta}$ = rate of change of sideforce coefficient with sideslip angle
D	Drag force = $1/2\ \rho V^2 S\ C_D$ (LB)
F	Force on wing member (LB)
f	Equivalent parasite drag area (SQ FT)
F_x	Axial component of tow cable tension (LB)
F_z	Normal component of tow cable tension (LB)
g	Acceleration due to gravity (= 32.2 FT/SEC^2)
$(H_A)_K$	Keel apex load which acts in the wing plane and normal to the keel (LB)
$(H_A)_{LE}$	Leading-edge apex load which acts in the wing plane and normal to the leading edge (LB)
H_K	Keel load acting in the wing plane and normal to the keel (LB)
H_{LE}	Leading-edge load acting in the wing plane and normal to the leading edge (LB)
$(H_{SB})_K$	Keel load at the spreader-bar joint, acting in the wing plane and normal to the keel (LB)
$(H_{SB})_{LE}$	Leading-edge load at the spreader-bar joint, acting in the wing plane and normal to the leading edge (LB)
i_w	Wing incidence angle, referenced to body zero
I_x, I_z	Moments of inertia about longitudinal and vertical axes respectively (SLUG-FT^2)
I_{xz}	Product of inertia (SLUG FT^2)

SYMBOLS (CONT)

K	Keel
k	Fraction of wing normal force on leading edge
L	Lift force = $1/2\ \rho\ V^2 S\ C_L$ (LB)
L	Rolling moment = $1/2\ \rho\ V^2 S\ b\ C_{\ell}$ (LB/FT)
LE	Leading edge
ℓ	Length of wing member (FT)
L/D	Lift/drag ratio
$(L/D)_{TD}$	Lift/drag ratio at touchdown
ℓ_k	Keel length (FT)
ℓ_s	Distance of strut drag force above center of gravity (FT)
M	Pitching moment = $1/2\ \rho V^2 S\ C_K\ C_m$ (LB/FT)
m	$\frac{W}{g}$ = mass of glider (SLUGS)
N	Yawing moment = $1/2\ \rho V^2 S\ b\ C_n$ (LB/FT)
N	Normal force (LB)
N_x	Forward load factor
N_y	Lateral load factor
N_z	Vertical load factor
P_{upper}	Pressure, upper wing surface, $\frac{lb}{ft^2}$
P_{lower}	Pressure, lower wing surface, $\frac{lb}{ft^2}$
q_∞	Dynamic pressure, free-stream, $\rho\ \frac{V^2}{2}$

SYMBOLS (CONT)

R	$D + \mu (W-L-t_c \sin \epsilon)$ = resistance of glider during takeoff ground run (LB)
S	Wing area (SQ FT)
S_G	Ground run distance (FT)
S_{wing}	Wing surface area (SQ FT)
t_c	Cable tension (LB)
V	Velocity (FT/SEC)
V	Velocity (KNOTS)
$(V_A)_K$	Keel apex load normal to wing plane (LB)
$(V_A)_{LE}$	Leading-edge apex load normal to wing plane (LB)
V_E	Equivalent airspeed (KNOTS)
$(V_F)_K$	Keel vertical load at the actuator fitting (LB)
V_{GLIDE}	Velocity along glide path (FT/SEC)
V_K	Keel load normal to wing plane (LB)
V_L	Limit speed (KNOTS)
V_{LE}	Leading-edge load normal to wing plane (LB)
V_{LO}	Velocity at lift-off (FT/SEC)
$(V_R)_K$	Keel vertical load at the aft keel fitting (LB)

SYMBOLS (CONT)

$(V_{SB})_K$	Keel load normal to wing plane and acting at the spreader-bar joint
$(V_{SB})_{LE}$	Leading-edge load normal to wing plane and acting at the spreader-bar joint
V_{STALL}	Velocity at stall
V_{TD}	Velocity at touchdown (FT/SEC)
W	Weight (LB)
w	Running load (LL/FT)
x	Chordwise length (FT)
X_{ac}	Distance of wing aerodynamic center from center of gravity, positive forward (FT)
X_{cp}	Distance to pressure coefficient of load on leading edge measured along leading edge (FT)
X_w	Distance of mid-keel point forward of CG positive forward (FT)
y	Spanwise distance (FT)
Z_{ac}	Distance of wing aerodynamic center above center of gravity, positive downward (FT)
Z_w	Distance of mid-keel point above CG, negative up (FT)
α_B	Angle of attack of body (DEG)
α_W	Wing angle of attack (DEG)
β	Sideslip angle (DEG)
γ	Flight path angle (DEG)

SYMBOLS (CONT)

ΔW	Increment in helicopter weight due to tow cable tension (LB)
ΔD_P	Increment in helicopter parasite drag due to tow cable tension (LB)
δ	Deflection (FT)
ϵ	Tow cable angle at glider (DEG)
η	Fraction of wing semi-span
θ_H	Tow cable angle at helicopter (DEG)
θ_{TUG}	Tow cable angle at TUG (DEG)
Λ_{LE}	Sweepback angle of leading edge (DEG)
λ_K	Angle, measured normal to the keel, between the membrane and the leading edge keel plane (DEG)
λ_{LE}	Angle, measured normal to the leading edge, between the membrane and the leading edge keel plane (DEG)
μ	Coefficient of rolling friction
μ_β	Coefficient of braking friction
ρ	Air density (SLUGS/CU FT)
ϕ_D	Depression angle (glider below horizontal reference through helicopter)

SUBSCRIPTS

cg	Center of gravity
w	Wing
B	Body
s	Struts
t	Tail

INTRODUCTION

The concept of the Flexible Wing Towed Universal Glider (TUG) was based on the need for an extremely versatile aerial cargo delivery vehicle of simple design and low cost for use in a highly mobile and dispersed combat environment. The design concept of the TUG system includes simplicity of construction, ease of maintenance, off-the-shelf components, and a design philosophy of cost effectiveness.

Preliminary design studies and the final detail design of a Flexible Wing Towed Universal Glider were accomplished, and four test vehicles were fabricated. Structural integrity was determined by stress analysis, and the performance and stability were determined by aerodynamic analysis. A flight test program determined handling qualities and performance of the vehicle. Initial ground taxi tow tests revealed excellent tracking and braking characteristics. All vehicles were utilized in both the ground and the flight tests.

Twenty-eight flight test operations were conducted on the TUG during 7 October-20 November 1964 and 4 October-2 November 1965. The towed flight envelope was expanded to a speed range of 40 to 80 KIAS, depending upon the glider gross weight and wing-incidence angle. Payloads of up to 2848 pounds were successfully towed.

SYSTEM DESCRIPTION

GENERAL

The Ryan Model 179 Flexible Wing Towed Universal Glider (TUG) system consists of the glider and includes cargo handling provisions, removable flexible fuel container, tow cable, and tow aircraft accessories. In use, it is loaded with fuel or cargo and towed by a helicopter to increase the load-carrying capacity of the helicopter by a factor of 2-1/2 to 3. The carrying capacity is 4000 pounds of dry cargo or 500 gallons of fuel, or a combination of the two. Normal airspeed is 60 -70 knots. It is easily collapsible for ground handling and can serve as a cargo trailer to be pulled by a jeep or truck.

The glider, shown in Figure 1, consists of the major assemblies defined in the following paragraphs.

Wing Assembly

The wing consists of a cloth membrane supported by an aluminum structure, as shown in Figure 2. The structure consists of leading edges, a keel, and a spreader bar, all made of aluminum alloy tubes. These members are composed of several relatively short telescoped sections of diameters proportioned to suit local bending moments and allowing easy replacement of individual sections by cutting to length and bolting in place. Various fittings for wing attachment and adjustment are incorporated.

The membrane is of Dacron cloth coated with neoprene rubber on both sides, and weighing 6 ounces per square yard. Assembly of the membrane is by machine stitching of numerous panels. Field repair may be made by hand sewing or cementing patches

Wing span is 36 feet, area is 554 square feet, keel length is 28 feet, and aspect ratio is 2.6.

Wing Support Struts

The wing support struts are constructed from standard aluminum alloy tubes. Three A-frames are used for wing supports. An electrically operated linear screw jack, mounted to the apex structure of the forward A-frame, shifts the center of gravity of the cargo with respect to the wing, thereby changing the trim angle of attack. The screw jack is controlled from the tow aircraft. The two aft A-frames form a pyramid and attach to a sheet aluminum fitting on the wing keel.

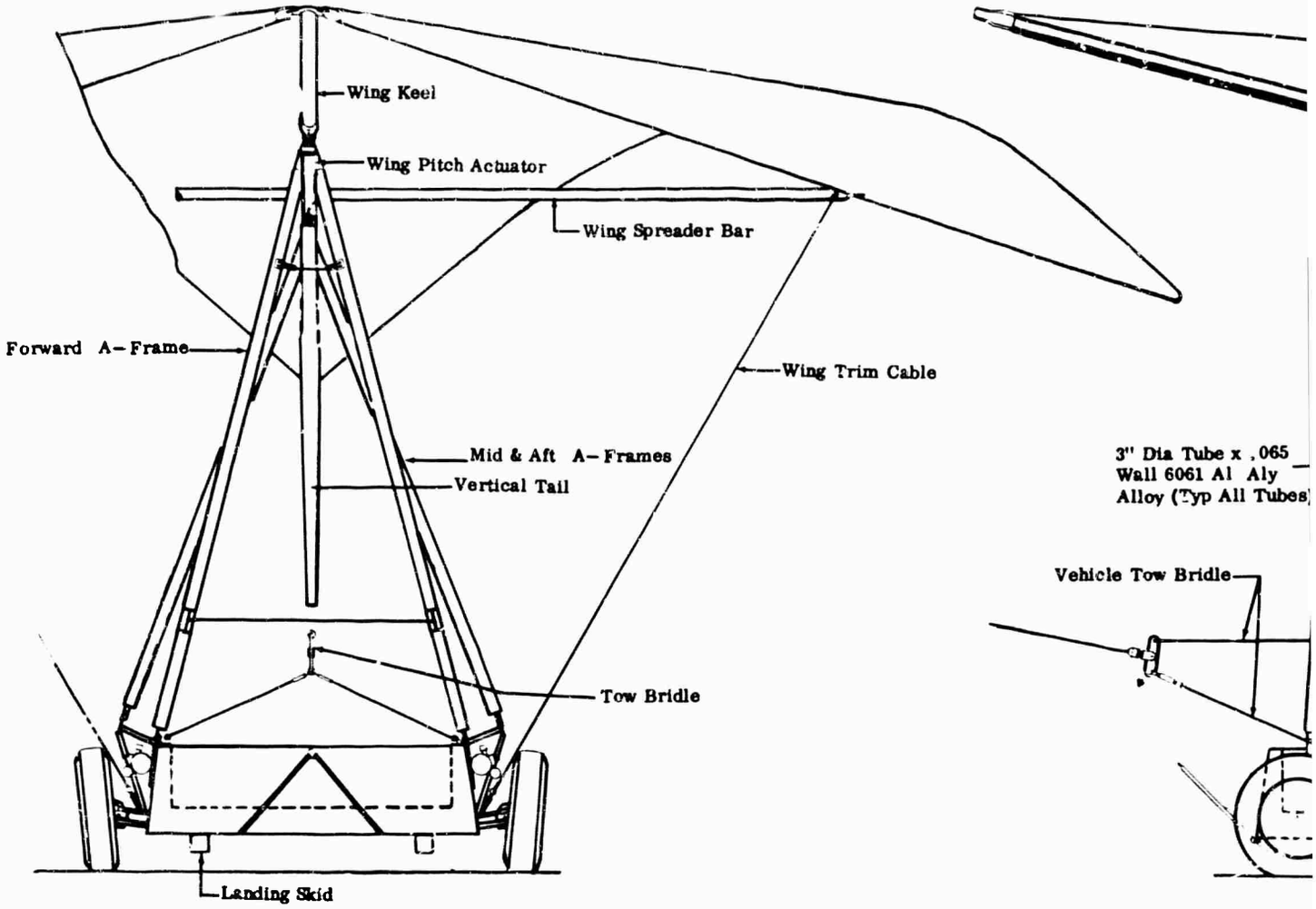

Front Elevation

Figure 1. Tow Universal Glider - General Arrangement

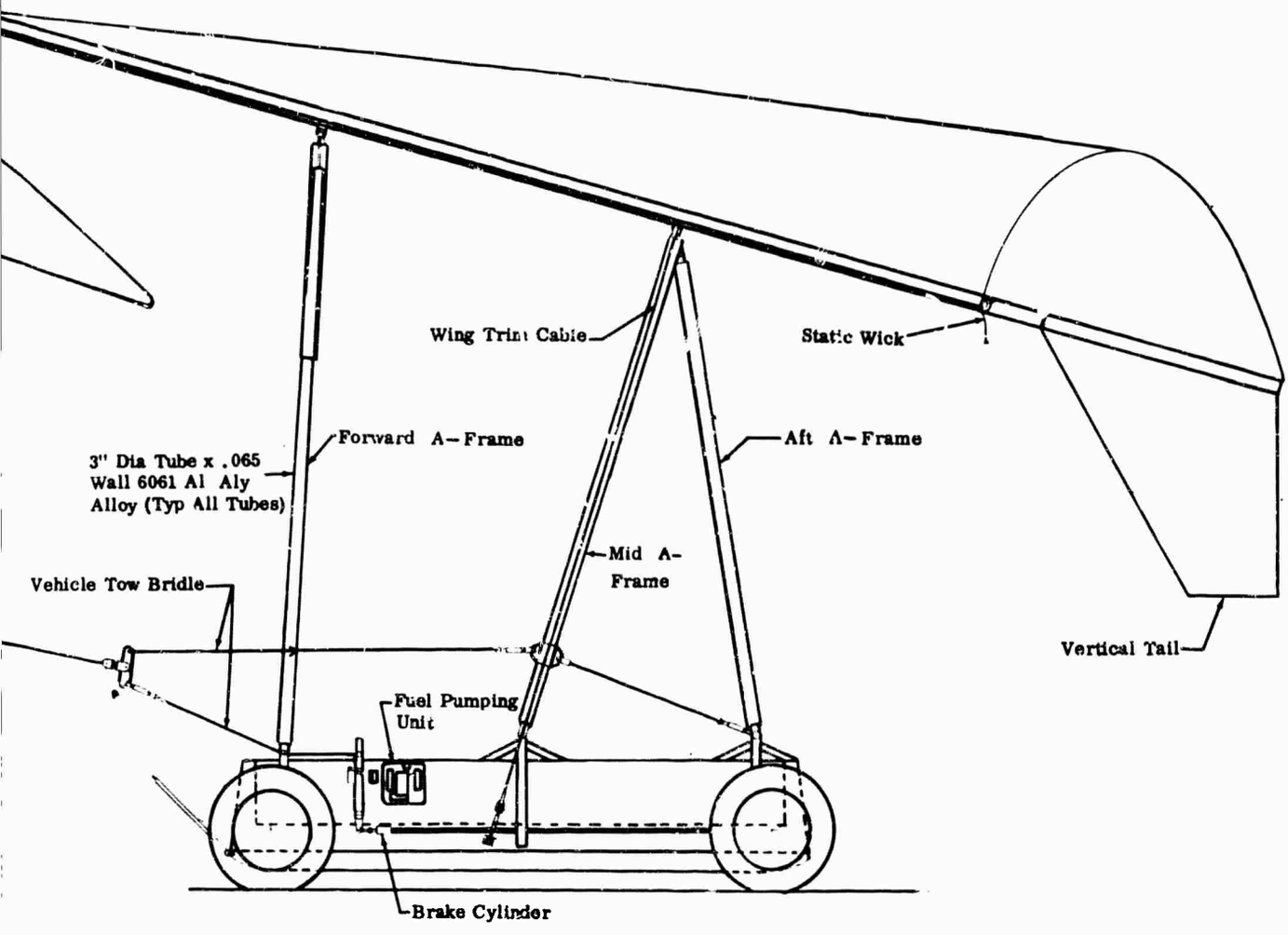

Side Elevation

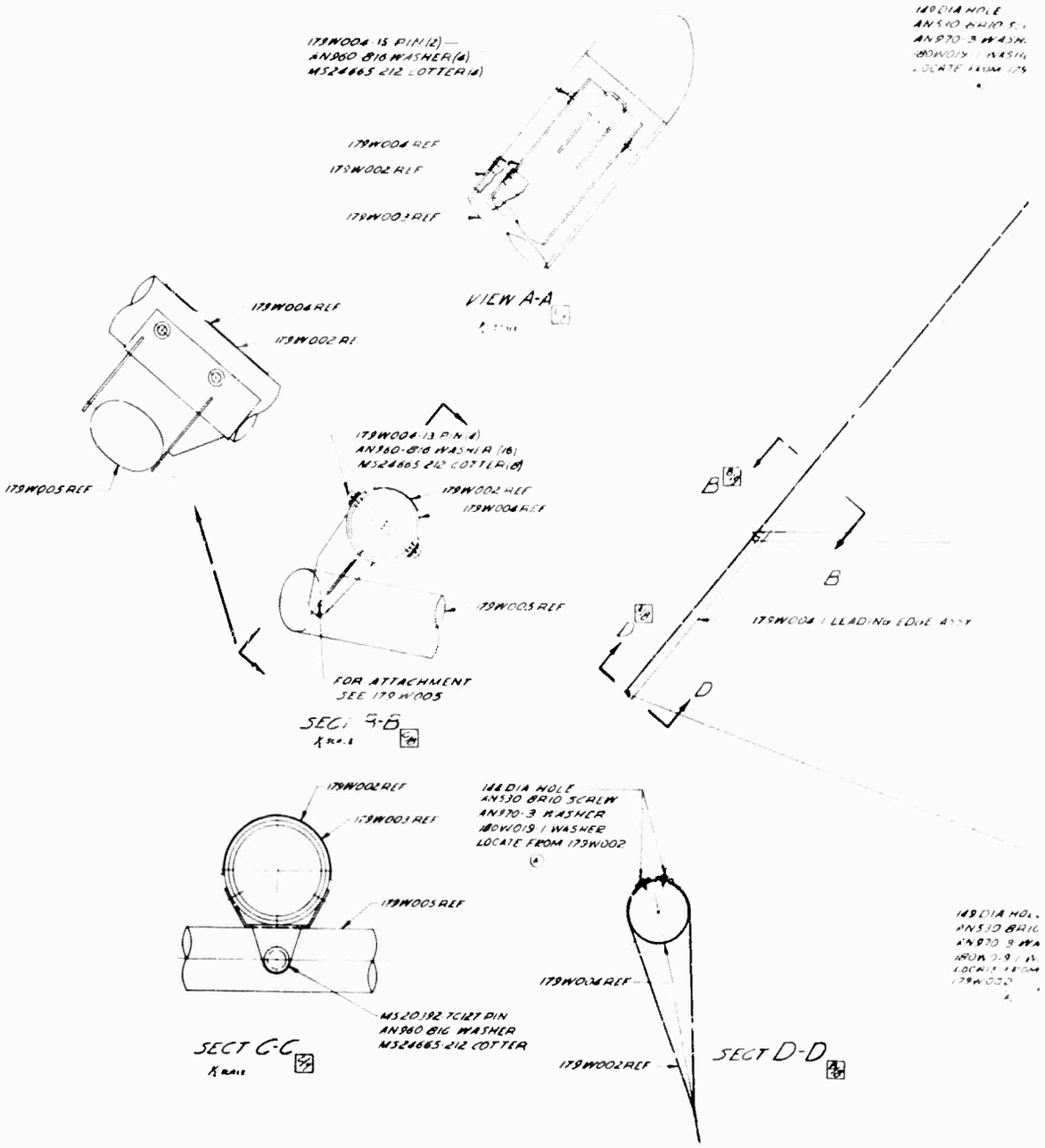

Figure 2. Wing Assembly

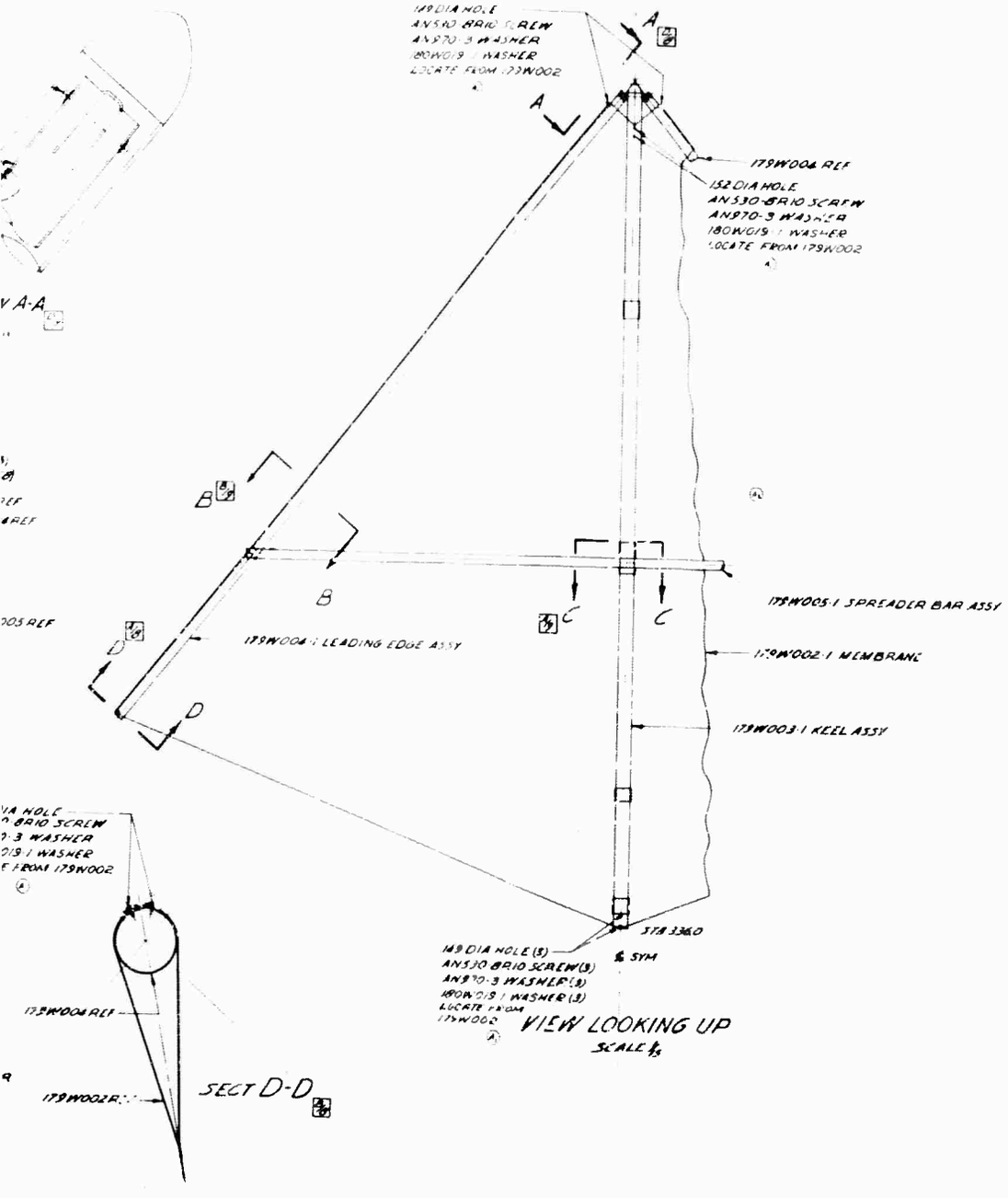
.149 DIA HOLE
AN530 BR10 SCREW
AN970-3 WASHER
180W019-1 WASHER
LOCATE FROM 179W002
179W004 REF
.152 DIA HOLE
AN530-BR10 SCREW
AN970-3 WASHER
180W019-1 WASHER
LOCATE FROM 179W002
179W005-1 SPREADER BAR ASSY
179W004-1 LEADING EDGE ASSY
179W002-1 MEMBRANE
179W003-1 KEEL ASSY
STA 336.0
& SYM
.149 DIA HOLE (3)
AN530 BR10 SCREW (3)
AN970-3 WASHER (3)
180W019-1 WASHER (3)
LOCATE FROM
179W002
VIEW LOOKING UP
SCALE 1/6
SECT D-D
179W004 REF

B

Assembly

This arrangement of A-frames takes all the loads to which the craft is subjected, except rolling moments about the wing keel. Rolling moment loads are taken by a pair of steel cables extending from the tips of the wing spreader bar to the sides of the glider body. The struts are attached to the glider body by simple sheet metal fittings that are easily removable for replacement of strut tubing.

Vertical Stabilizer

The vertical stabilizer, shown in Figure 3, fabricated of sheet aluminum alloy with two aluminum spars, has a conventional airfoil shape of 8% thickness, an aspect ratio of 1.4, and an area of 14 square feet. The vertical stabilizer is attached to the keel with four quick-disconnect pins.

Body Assembly

The glider body is shaped like that of a conventional pickup truck, with a cargo deck and tie-down fittings, a cargo divider with fixed sides and front, and a removable tail gate. Two dock boards, stowed on the sides of the body, are manually positioned on the aft end of the cargo deck for rolling wheeled cargo in and out of the body.

A tow bar attached to the front end of the body mates with existing military tow hooks for ease in ground handling before and after flights. Mounting for a fuel pump system is provided on each side of the body, allowing two pumps to be carried. The body, shown in Figure 4, is constructed of metal frames and conventional load-carrying longitudinal beams. The cargo compartment floor and sides are constructed from aluminum-covered plywood. All sections throughout are uniform; special contouring is not required.

Takeoff and Rolling Gear

A rolling gear with a track of 104 inches and a wheel base of 123 inches supports the body. The gear is designed for ground handling and takeoff runs. Its suspension allows vertical deflection to absorb jolts during ground runs. Two longitudinal wooden skids, attached to the underside of the body, absorb major landing loads. The suspension deflects sufficiently to allow all loads greater than 2 G's to be taken by the skids, significantly reducing both body and landing gear structural weight. The skids also reduce any tendency of the glider to bounce during hard landings, and they minimize ground run-outs.

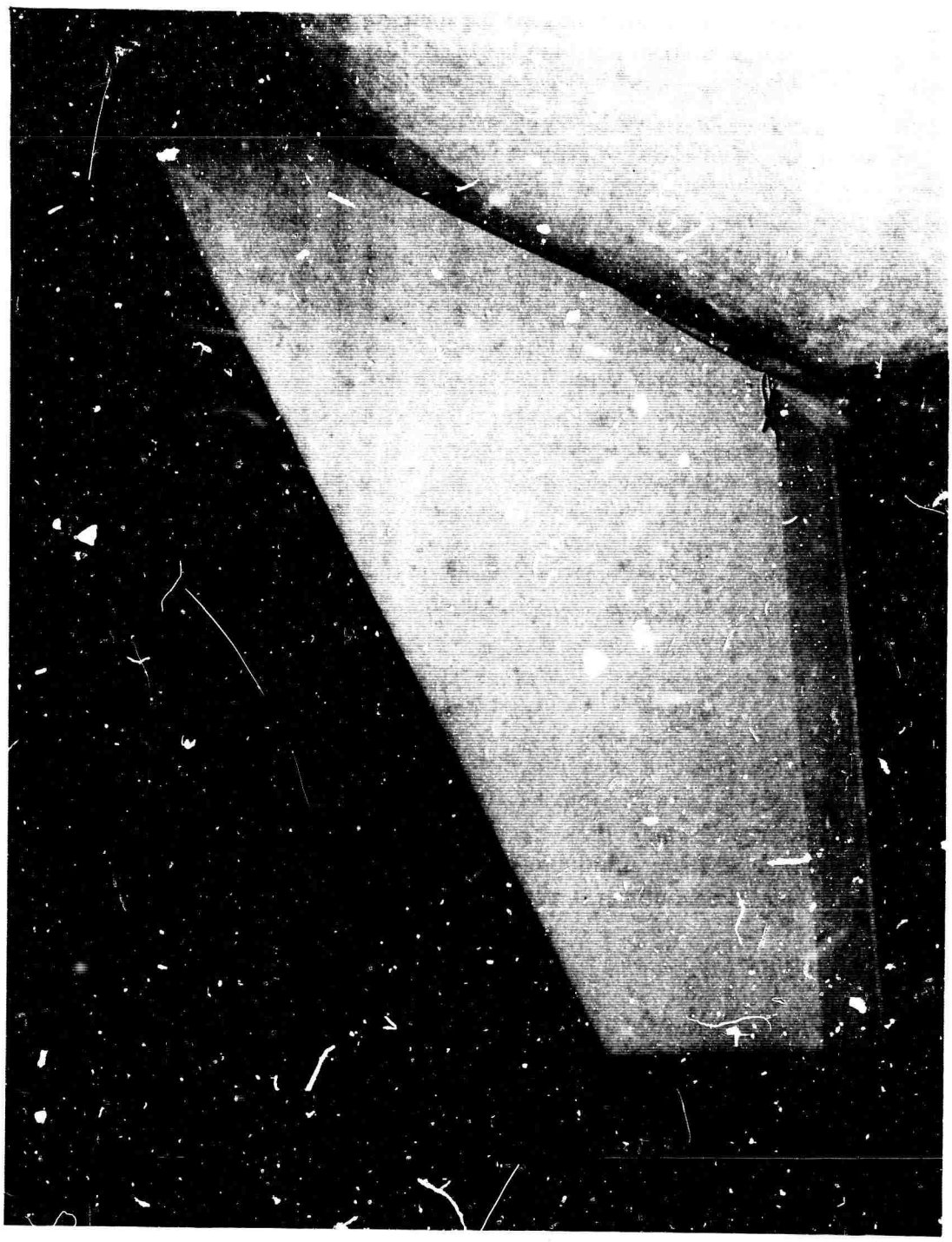

Figure 3. Vertical Stabilizer

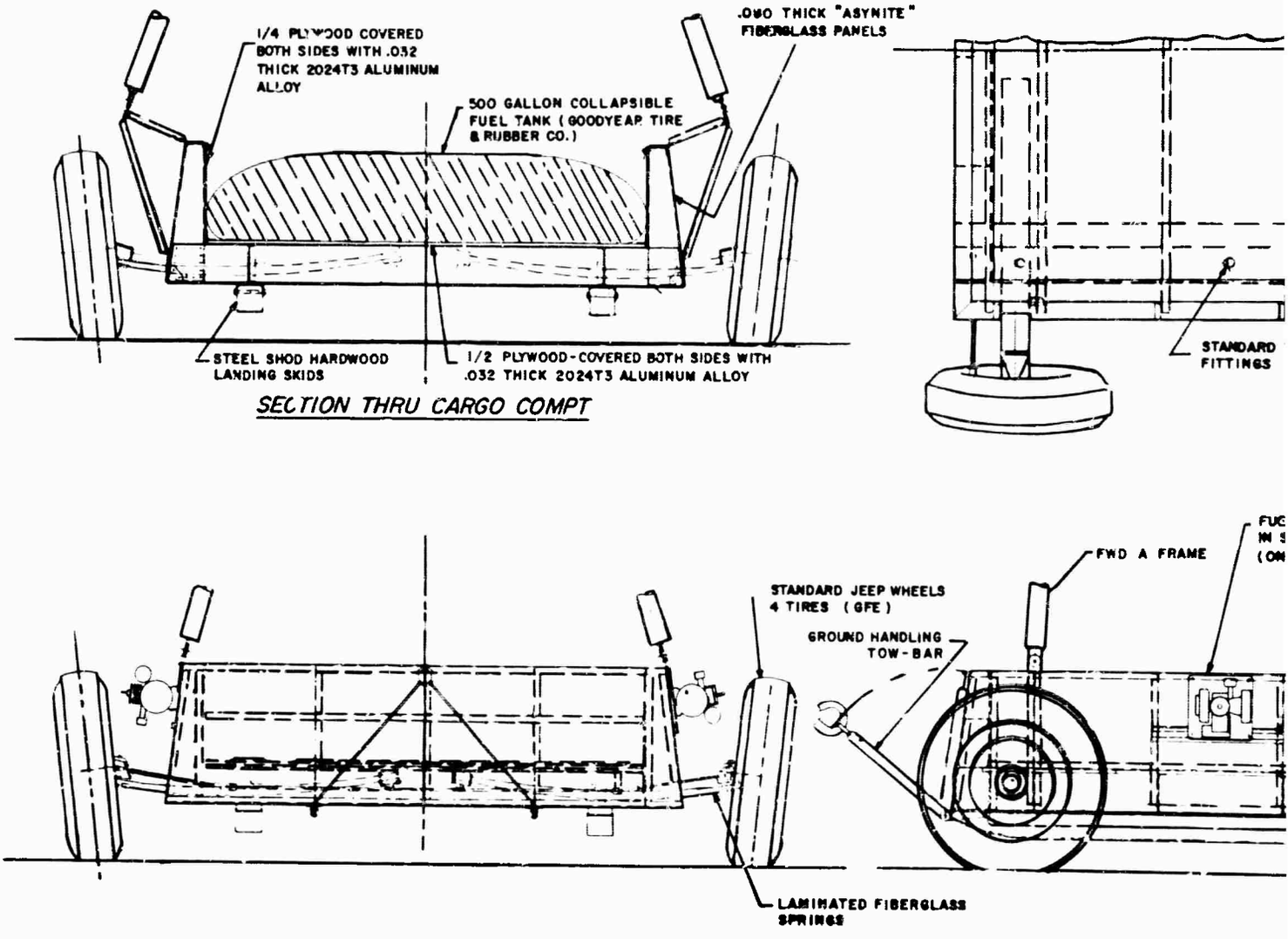

Figure 4. Body Assembly

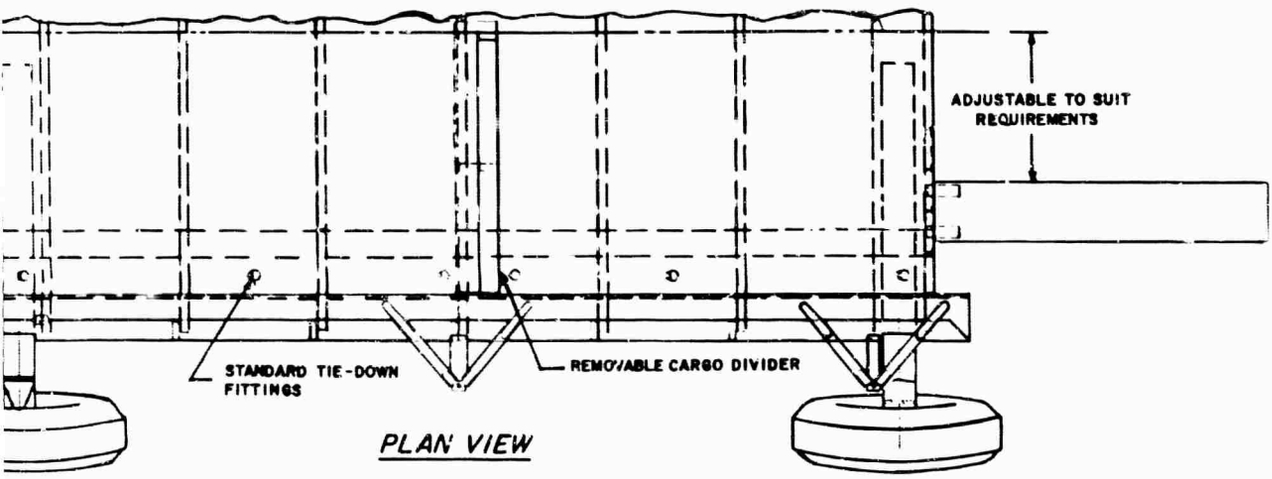

PLAN VIEW

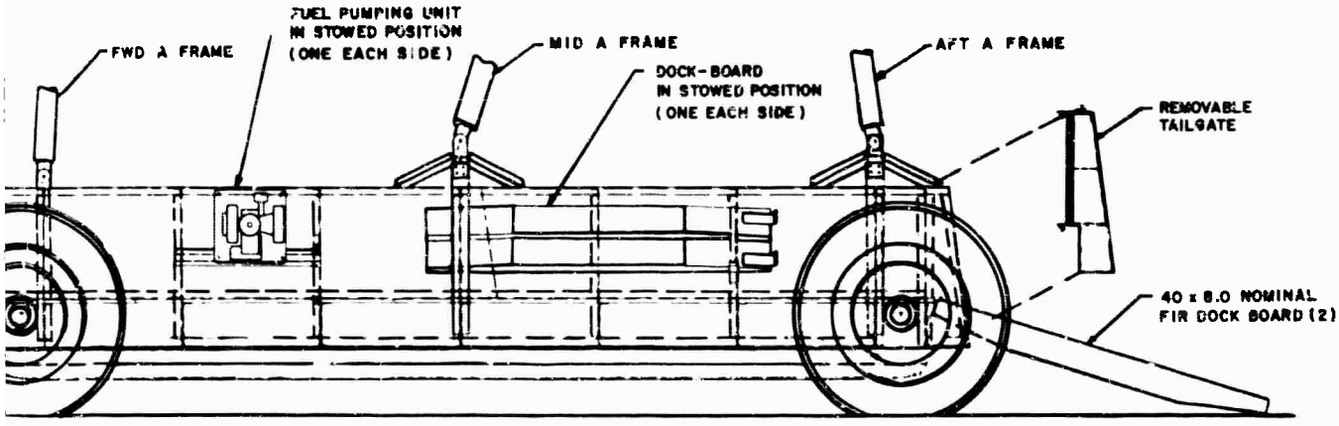

SIDE VIEW

The rolling gear springs, in the form of conventional single flat leaf springs, are manufactured from Fiberglas. The springs are similar to those developed and tested for the flexible wing utility vehicle (Project XV-8A, Contract DA 44-177-AMC-874(T)). The wheels and brakes are standard Government-furnished jeep equipment. The forward wheel installation provides the castering required for successful shimmy-free ground towing. The aft wheel installation acts as the braking system for the vehicle.

The brake system consists of a master brake cylinder, a brake lever, a tension spring, and the brake line tubing (Figure 1). The system applies brake pressure to the two rear glider wheels and brakes when the tow cable is slack. The brake pressure can also be controlled manually for ground handling.

Tow Bridle Assembly

The tow bridle assembly, shown in Figure 1, consists of four 1/4-inch-diameter woven wire cables, two connected to the forward end of the glider body and two connected to the mid-wing support strut. An adjustable tension cable runs from the mid-wing support strut to the aft wing support strut attach fitting, to relieve the mid-wing strut of tow loads. The lower left of the four cables is not attached directly to the body; it runs through a fairlead to the brake lever. When there is sufficient tension in the cable to overcome the brake spring, the lever yields and releases the brakes. The forward ends of the cables attach through a swivel fitting to a whiffletree which induces corrective pitching moments for any off-trim tow conditions. Thirteen electrical wires run the full length of the tow cable, with quick-disconnects on each end to allow separation of the cable from the glider or the helicopter.

Electrical System

The electrical system (Figure 5) consists of a 28-volt aircraft battery, an electrically operated linear actuator, and six control relays. Four control relays are operated from the helicopter to command glider power on, wing up, wing down, and glider release. The other two relays are for wing up and wing down limits.

Momentary switches are located in the glider to control the system during ground checkout.

Fuel Container

The fuel container is a flexible, collapsible 500-gallon container made of rubberized fabric in a convenient pillow design. Only one fitting is needed for both the filling and the draining operations. The filled container is held in place by tie-down straps attached to the floor of the cargo body. The container is 130 inches long by 70 inches wide by 13 inches high when filled.

Tow Cable

The tow cable is a standard woven-wire strain cable wrapped with electrical wires and covered with a neoprene jacket. The tow cable is approximately 400 feet in length.

The cable has an attaching ring, weak link and load link on the tow aircraft end, and a standard releasable type cargo hook on the glider end. Electrical connections made through quick-disconnects at both ends allow separation of the cable from the glider or the helicopter.

Tow Aircraft Provisions

Modifications to the helicopter are necessary to accommodate the attachment fittings for the tow bridle and to tie in the electrical system for the tow operation (Figures 6, 7, and 8).

The helicopter tow bridle consists of two 5/16-inch-diameter woven-wire strain cables that attach to the structural shelf aft of the main doors. These cables in turn attach to the forward end of a triangular-shaped metal plate. A standard releasable-type cargo sling hook is attached to the aft end of this plate. The hook accepts the tow cable attaching ring. Both the existing electrical and manual sling releases in the helicopter are utilized for tow cable release at the helicopter.

A glider control panel is included in the conversion. This panel mounts the switches to command glider power on, wing up, wing down, and glider release. Also on the panel is a display of cable tension and indicator lights for wing motior and glider power on.

AERODYNAMICS ANALYSIS

Summary

This section contains the estimated performance and stability characteristics of the Flexible Wing Towed Universal Glider (TUG) system.

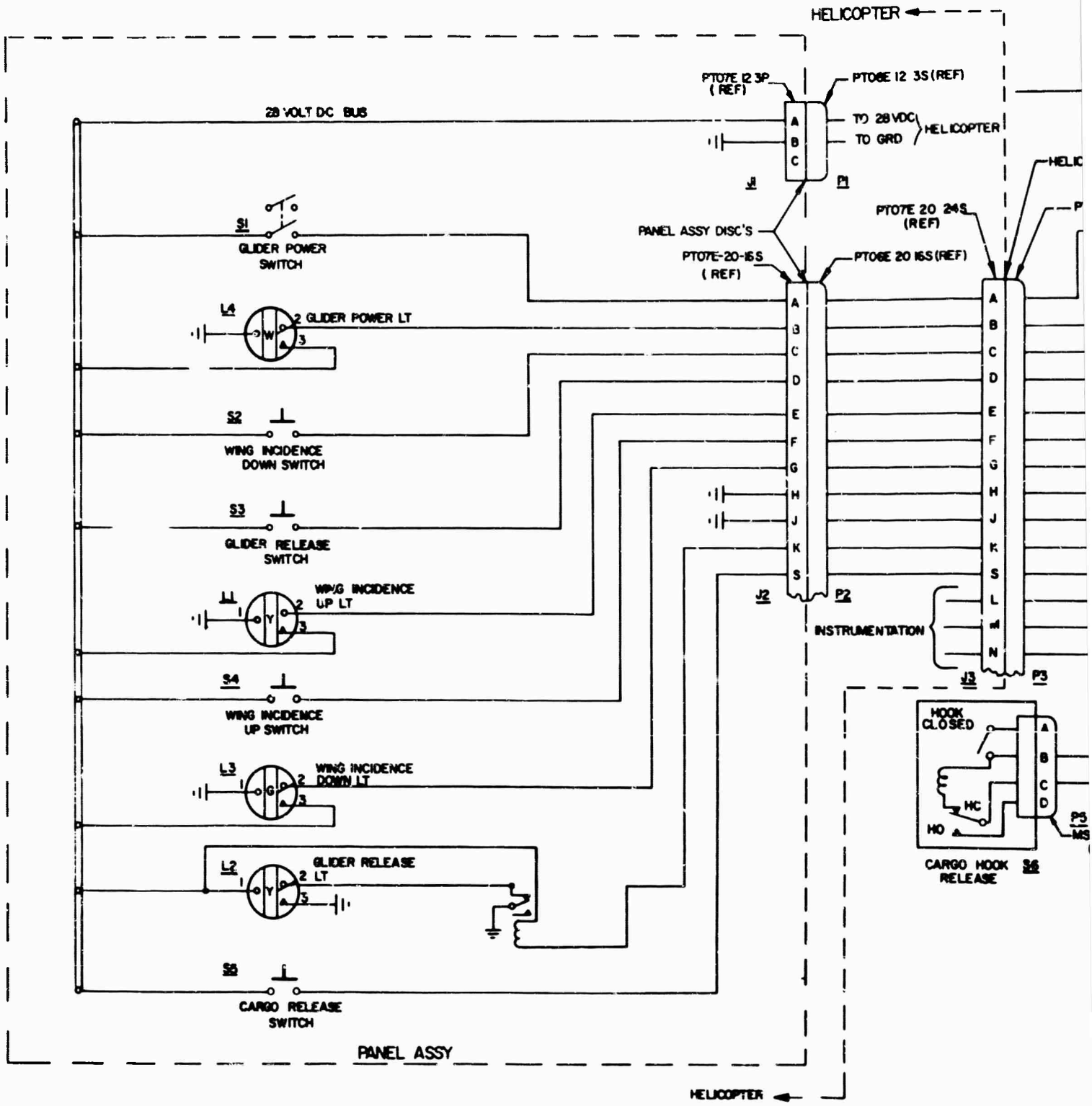

Figure 5. Electrical System

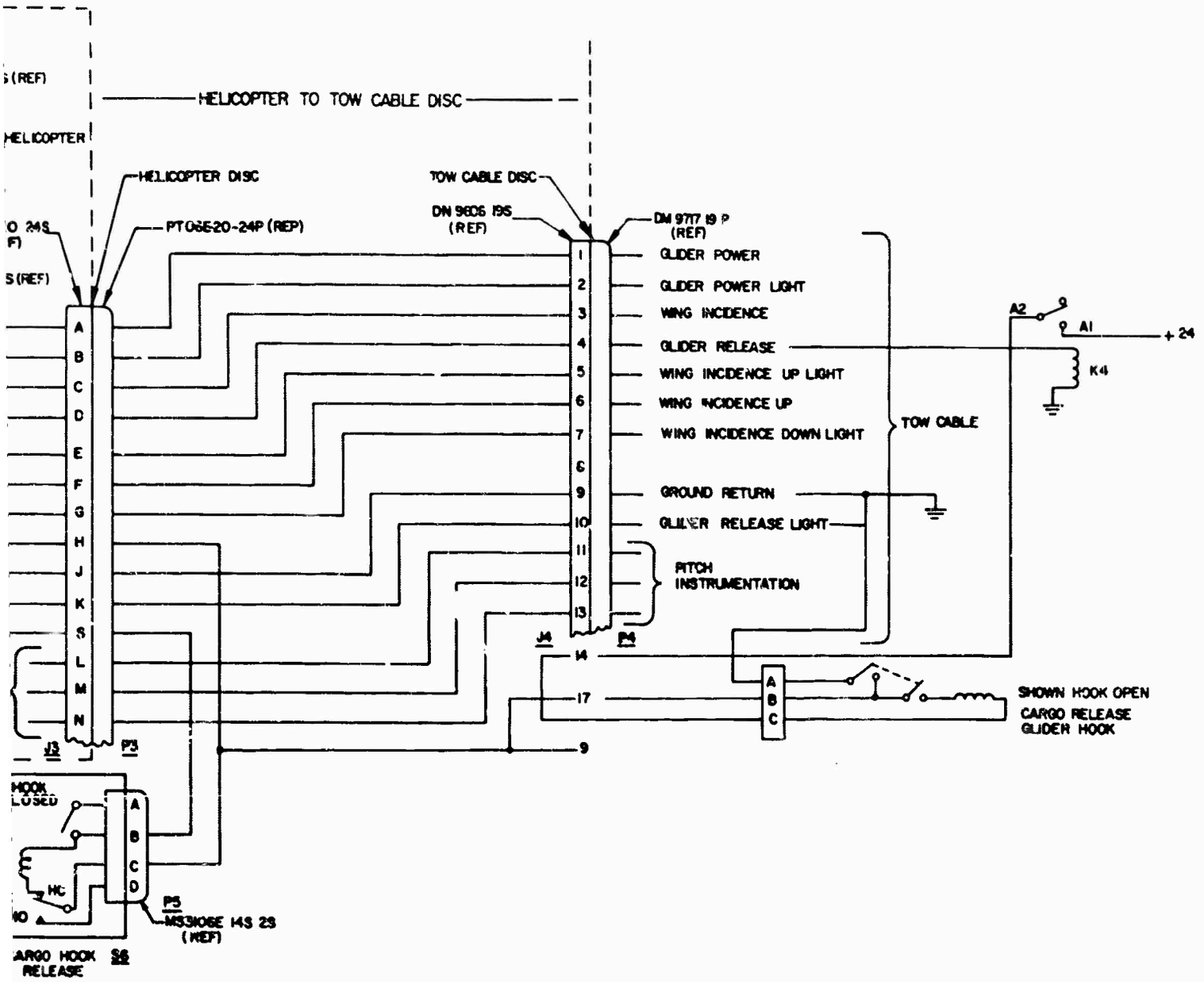
HELICOPTER TO TOW CABLE DISC
HELICOPTER DISC
TOW CABLE DISC
PT06E20-24P (REP)
DN 9606 19S (REF)
DM 9717 19 P (REF)
GLIDER POWER
GLIDER POWER LIGHT
WING INCIDENCE
GLIDER RELEASE
WING INCIDENCE UP LIGHT
WING INCIDENCE UP
WING INCIDENCE DOWN LIGHT
GROUND RETURN
GLIDER RELEASE LIGHT
PITCH INSTRUMENTATION
TOW CABLE
A2
A1
+ 24
K4
J4
P4
J3
P3
SHOWN HOOK OPEN
CARGO RELEASE
GLIDER HOOK
P5
MS3106E 14S 2S (REF)
CARGO HOOK RELEASE
S6

B

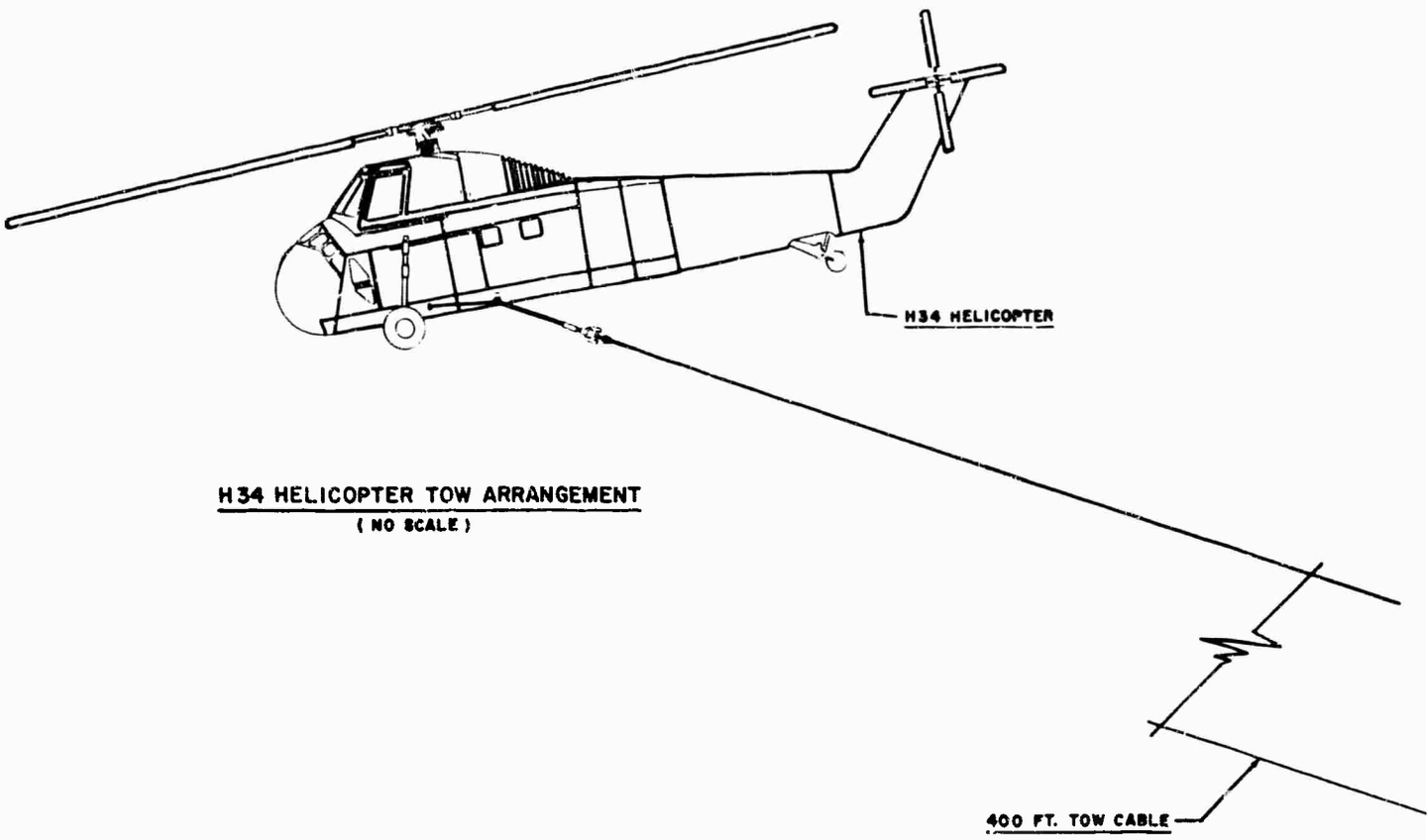

H34 HELICOPTER TOW ARRANGEMENT
(NO SCALE)

Figure 6. Tow Arrangements

TER

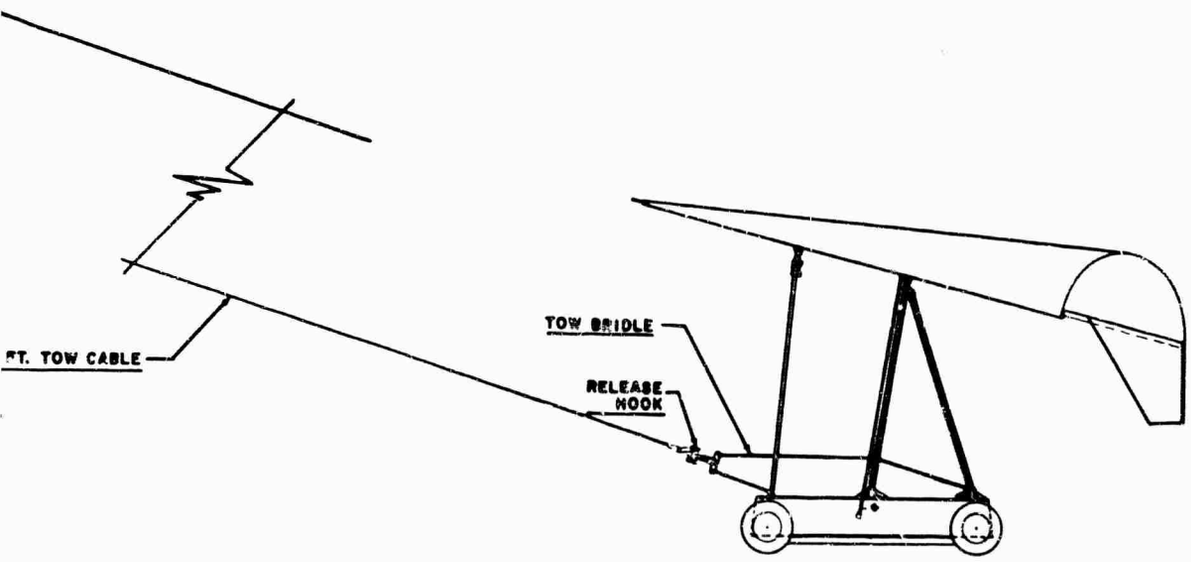

B

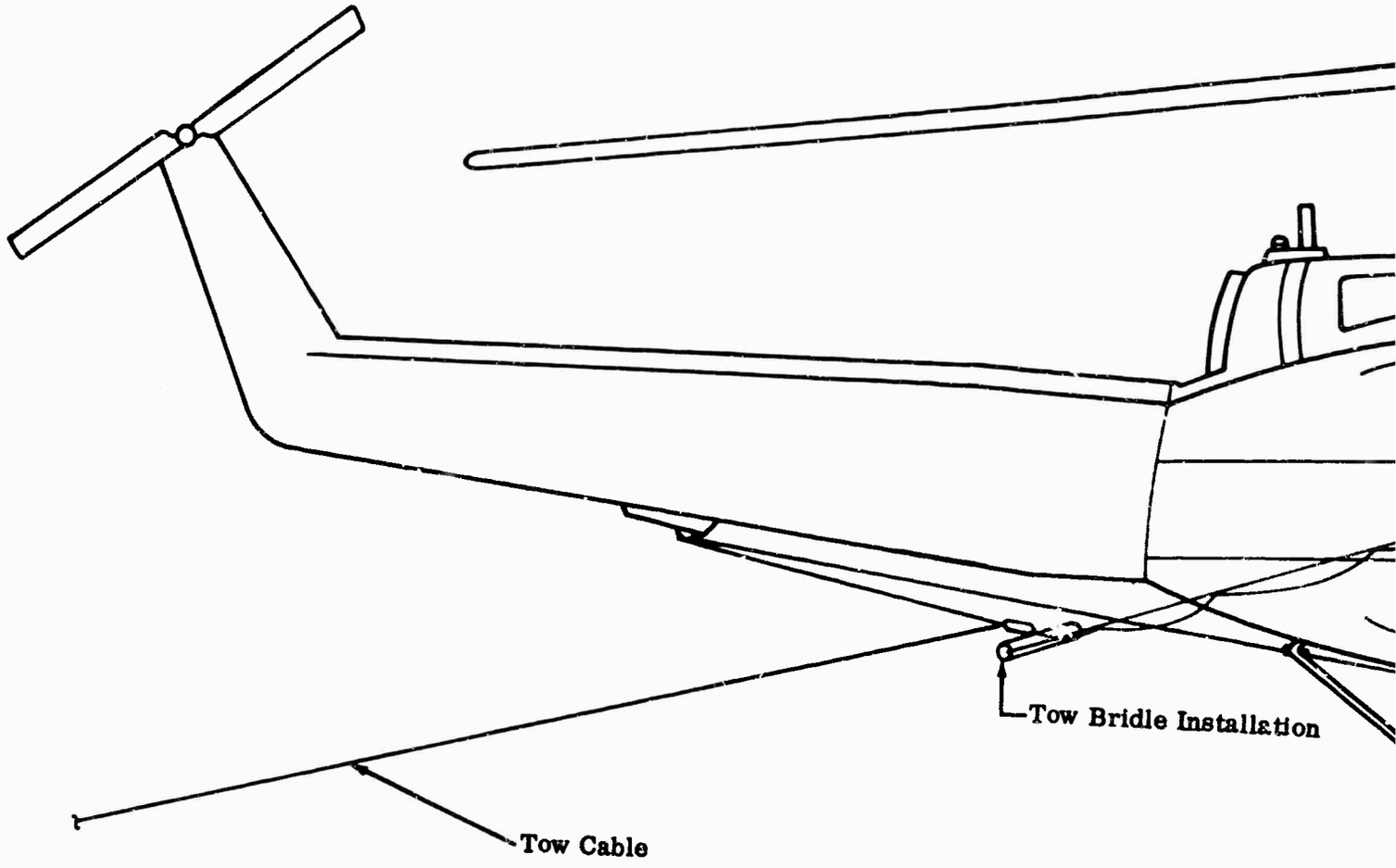

Figure 7. UH-ID Helicopter Tow Arrangement

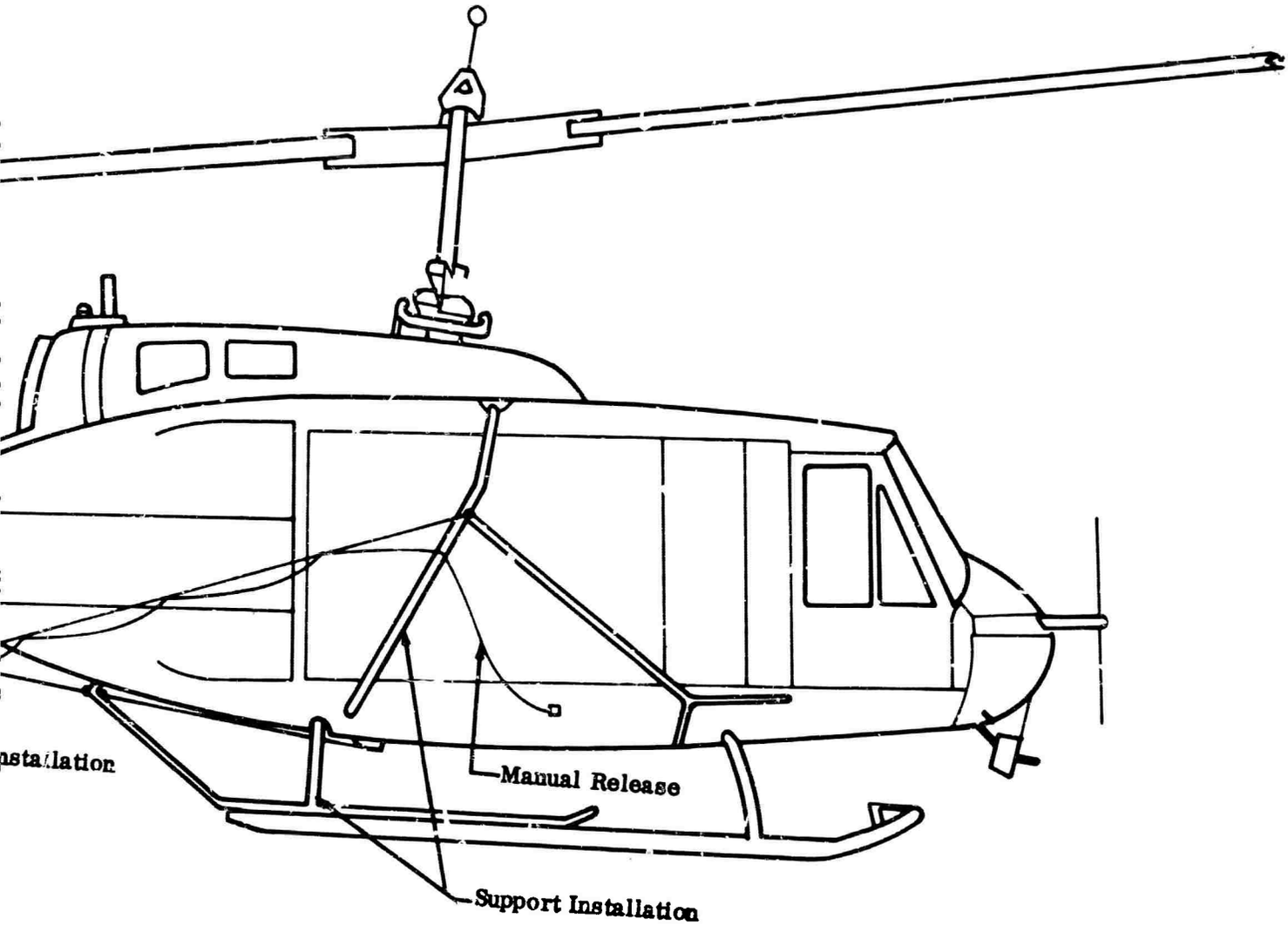

B

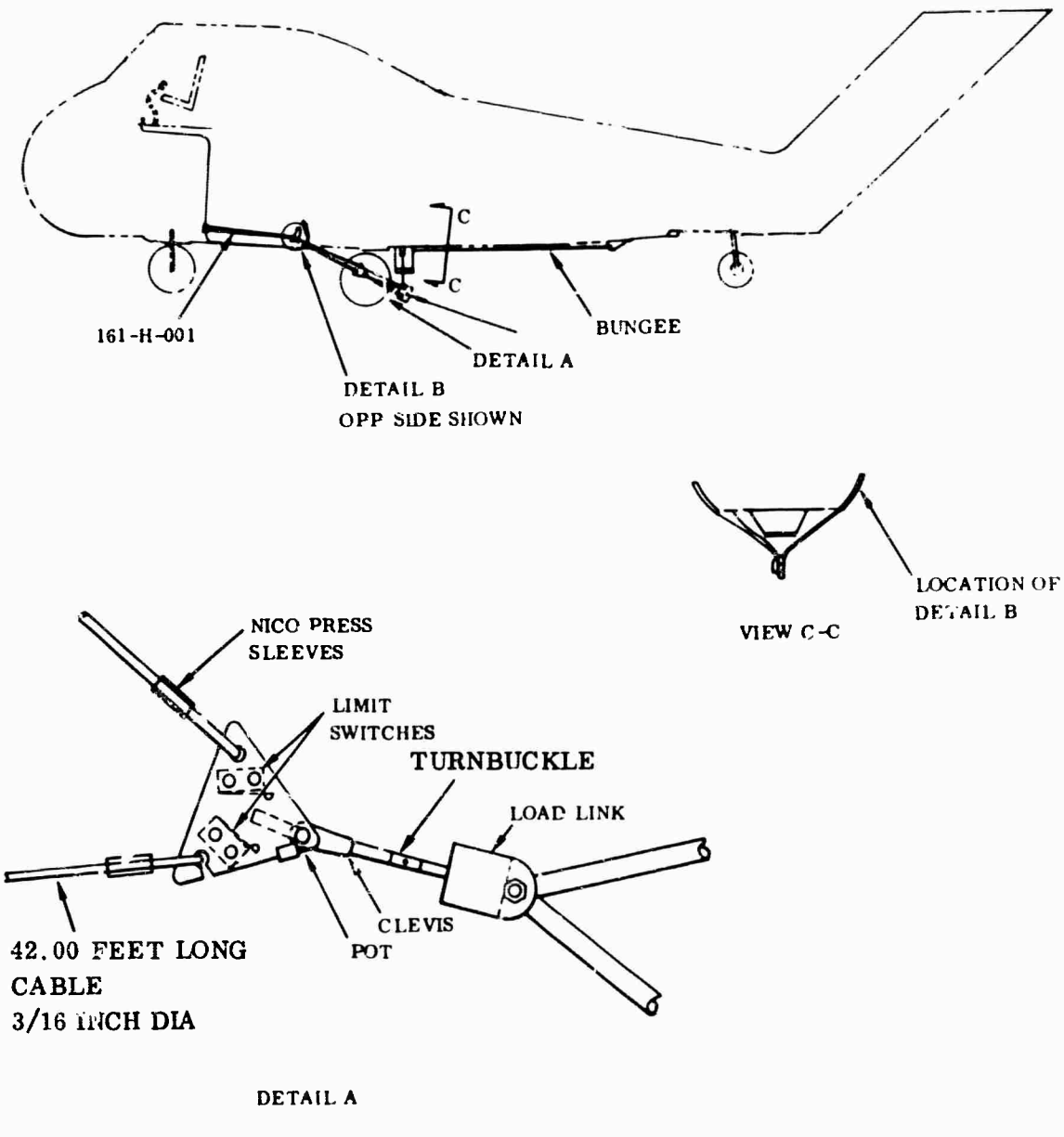

Figure 8. CH-34 Helicopter Modifications

The empty weight estimate of the TUG was less than the actual empty weight of the vehicle as flight tested. Data are therefore presented herein for a TUG gross weight of 4,200 pounds, which represents a 500-gallon payload of fuel based on the estimate of empty weight, and for a gross weight of 5,100 pounds, which represents a 500-gallon payload based on the actual empty weight of the TUG.

Using the UH-1B for towing, a sea level takeoff ground run of approximately 1,400 feet at a gross weight of 5,100 pounds was calculated for the TUG. Rate of climb at sea level and normal rated power with this payload was 530 feet per minute. A maximum tow speed of approximately 70 knots was determined.

Analysis indicated that the UH-1B is capable of towing the glider 117 nautical miles at a gross weight of 4,200 pounds and an altitude of 5,000 feet. This allows 10% of usable fuel for reserve. In this case the takeoff ground run was 800 feet, the maximum possible tow speed was 72 knots, and the landing ground run was 290 feet.

The TUG was shown to be both statically and dynamically stable in all configurations investigated, and both longitudinal and lateral-directional oscillatory characteristics were more than adequate for an unmanned vehicle.

Data Basis

The aerodynamic data used as a basis for estimating TUG performance were obtained for the most part from Ryan and NASA-conducted wind-tunnel tests. Aerodynamic characteristics of untested components were estimated, using standard estimating techniques.

A drag buildup for the TUG at zero lift is tabulated in Table 1. Drag due to lift was added to C_{D_O} to provide the drag polar presented in Figure 9. The lift curve is shown in Figure 10.

Lift-to-drag ratios are plotted in Figure 11, which shows maximum L/D to be 3.72.

Horsepower Required and Available

Horsepower required for the UH-1B-TUG combination in level flight was determined by first calculating an "equivalent helicopter" and then solving for power required using standard helicopter analysis. The "equivalent helicopter" is defined as a helicopter exhibiting the same performance characteristics as the helicopter-plus-glider combination.

TABLE I
DRAG BUILDUP

ITEM	f (SQ FT)	ΔC_{D_O}
Body	11.85	0.0214
Skids	0.22	0.0004
Wheels	2.49	0.0045
Wheel Struts	0.89	0.0016
Wing-Body Struts	16.79	0.0303
Roll Cables	0.44	0.0008
Tow Line Attaching Cables	0.11	0.0002
Pitch Actuator	1.50	0.0027
Vertical Tail	0.16	0.0003
Fuel Pumping Units	0.44	0.0008
A-Frame Supports	0.88	0.0016
SUBTOTAL	35.77	0.0646
Miscellaneous (5% of SUBTOTAL)	1.79	0.0032
Wing	38.81	0.0700
TOTAL	76.37	0.1378

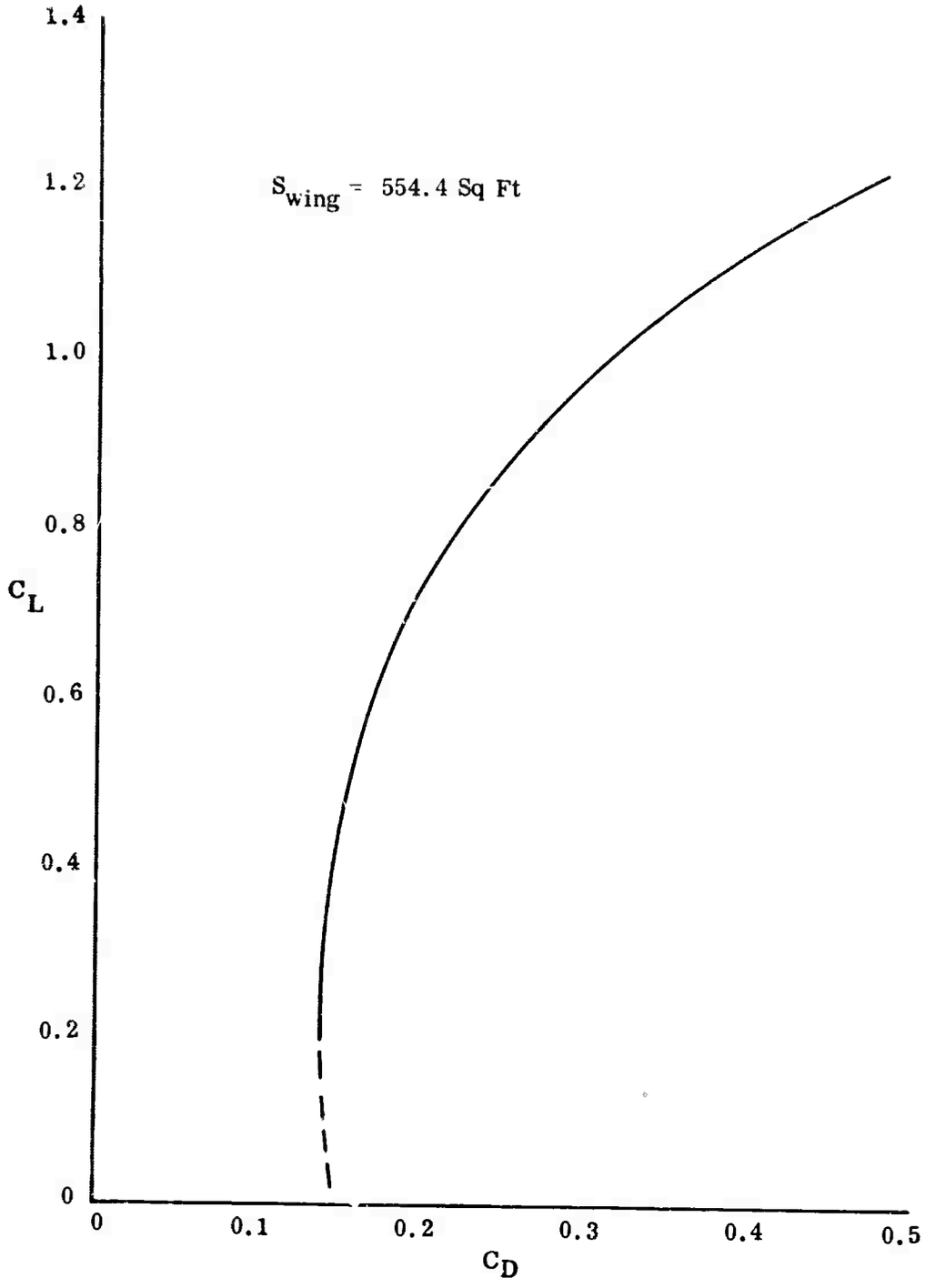

Figure 9. Drag Polar

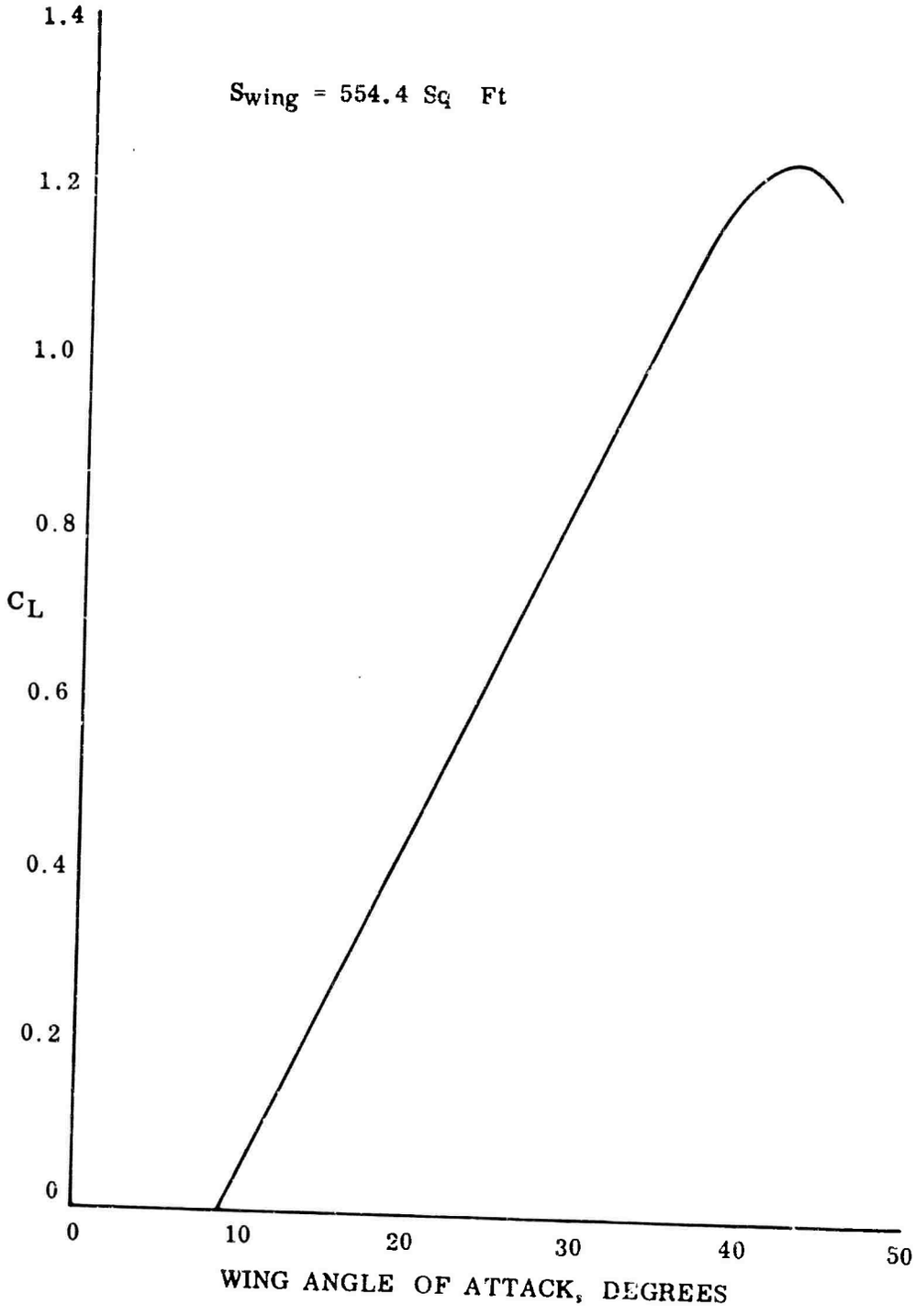

Figure 10. Lift Curve

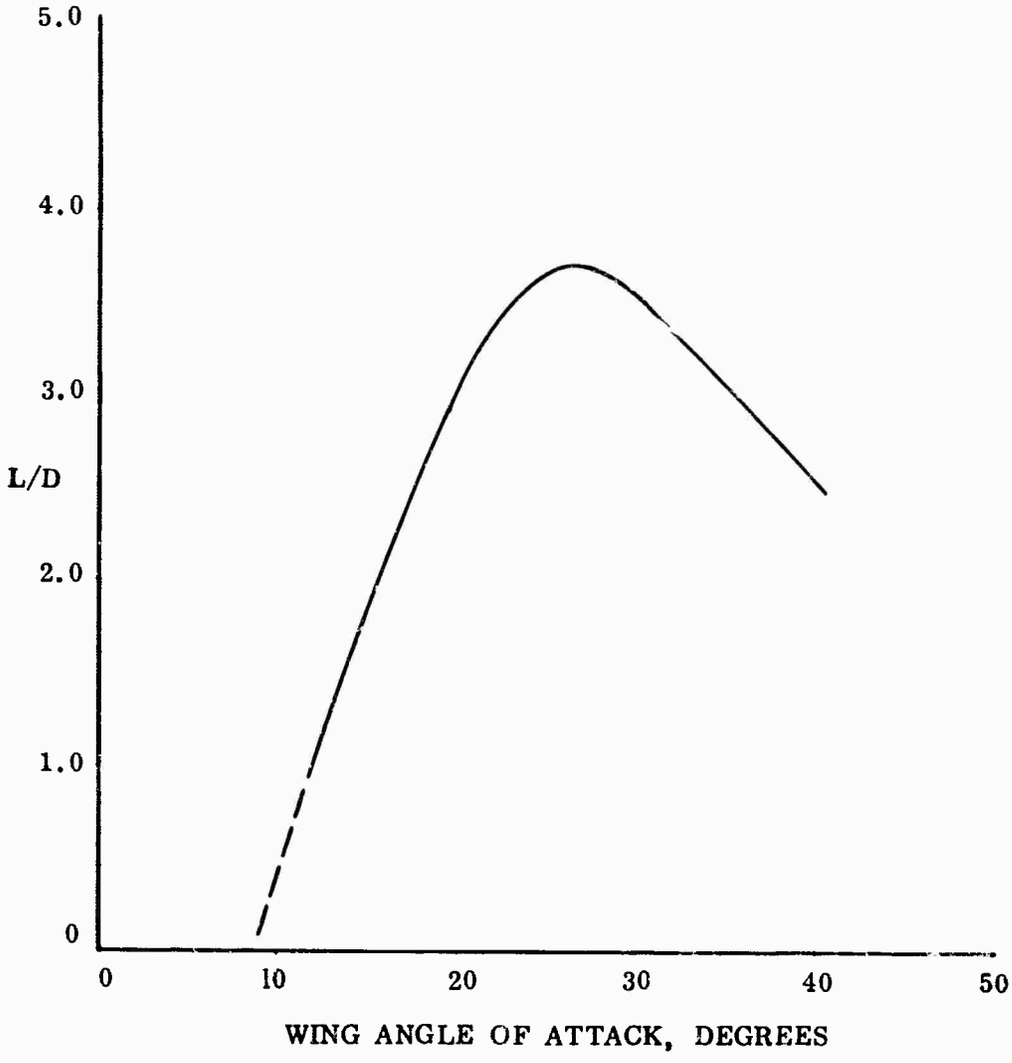

Figure 11. Lift-Drag Ratios

The "equivalent helicopter" was determined as follows:

1. Cable tension and cable angle at the helicopter were obtained from a tow cable characteristics program solved by an IBM-704 computer.

2. The cable tension was resolved into two components: one in the drag direction and one in the weight direction.

3. The weight component was added to the helicopter gross weight and the drag component was considered as additional parasite drag.

The tension components were resolved using the following force diagram:

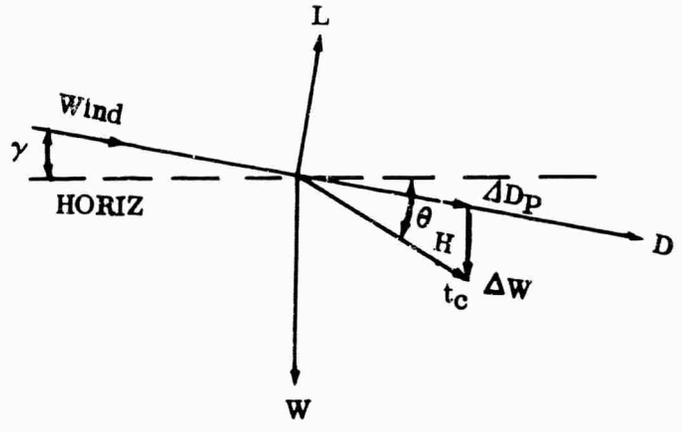

$$t_c/\sin(90+\gamma) = \Delta W/\sin(\theta_H-\gamma) = \Delta D_P/\sin(90-\theta_H)$$

$$\Delta W = \frac{t_c \sin(\theta_H-\gamma)}{\sin(90+\gamma)}$$

$$\Delta D_P = \frac{t_c \sin(90-\theta_H)}{\sin(90+\gamma)} = \frac{t_c \cos\theta_H}{\sin(90+\gamma)}$$

where

γ = flight path angle

θ_H = cable angle below horizontal

t_c = cable tension

ΔW = weight component of cable tension

ΔD_P = parasite drag component of cable tension

For level flight $\gamma = 0$ and the expressions for ΔW and ΔD_P reduce to:

$$\Delta W = t_c \sin \theta_H$$

$$\Delta D_P = t_c \cos \theta_H$$

The total power required at the helicopter rotor shaft for the UH-1B-TUG combination was calculated by IBM-704 computer, utilizing the computation methods of References 1 and 2. The digital program does not use small-angle assumptions regarding blade section inflow angles and velocities. Allowance is made for stall in the reversed flow region.

The calculated power required does not include power losses due to transmission, cooling, antitorque, etc. These losses are accounted for in the power available, which is reduced by 10% for this purpose. Figures 12 and 13 present power required and available for the UH-1B plus TUG for sea level and 5,000 feet respectively. The engine assumed for the UH-1B is the Lycoming T-53-L-9 rated at 1,100 horsepower at sea level.

Maximum Tow Speeds

Power-limited maximum speeds were obtained from the intersection of the power required and power available curves. Maximum speed at sea level at a gross weight of 5,100 pounds is 70 knots and at 5,000 feet is 66 knots.

Rates of Climb

Rates of climb were calculated using the equation:

$$R/C = \frac{(\text{HP AVAIL} - \text{HP REQ})\ 33{,}000}{\text{WEIGHT (UH-1B + TUG)}}$$

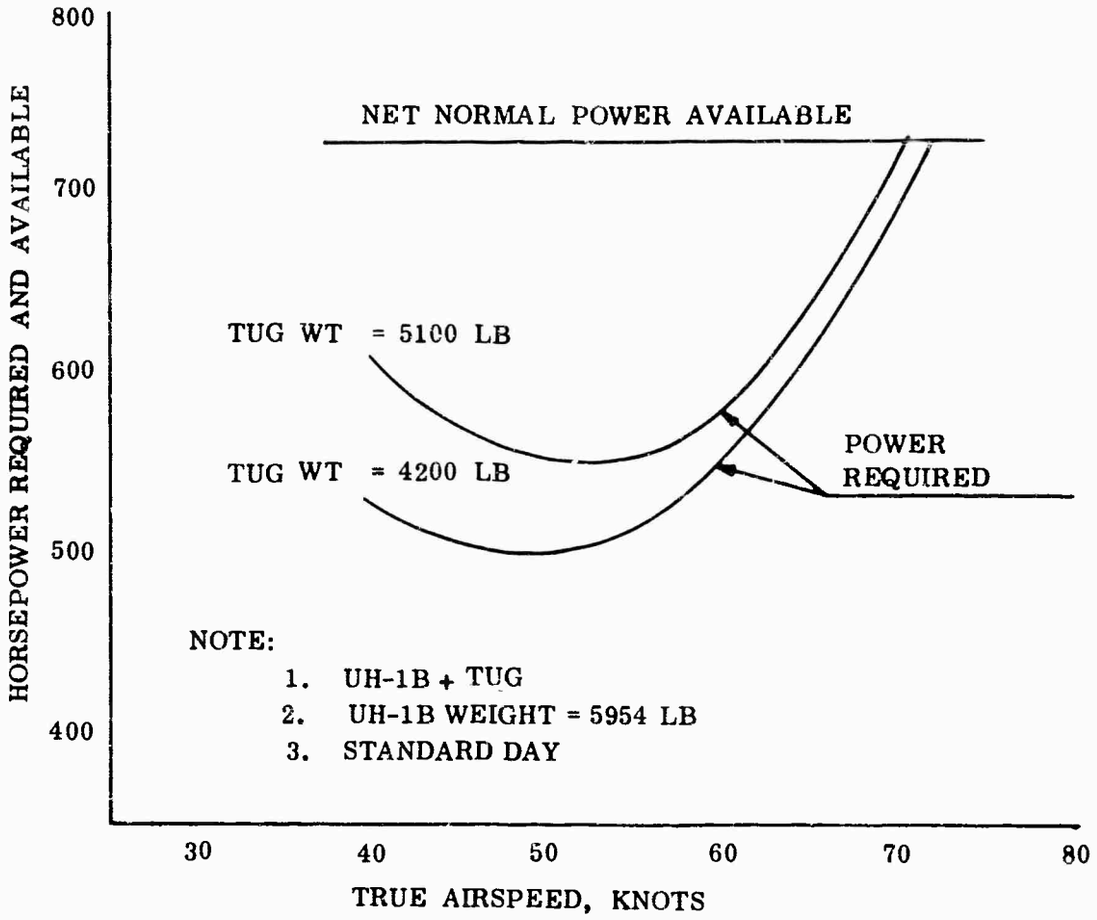

Figure 12. Horsepower Required and Available at Sea Level

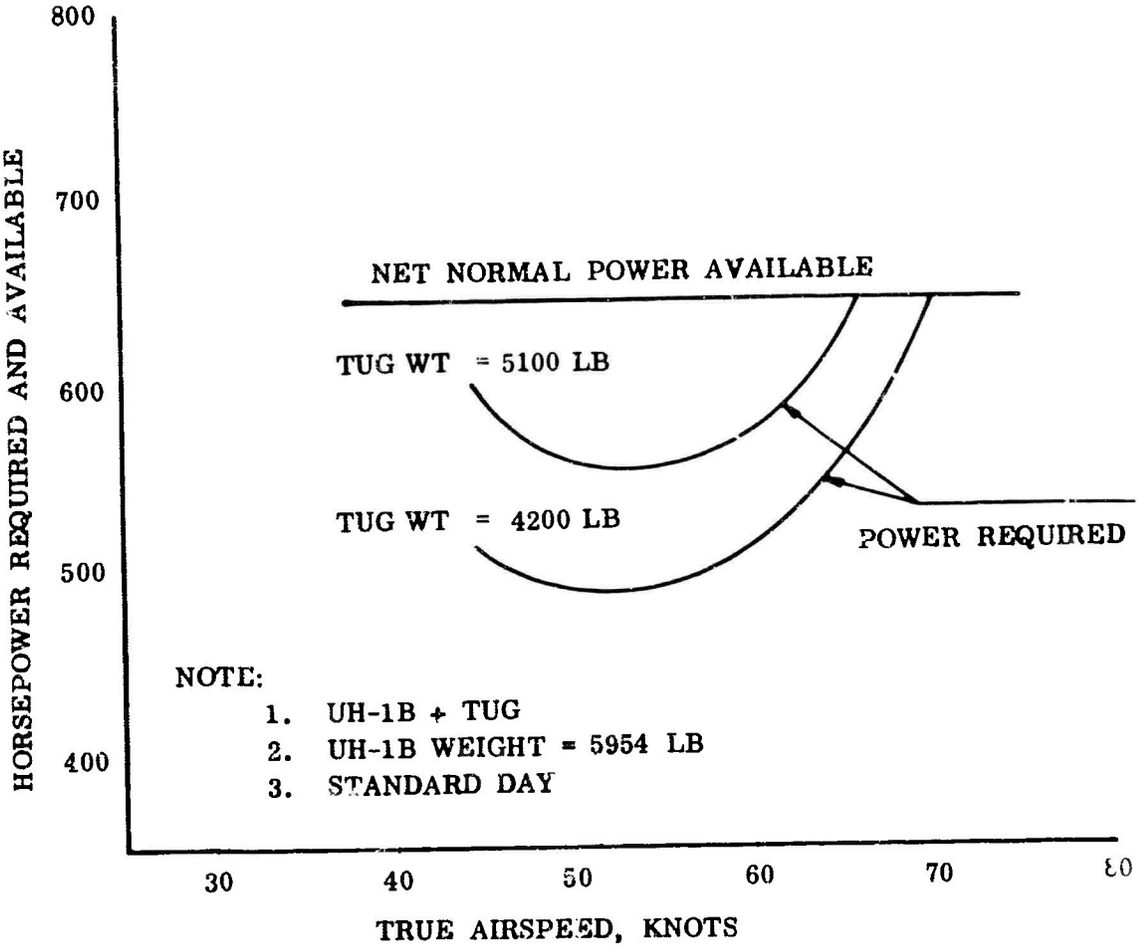

Figure 13. Horsepower Required and Available at 5000 Feet

Available and required horsepowers are for the equivalent helicopter and were obtained from Figures 12 and 13.

The results are plotted on Figure 14.

Glide Performance

Still-air glide range is plotted in Figures 15 and 16, as a function of altitude and speed, for TUG weights of 4,200 and 5,100 pounds respectively. Maximum range, attained at maximum L/D, occurs at speeds of 64.5 and 71 knots. Glide velocities at sea level are presented in Figure 17, with equivalent rates of descent shown in Figure 18. Glide performance was determined as follows:

Consider the force diagram representing gliding flight:

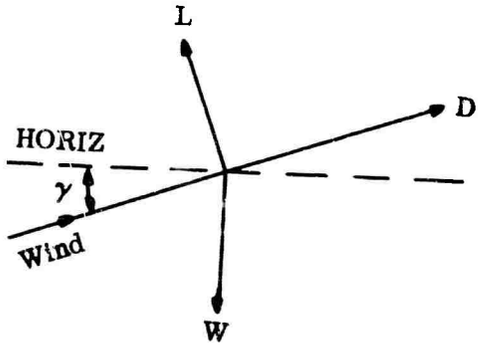

where

L = lift

D = drag

W = weight

γ = flight path angle

$L = W \cos \gamma$

$D = W \sin \gamma$

$L/D = (\cot \gamma)$

$$V_{GLIDE} = \sqrt{\frac{2W \cos \gamma}{C_L \rho S}}$$

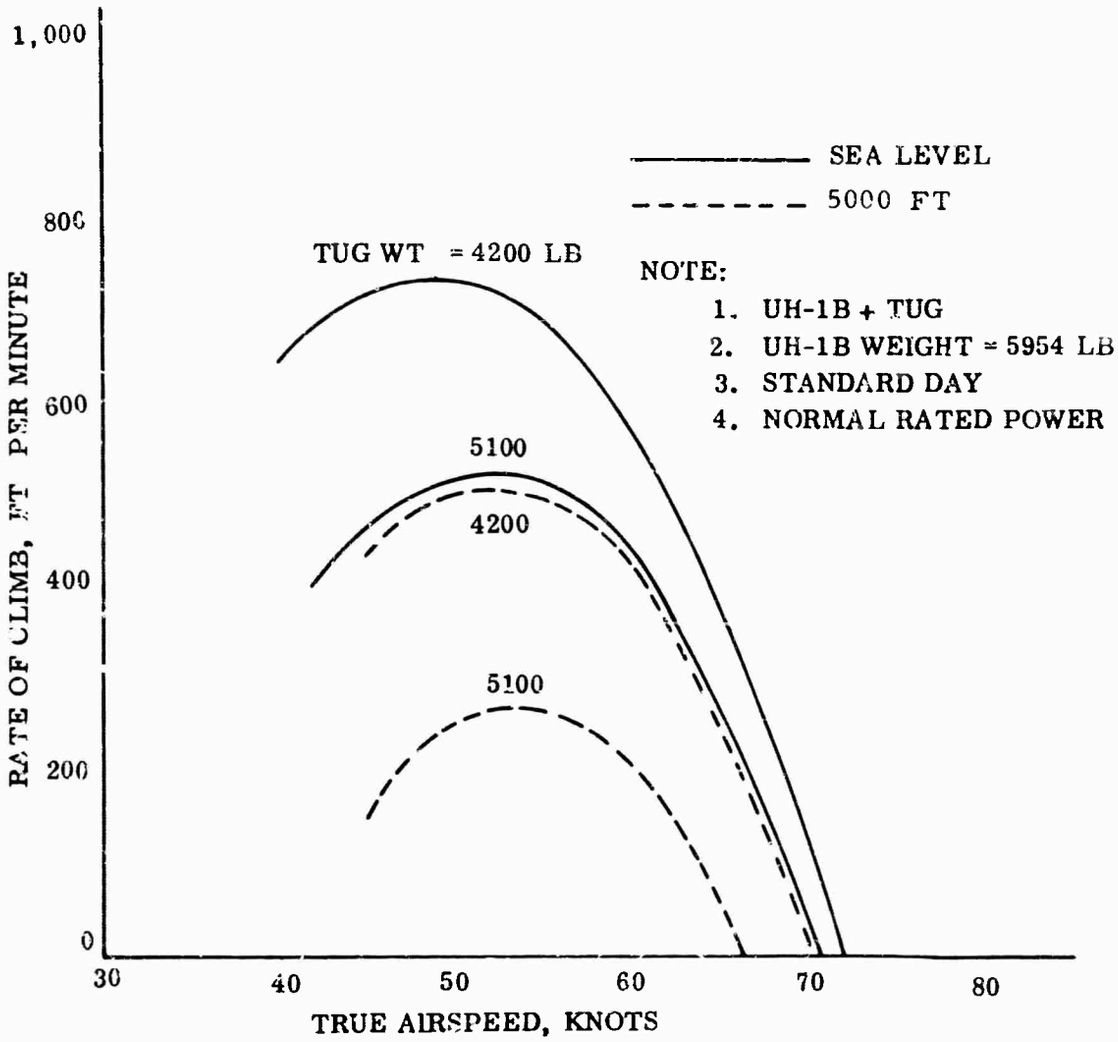

Figure 14. Rates of Climb

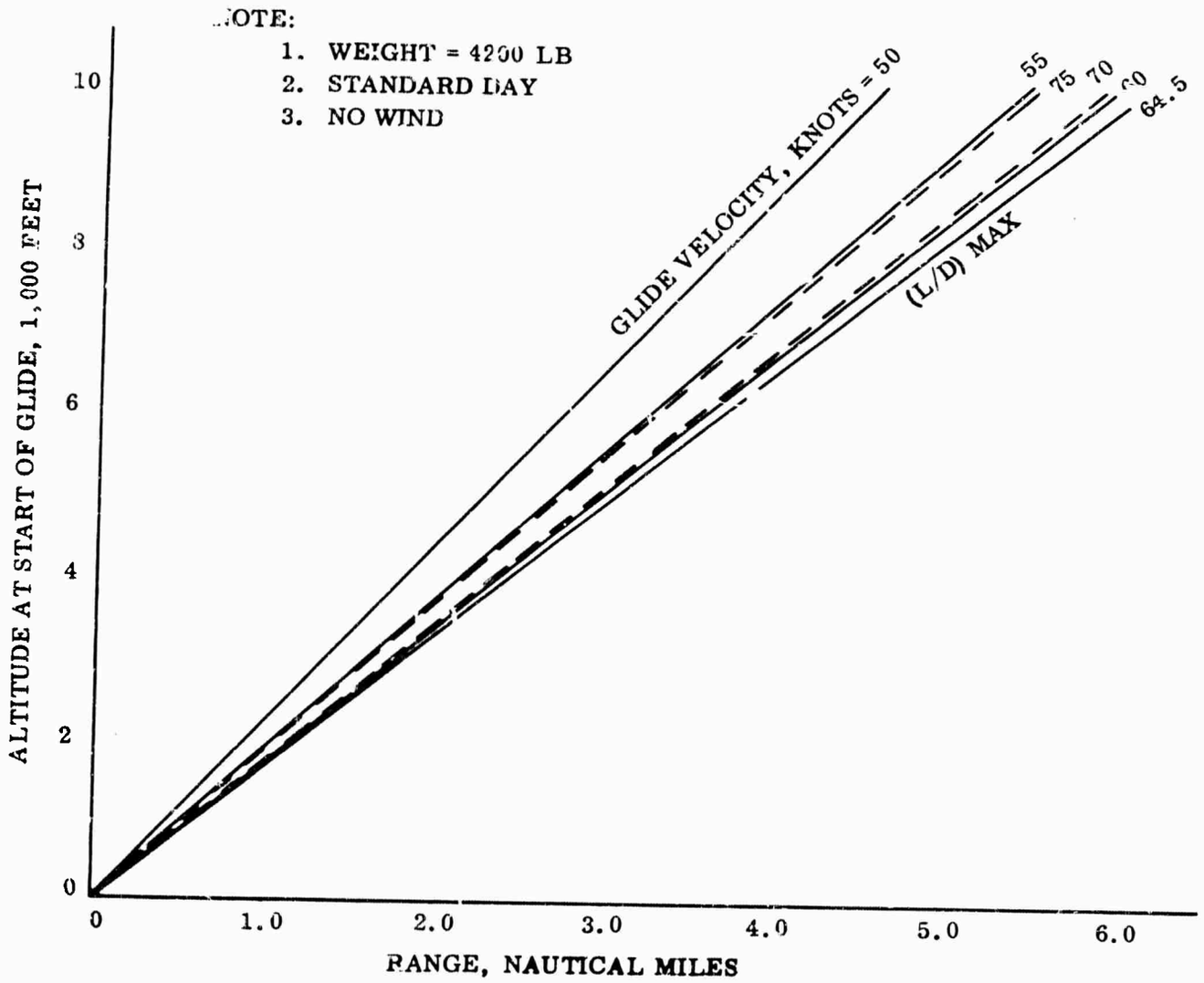

Figure 15. Glide Range at TUG Weight of 4200 Pounds

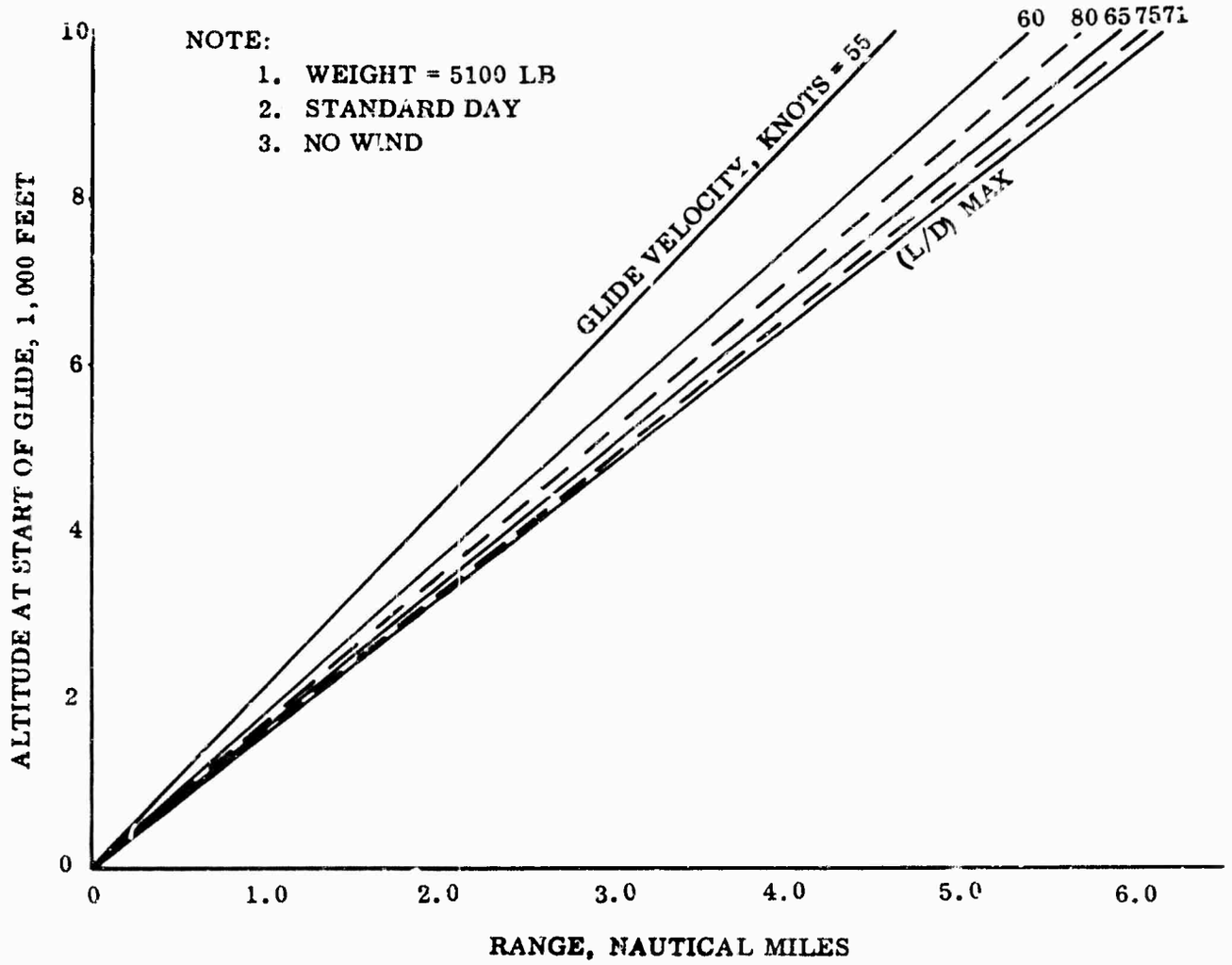

Figure 16. Glide Range at TUG Weight of 5100 pounds

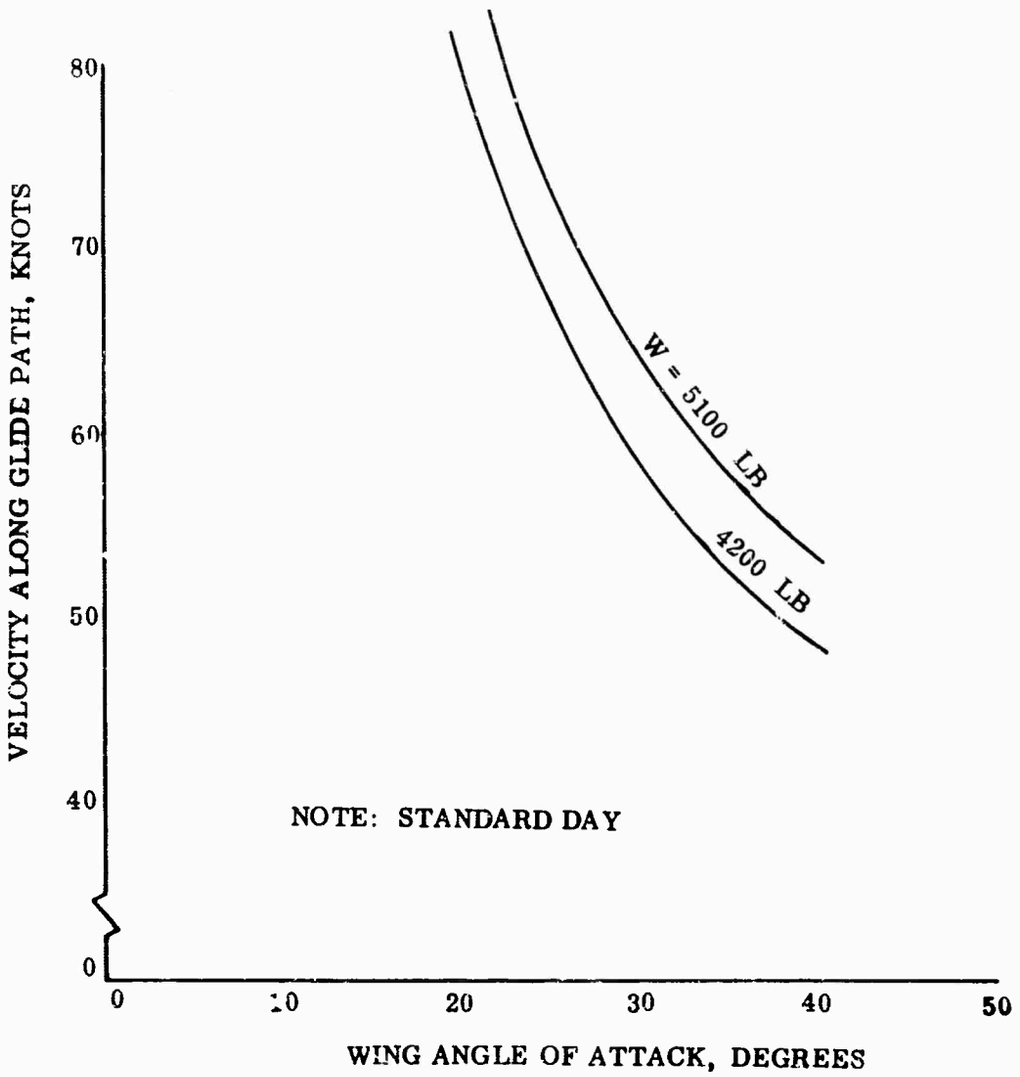

Figure 17. Glide Velocity at Sea Level

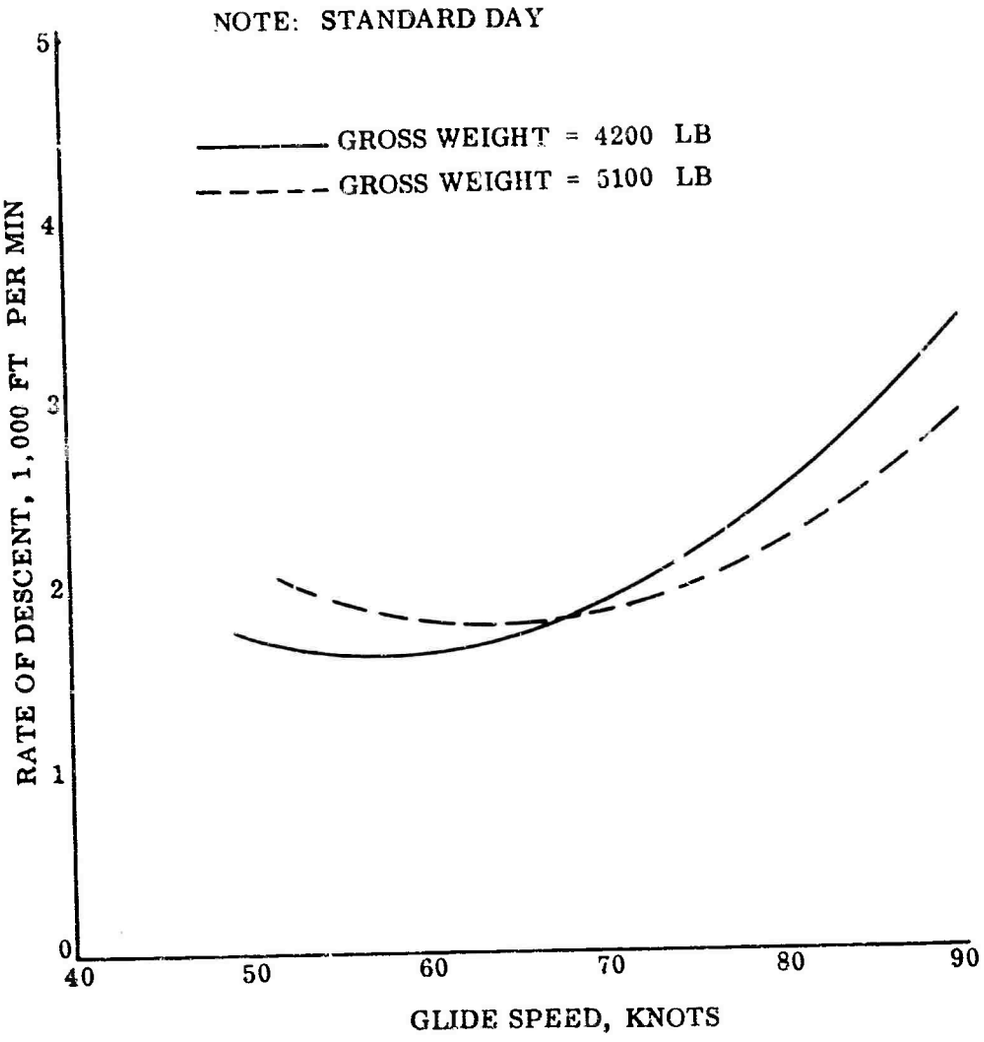

Figure 18. Rate of Descent Versus Glide Speed

rate of descent = $V_{(GLIDE)} \sin \gamma$

glide range = altitude at start of glide/tan γ

Takeoff

Takeoff performance is presented in Figure 19 as takeoff ground run versus TUG gross weight. This was derived as follows:

$$a = \frac{dv}{dt} = 1/2 \frac{dv^2}{ds}$$

$$S_G = \int_0^{V_{LO}} \frac{dv^2}{a}$$

The above equation may be solved graphically, knowing the acceleration (a) which is found by consideration of the force diagram representing the glider forces:

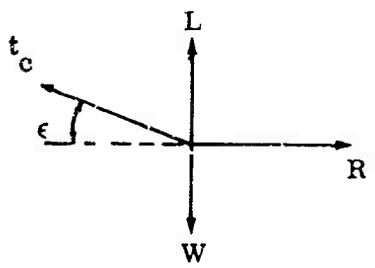

$$a = \frac{t_c \cos \epsilon - R}{m}$$

where

t_c = cable tension at glider, pounds

ϵ = cable angle, degrees

m = mass of glider, slugs

L = lift, pounds

W = weight of glider, pounds

R = resistance = $D + u\ (W - L - t_c \sin \epsilon)$

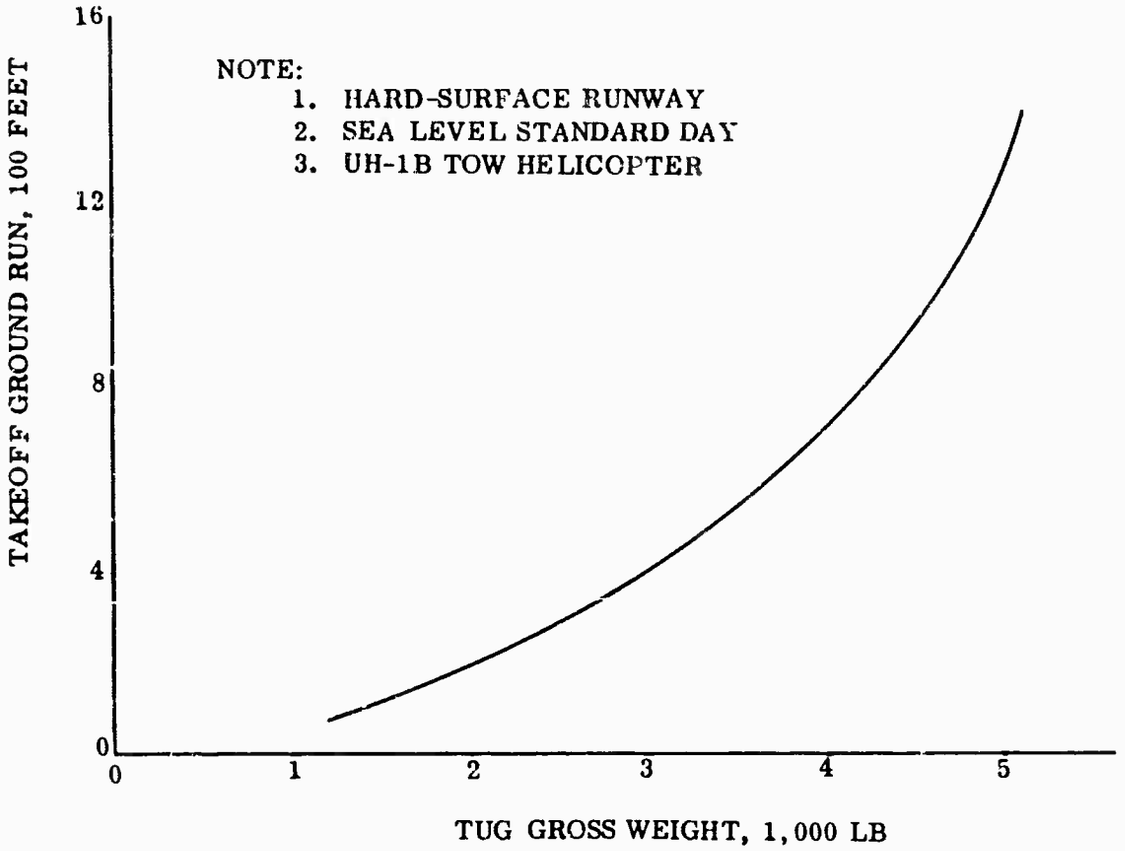

Figure 19. Takeoff Performance

D = drag, pounds

μ = coefficient of rolling friction = 0.025

Wing-body incidence angle is 22° throughout ground run and lift-off.

Landing

The landing ground run is presented in Figure 20 as a function of gross weight of the TUG. A touchdown speed of 1.20 percent of stall speed was assumed for the calculations, and the following equation was used:

$$S_G = \frac{0.1022\ V_{TD}^2}{\mu_\beta - (D/L)_{TD}} \log_{10} \left[\mu_\beta\ (L/D)_{TD}\right]$$

where

S_G = ground run, feet

V_{TD} = touchdown velocity, knots

$(L/D)_{TD}$ = lift/drag ratio at touchdown C_L

μ_β = braking coefficient = 0.4 for turf runway assumed

Stall Speeds

Sea level, standard day stall speeds are shown in Figure 21 as a function of gross weight. These values are determined using:

$$V_{STALL}\ (KNOTS) = \sqrt{\frac{GROSS\ WEIGHT\ X\ 295}{S_w\ X\ C_{L\ MAX}}}$$

Stall speed at the design gross weight of 5,100 pounds is 46.8 knots.

Range

The mission profile for the TUG plus UH-1B helicopter combination is presented in Figure 22. The TUG has a gross weight of 4,200 pounds. Allowance for

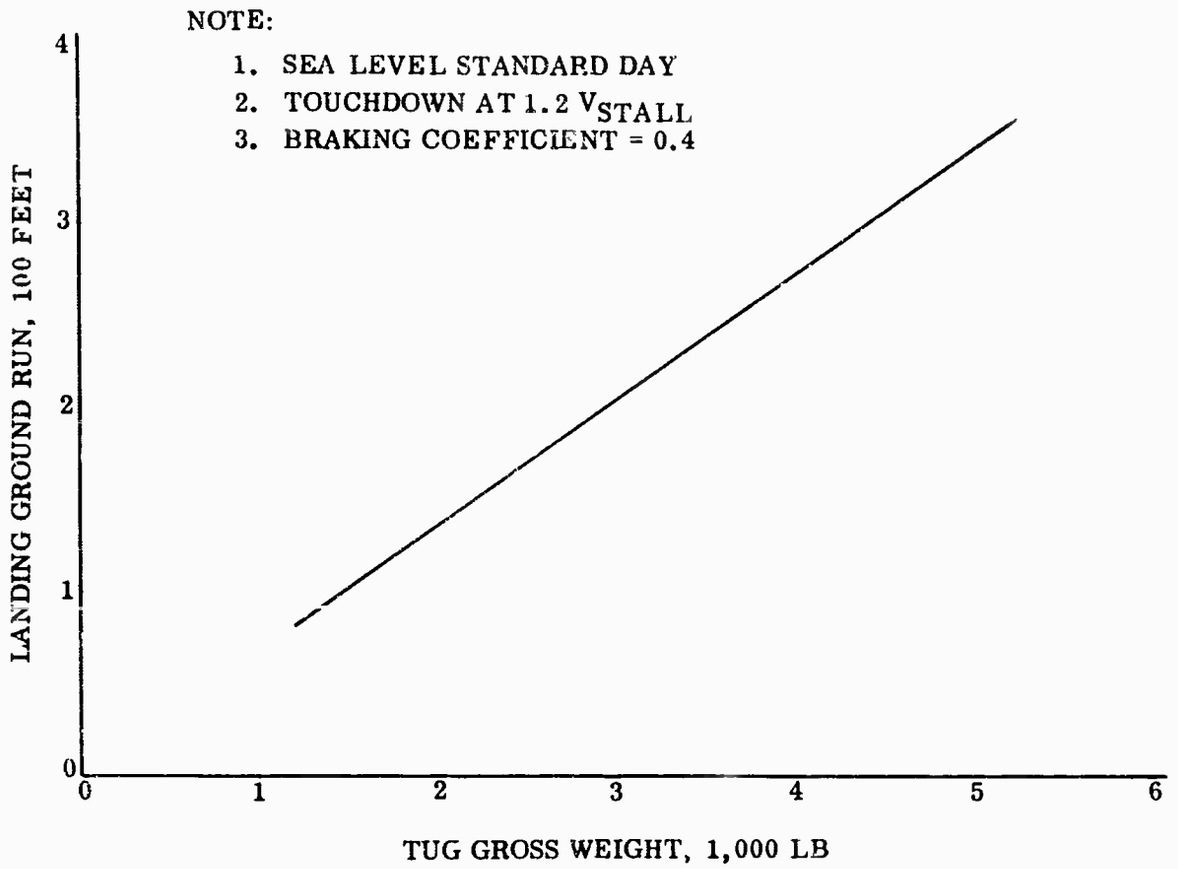

Figure 20. Landing Performance

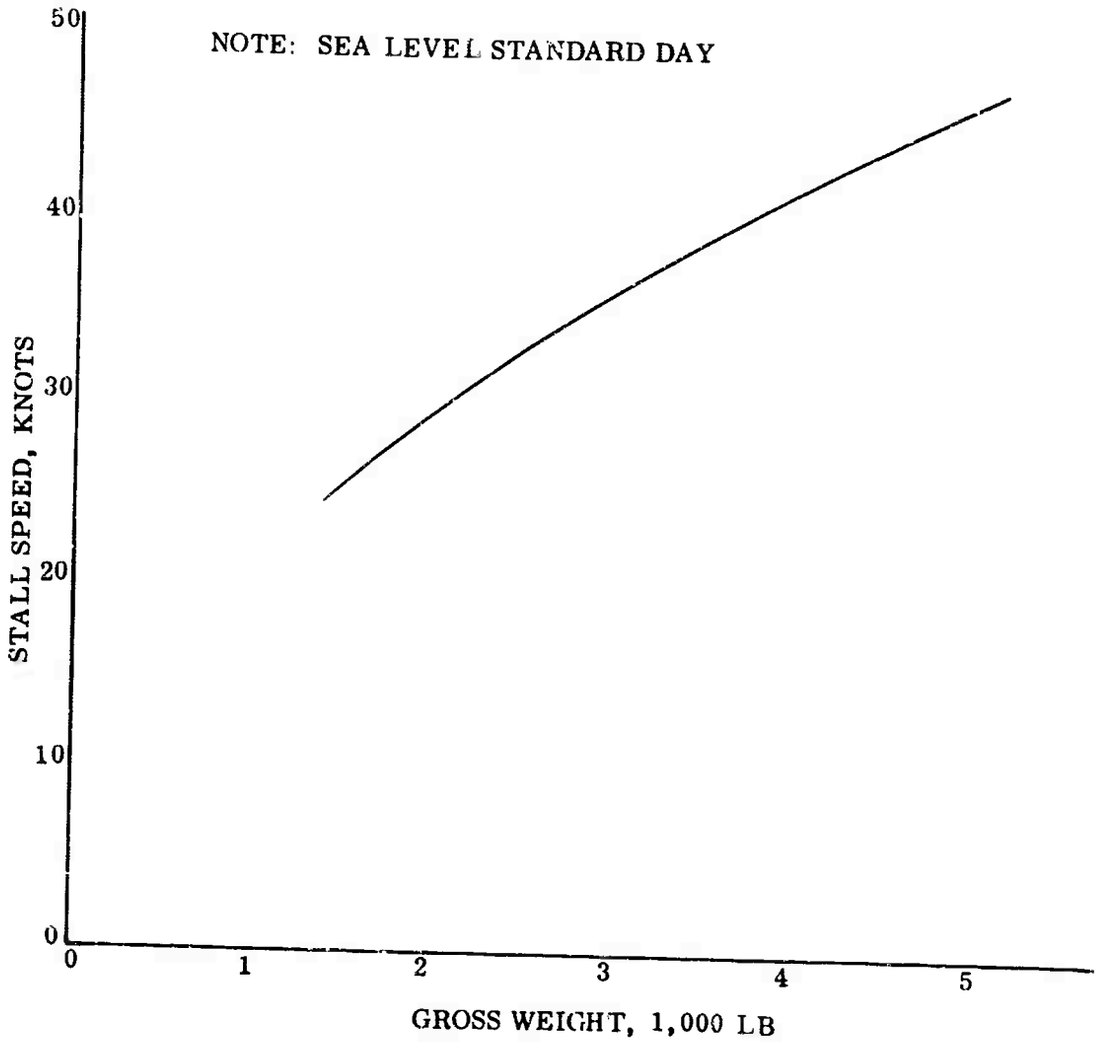

Figure 21. Stall Speeds

NOTE:

1. UH-1B TOW HELICOPTER
2. CRUISE ALTITUDE = 5000 FT
3. STANDARD DAY
4. TUG GROSS WEIGHT = 4200 LB

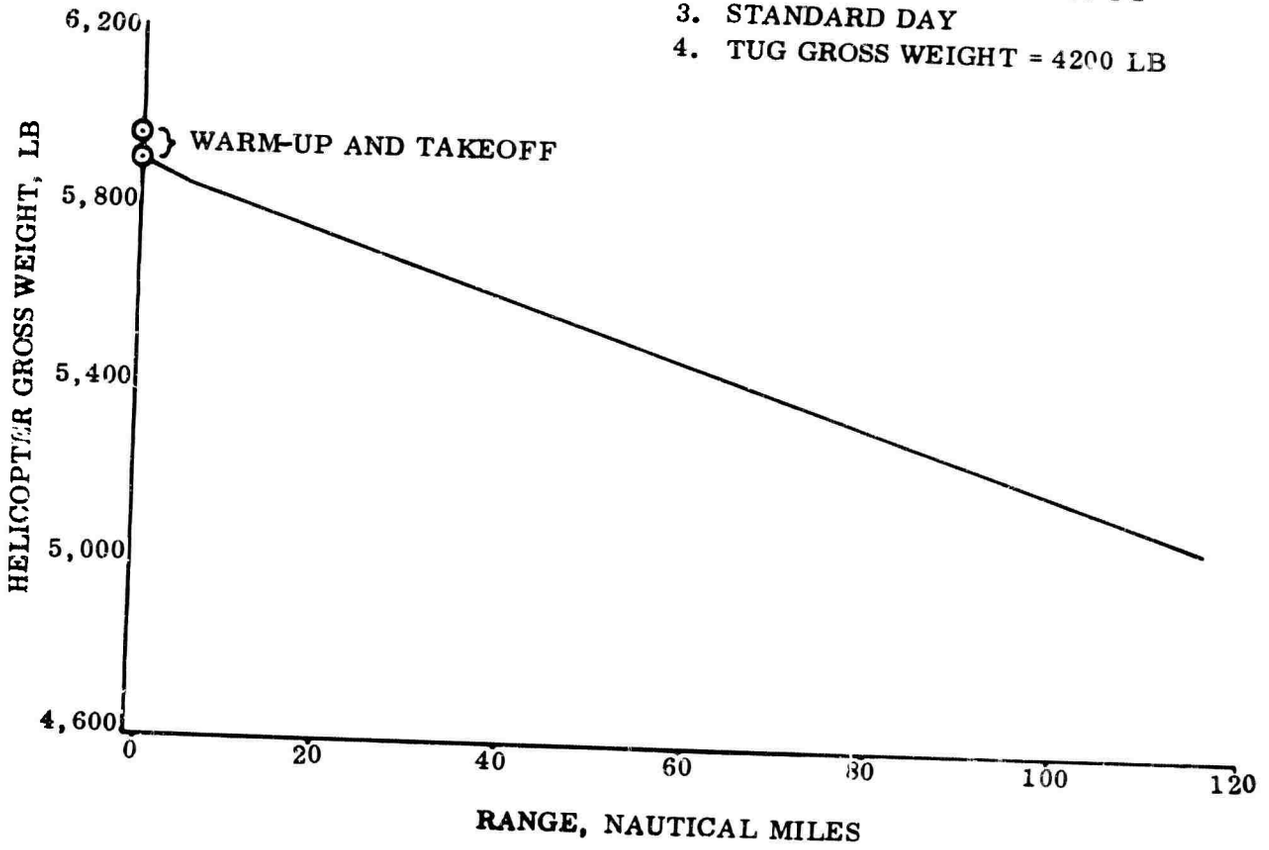

Figure 22. Mission Profile

warm-up and takeoff is the fuel required for 5 minutes at normal rated power at sea level. Fuel to climb was calculated at maximum normal rated power. Cruise speed is 67 knots. Ten percent of total usable fuel is allowed for landing and reserves. The maximum range for these conditions is shown to be 117 nautical miles.

Longitudinal Trim

Longitudinal trim analyses have been performed for both on-tow and 1-g gliding flight conditions.

Pitching moment coefficients for gliding flight were calculated as functions of angle of attack and wing-body incidence from the following equation for pitching moment coefficient about the glider's center of gravity.

$$C_{m_{cg}} = C_N\left(\frac{X_{ac}}{C_K}\right) + C_A\left(\frac{Z_{ac}}{C_K}\right) + C_{m_{o_w}} + C_{D_S}\left(\frac{\ell_s}{C_K}\right) + C_{m_{\alpha_B}}\alpha_B$$

The symbols in the following diagram are defined in the list of symbols.

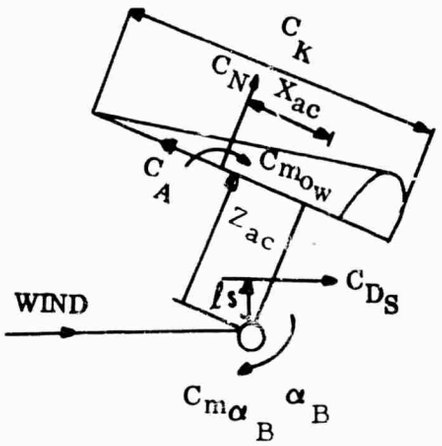

X_{ac} and Z_{ac} are functions of the wing incidence as shown in Figure 23. The wing normal and axial force coefficients C_N and C_A are plotted versus angle of attack in Figure 24.

Example $C_{m_{cg}}$ versus α curves are presented in Figure 25 for off-tow conditions. Trim angles of attack were read at the point of zero pitching moment to provide the curve of wing incidence versus trim angle of attack presented in Figure 26. From these data, trim airspeed was calculated and is plotted in Figure 27 versus wing angle of attack.

Curves of wing incidence versus trim airspeed are presented in Figure 28 for two gross weights at sea level standard day conditions. Values used for Figure 28 were obtained from Figures 26 and 27.

On-tow trim was calculated by means of a digital computer program which includes the effect of tow-cable tension on lift, drag and pitching moment. The equations of motion used and a description of the program may be found in Reference 5.

Data obtained from the computer include vertical separation between the glider and helicopter, tow-cable angles, cable tension and trim wing incidence. These data are presented in Figures 29 through 33.

Longitudinal Static Stability

Values of the off-tow longitudinal static margin $C_{m_{C_L}}$ were calculated using data from Figures 10 and 25. The variation of $C_{m_{C_L}}$ with C_L is shown in Figure 34 and indicates stable values throughout the C_L range.

Lateral-Directional Static Stability

The lateral-directional stability parameters C_{y_β}, C_{N_β} and C_{ℓ_β} for the wing alone are presented in Figure 35. These are based on Ryan and NASA wind-tunnel tests. Body, strut and tail contributions were calculated using standard estimating techniques.

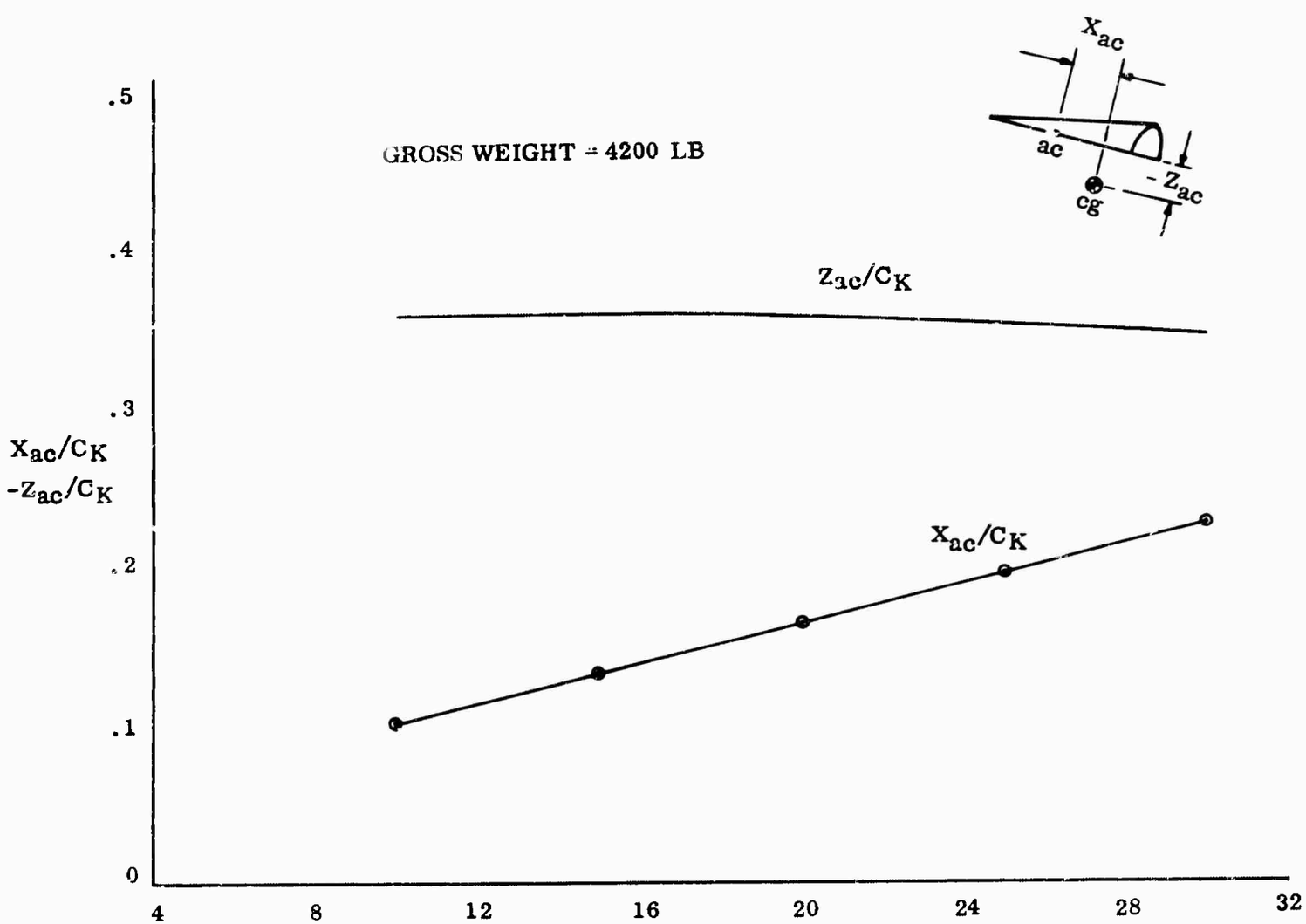

Figure 23. Center of Gravity Positions

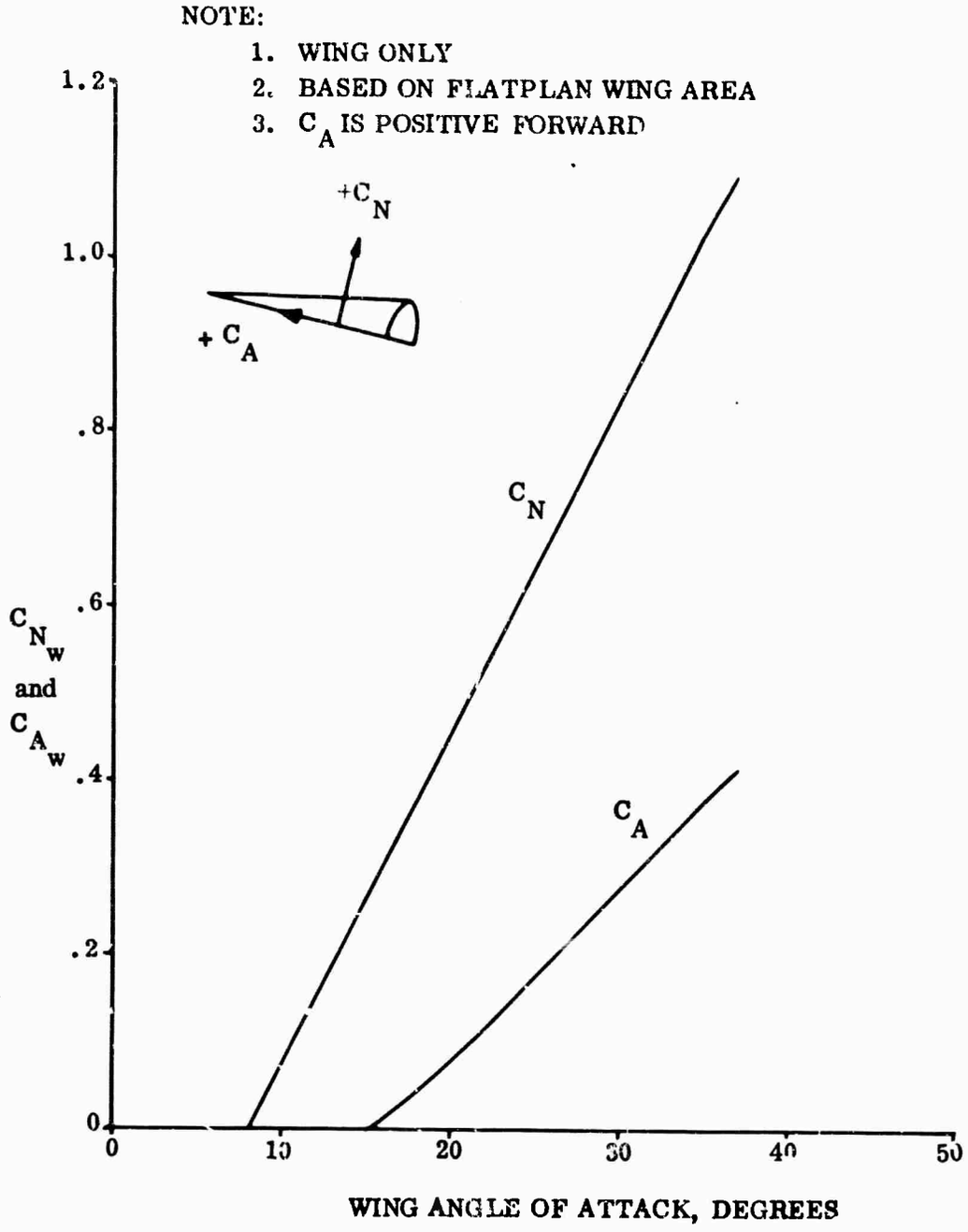

Figure 24. Flex Wing Normal and Axial Forces

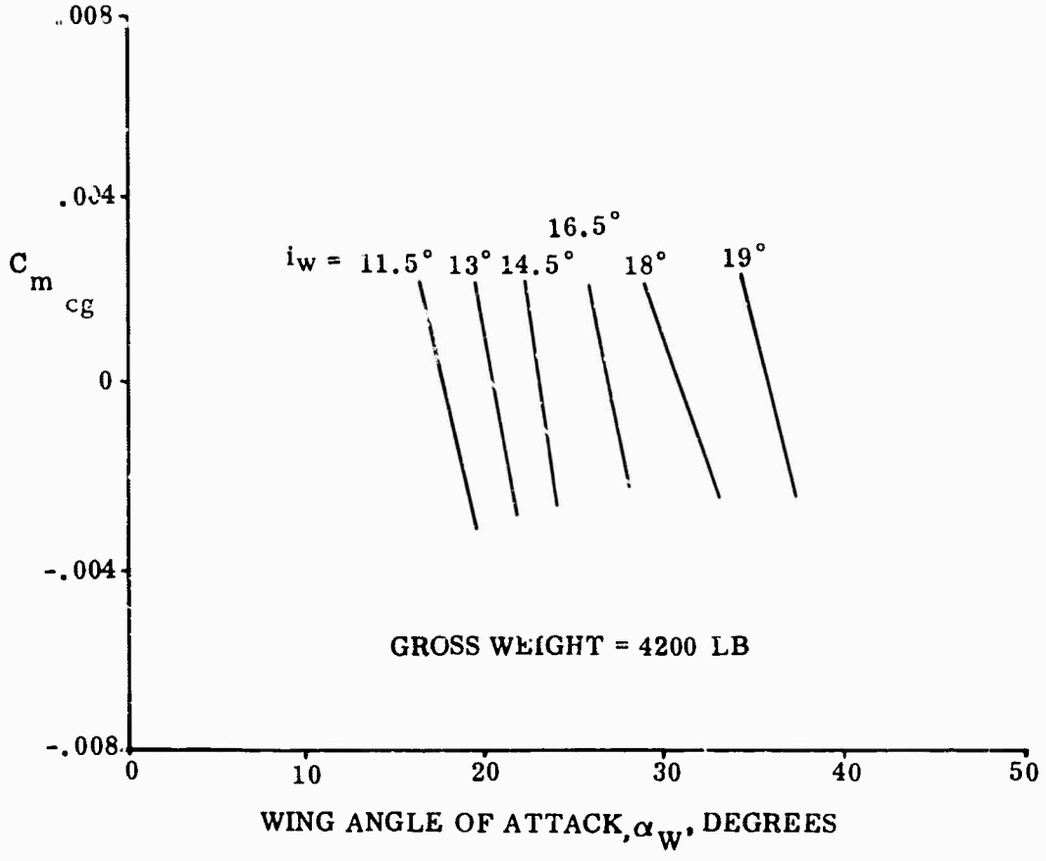

Figure 25. Pitching Moment Coefficient about Center of Gravity

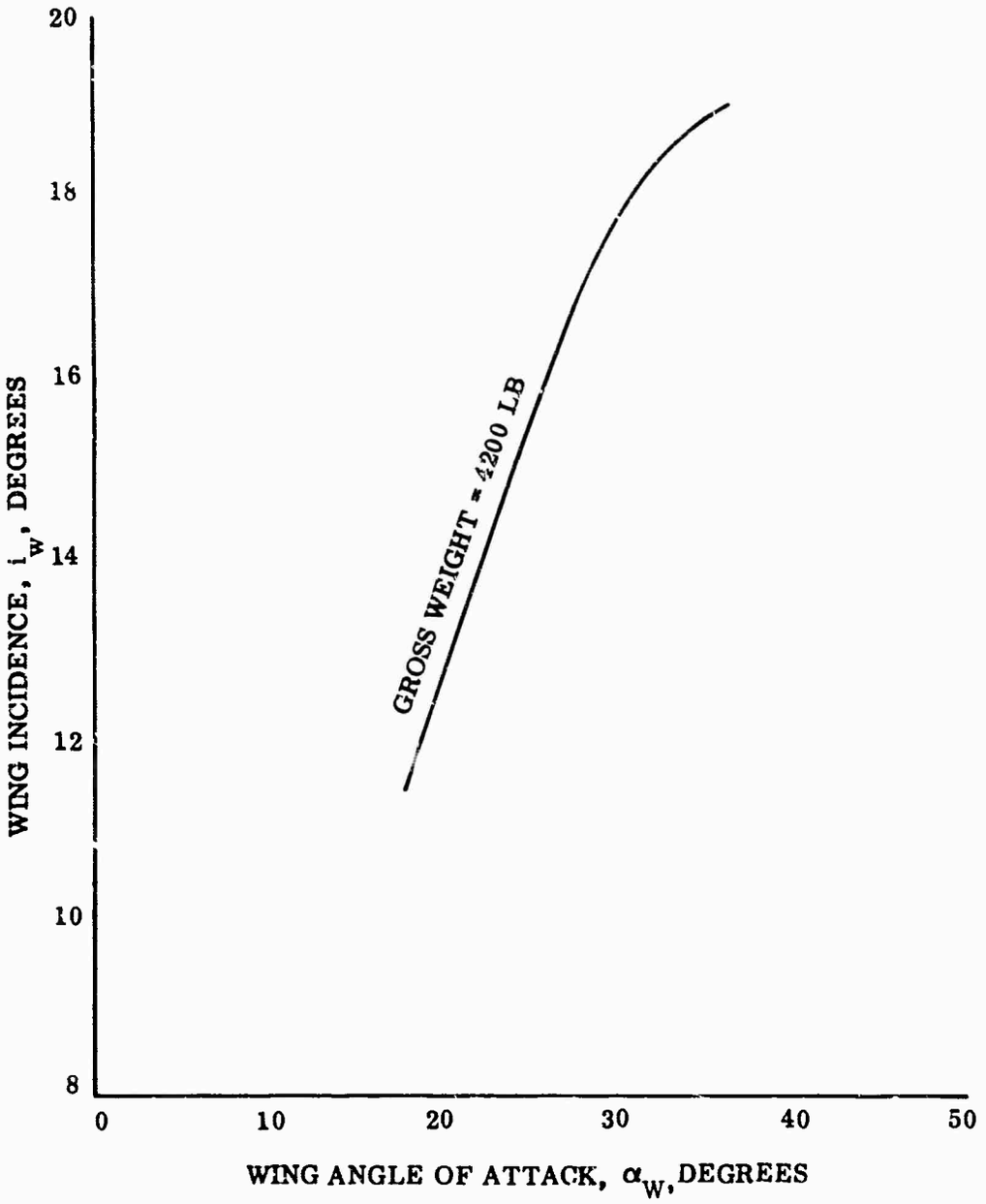

Figure 26. Wing Incidence Versus Wing Angle of Attack

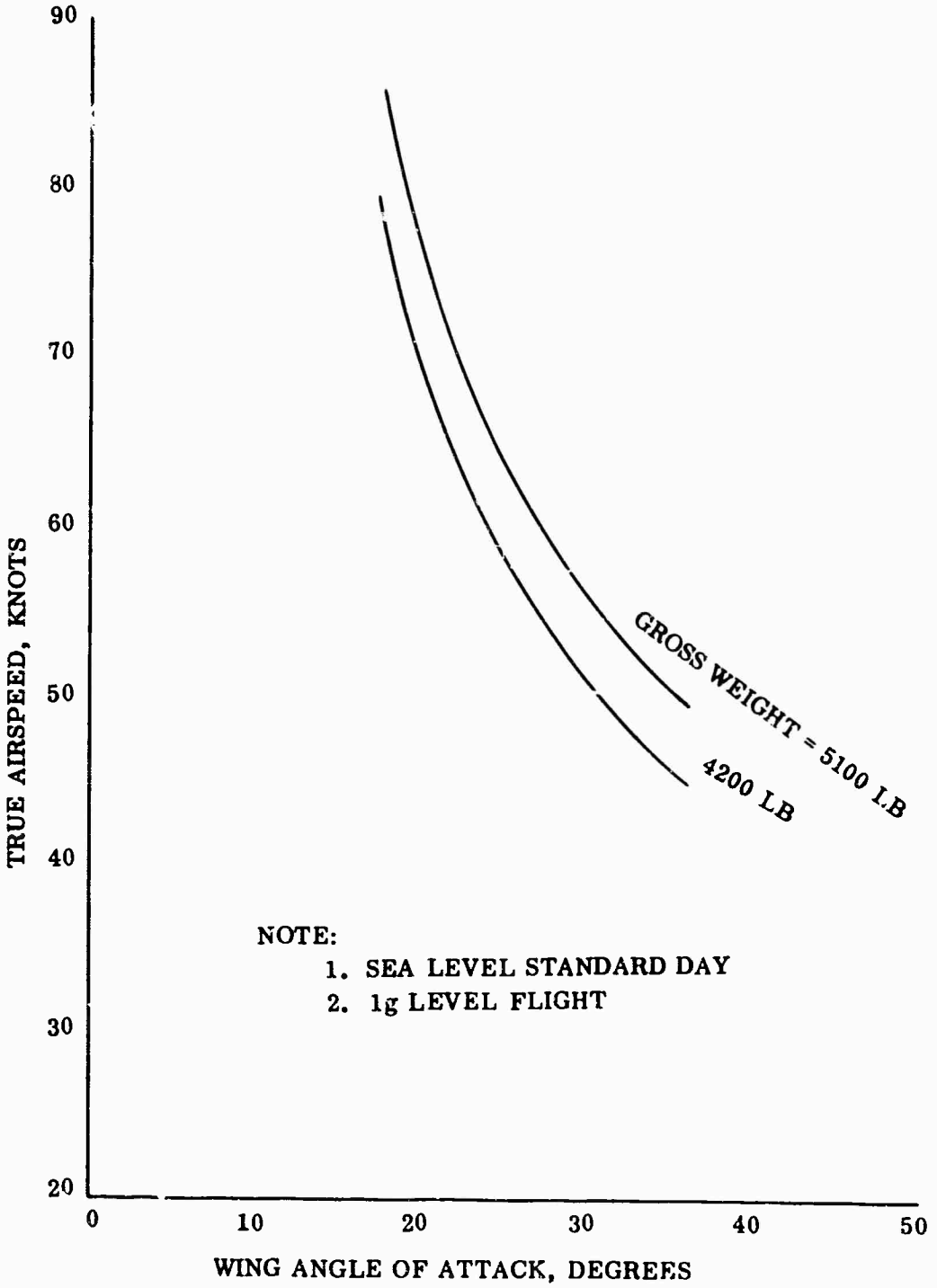

Figure 27. True Airspeed Versus Wing Angle of Attack for Trimmed Flight

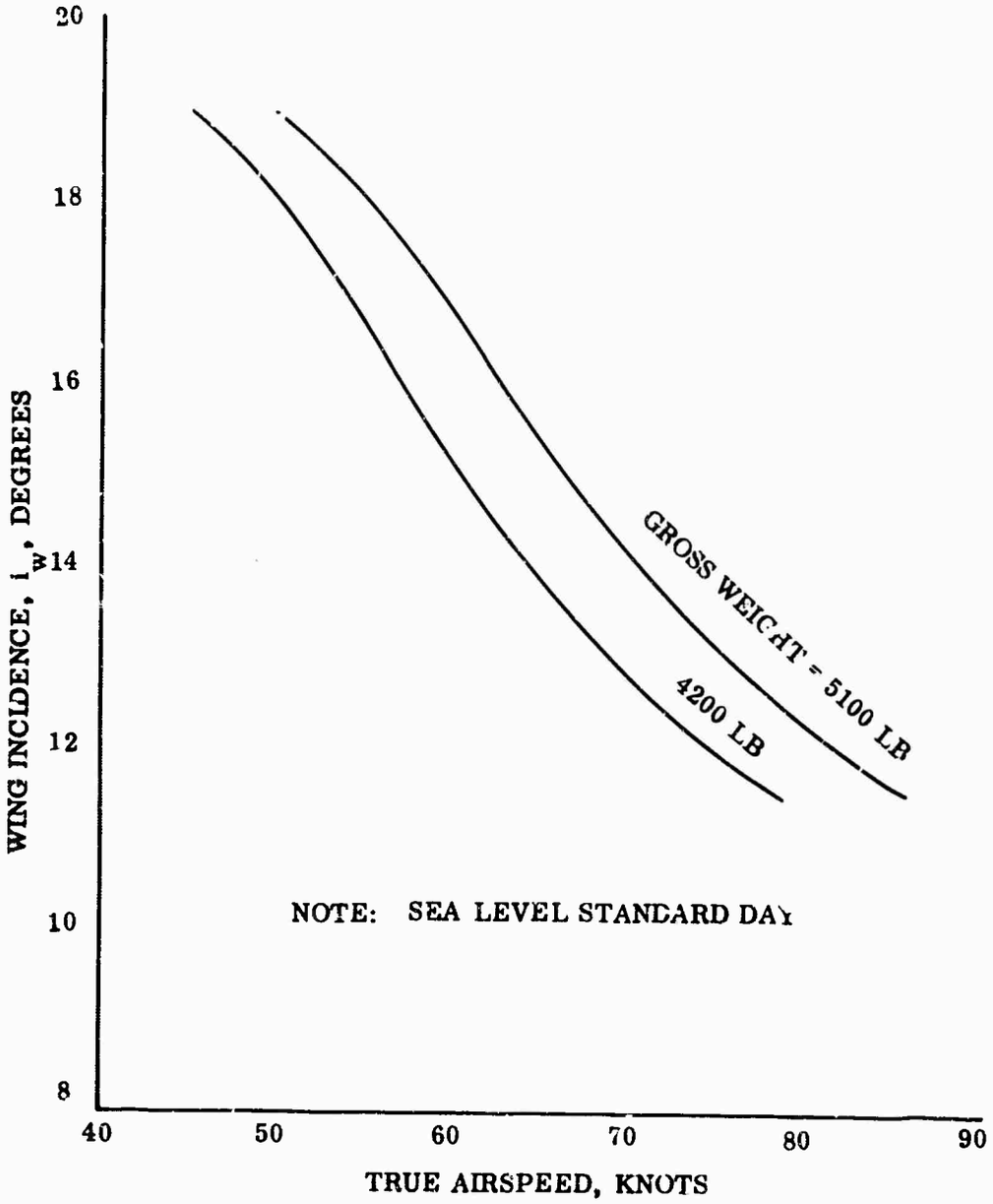

Figure 28. Wing Incidence Angles

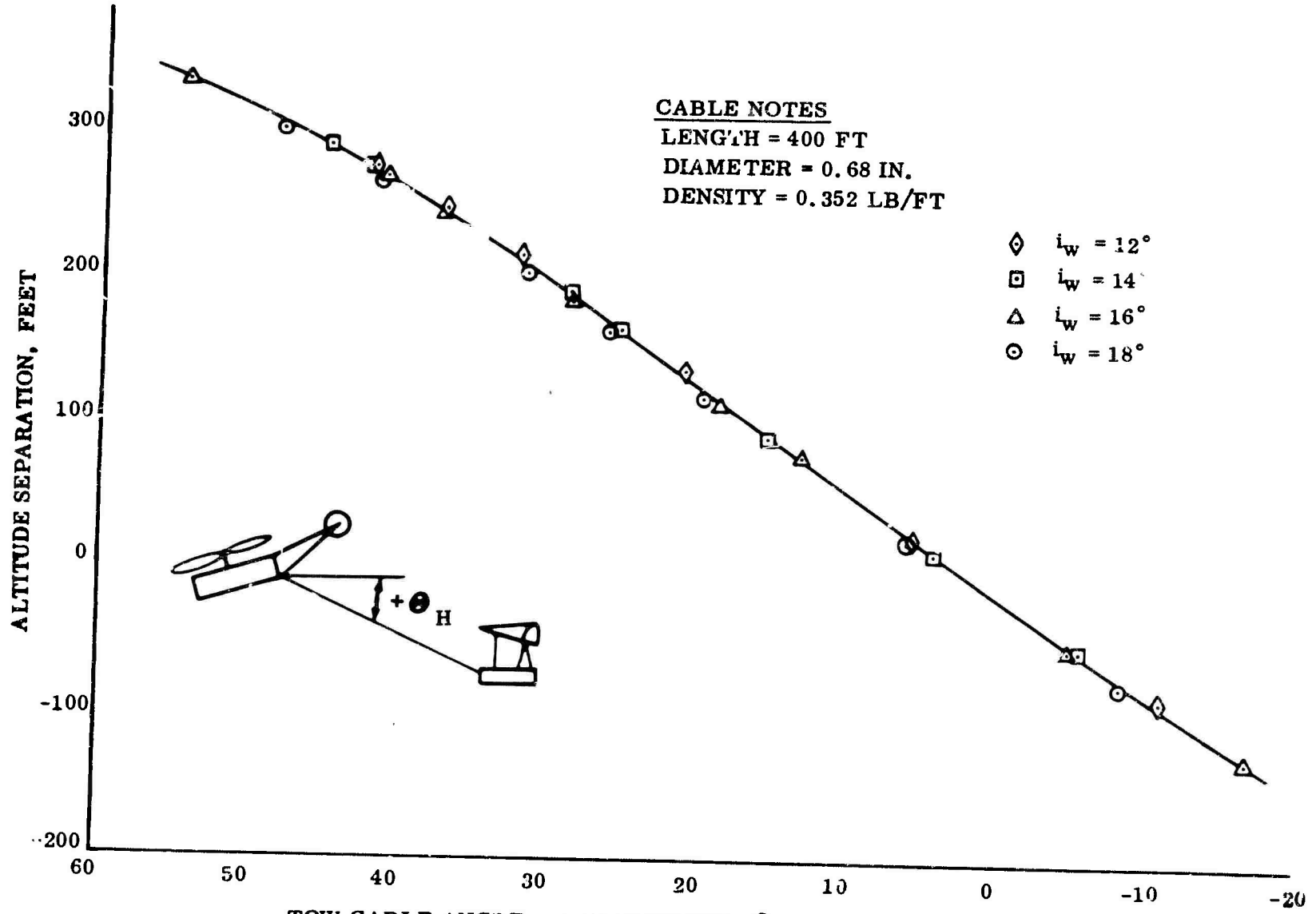

Figure 29. Vertical Separation Versus Tow Cable Angle

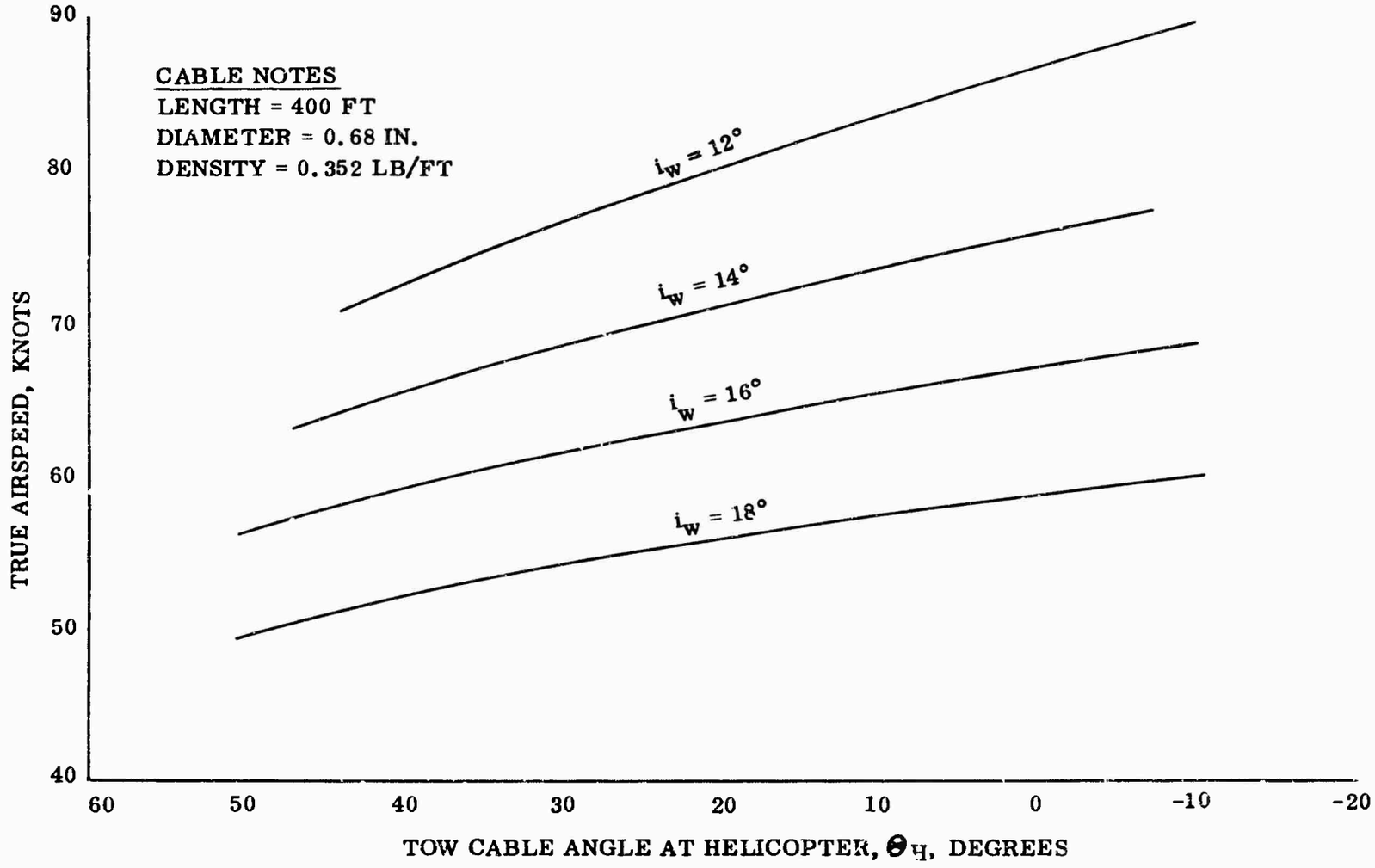

Figure 30. True Airspeed Versus Tow Cable Angle

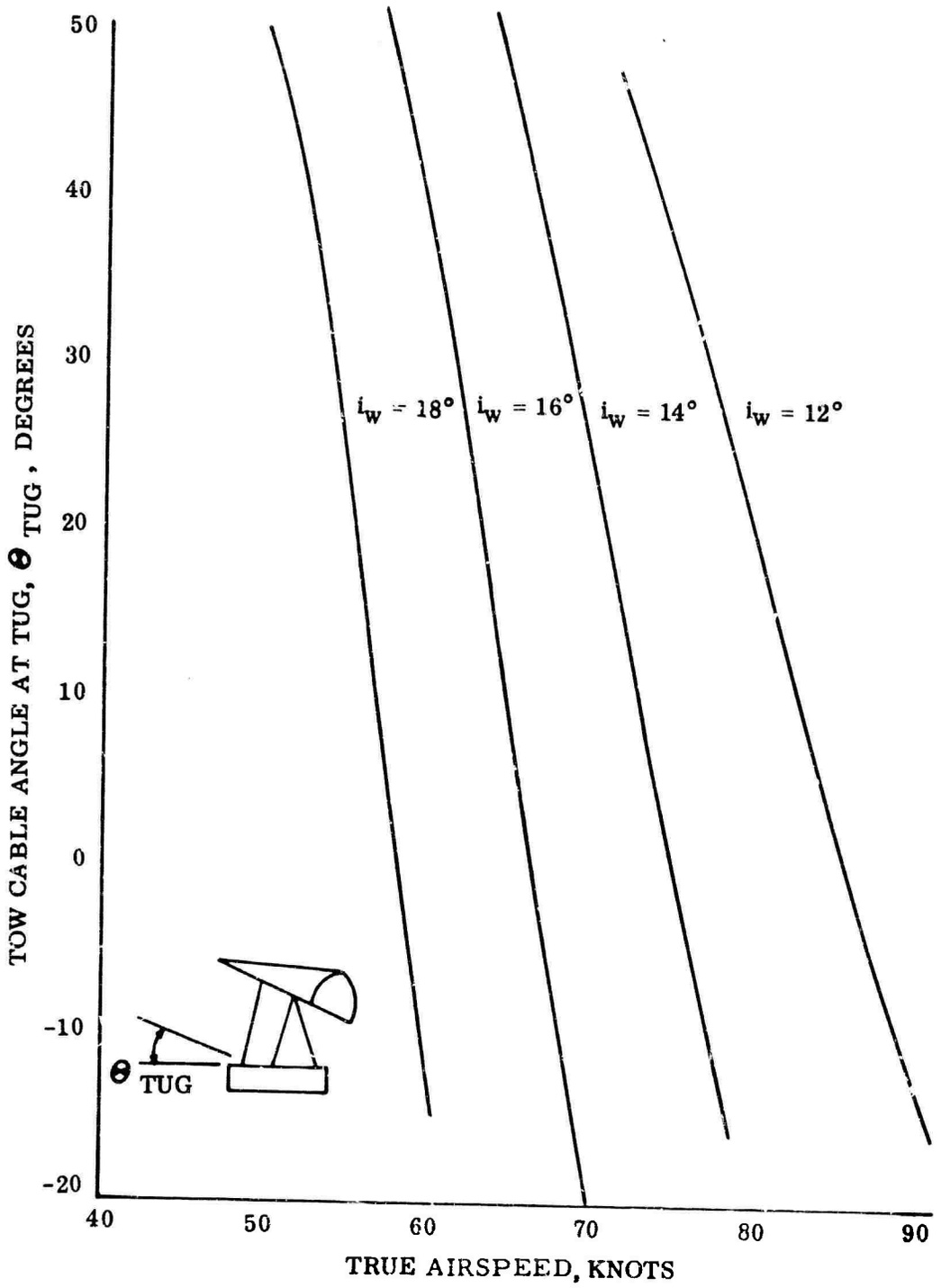

Figure 31. Tow Cable Angle at TUG

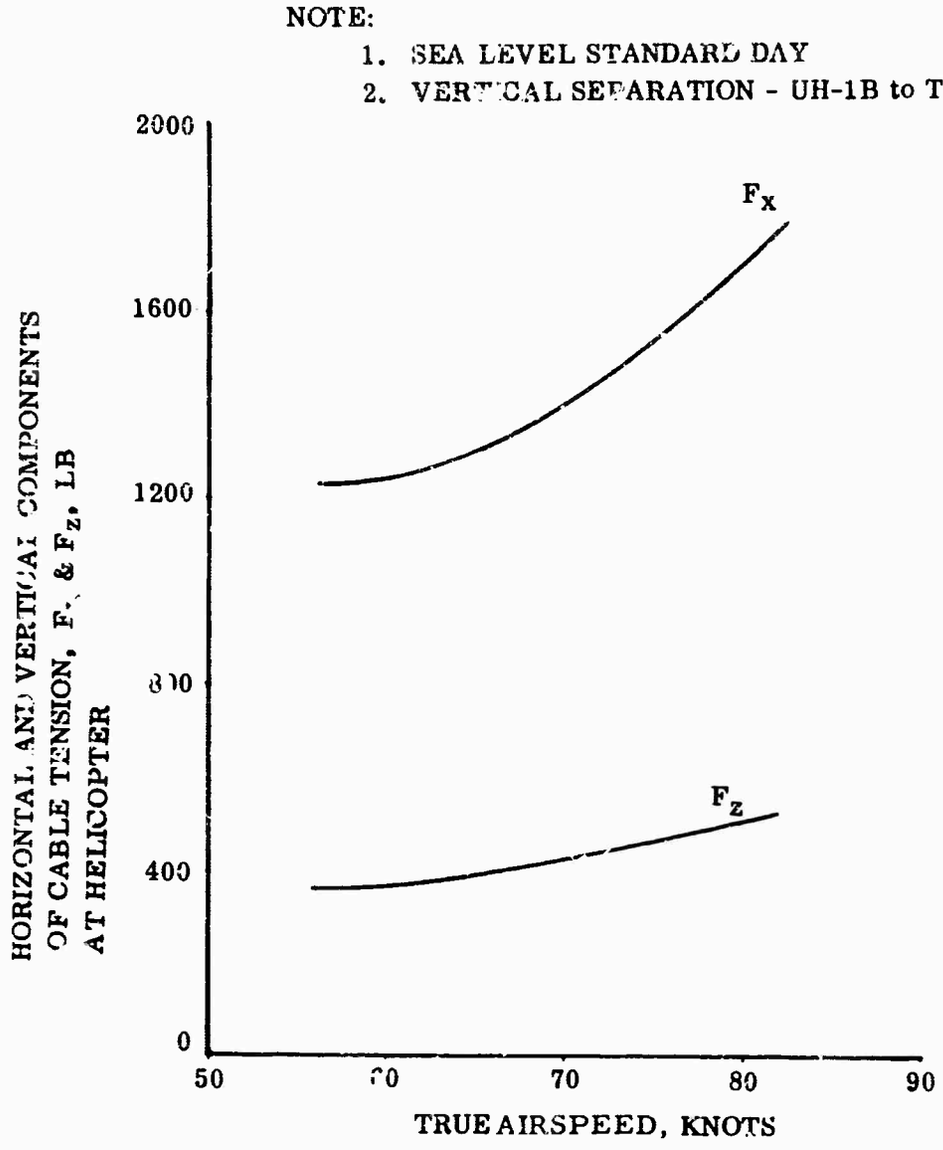

Figure 32. Tow Cable Tension

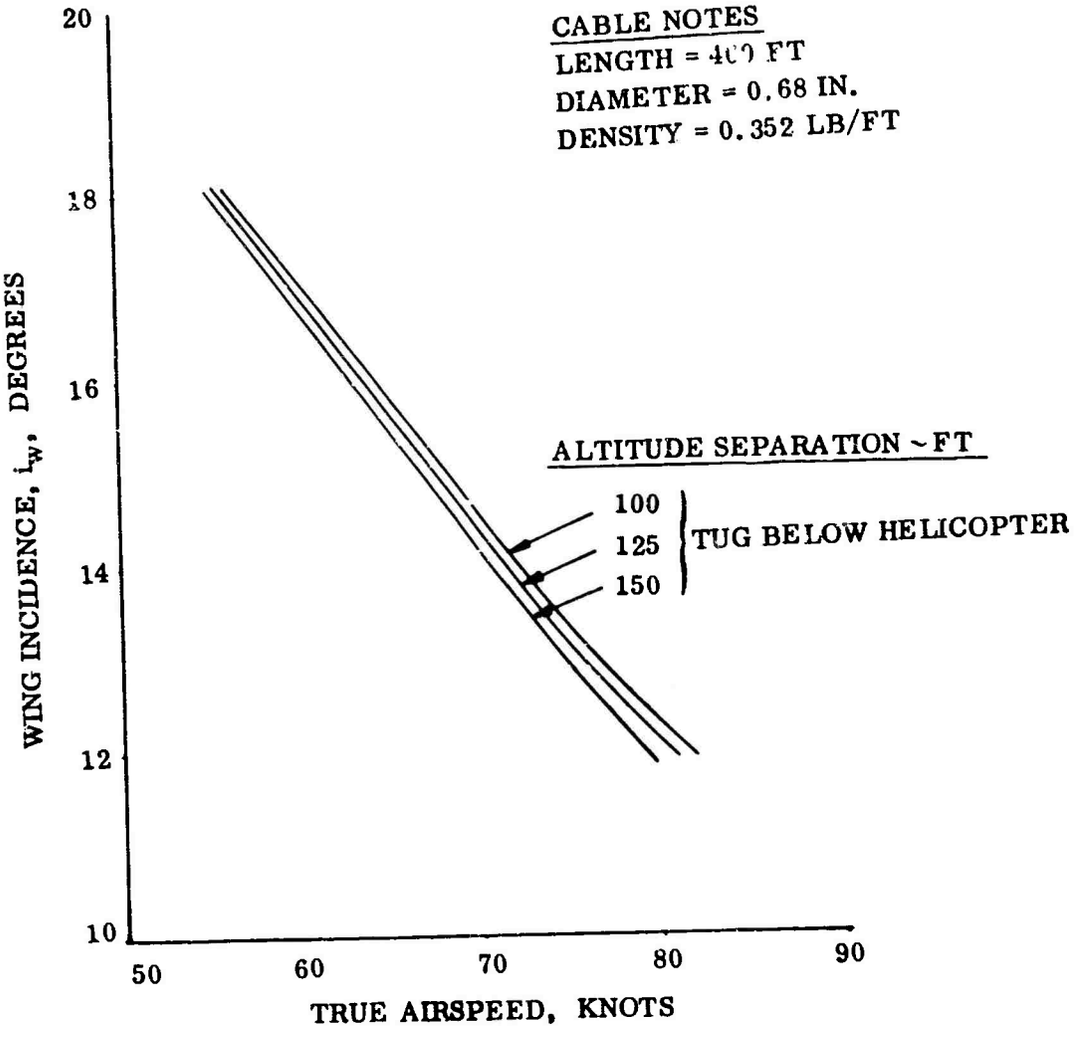

Figure 33. Wing Incidence Versus True Airspeed

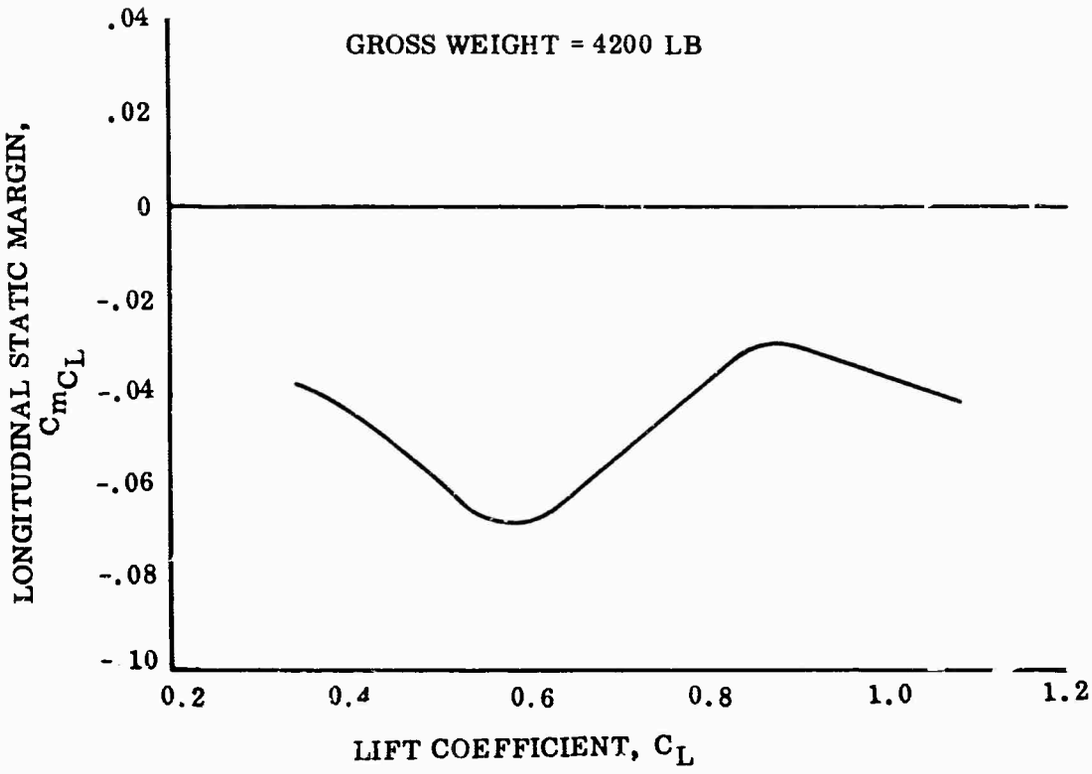

Figure 34. Longitudinal Static Margin

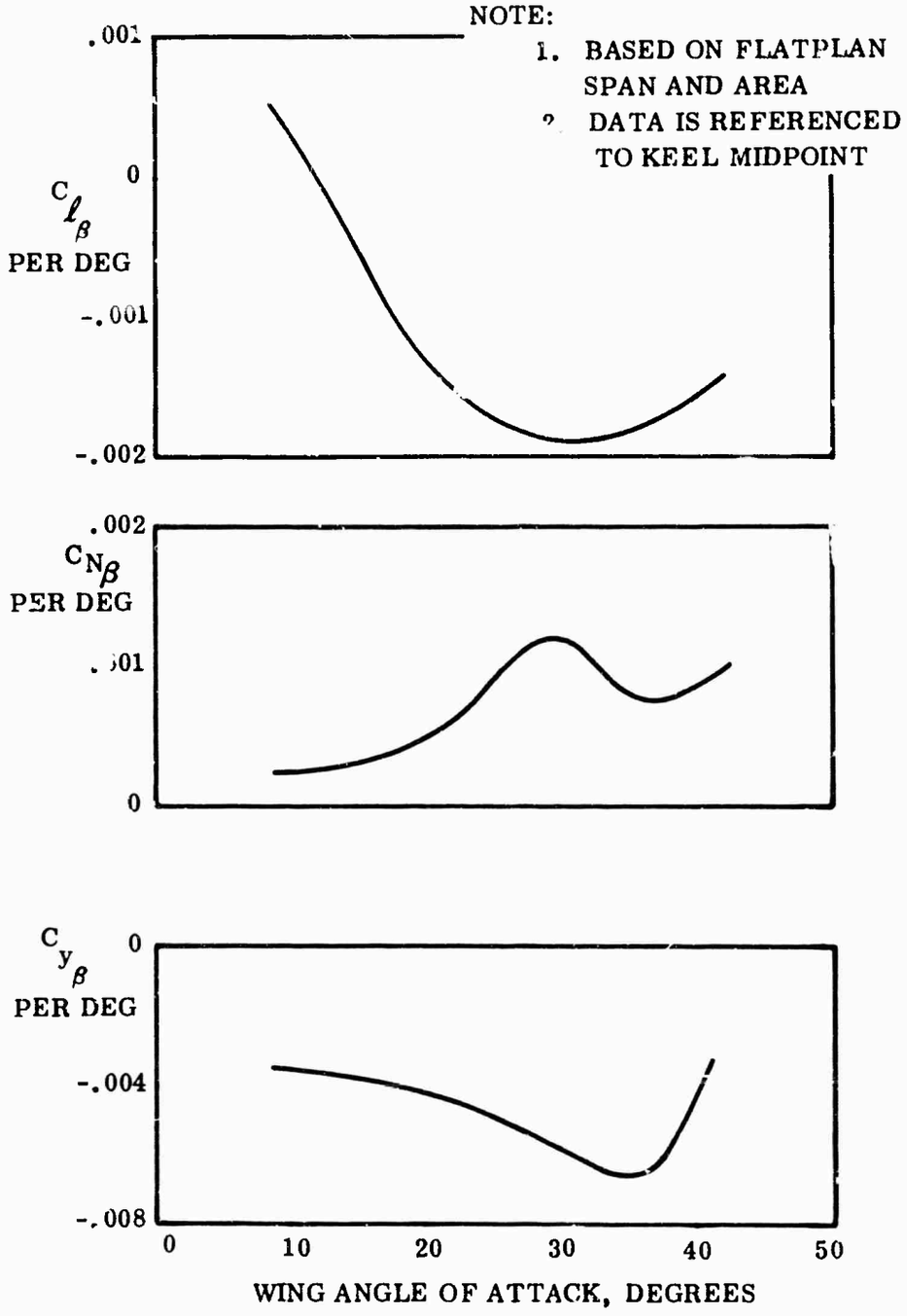

Figure 35. Lateral-Directional Static Stability of Wing Only

C_{y_β}, C_{N_β} and C_{ℓ_β} for the complete glider off-tow were obtained by transferring the wing terms to the aircraft center of gravity and by adding the body, strut and tail terms as follows:

$$C_{y_{\beta_{cg}}} = C_{y_{\beta_w}} + C_{y_{\beta_B}} + C_{y_{\beta_s}} + C_{y_{\beta_t}}$$

$$C_{N_{\beta_{cg}}} = C_{N_{\beta_w}} + C_{N_{\beta_B}} + C_{N_{\beta_s}} + C_{N_{\beta_t}}$$

where

$$C_{N_{\beta_w}} = C'_{N_{\beta_w}} + C_{y_{\beta_w}} \frac{(X_w)}{\beta}$$

$$C_{\ell_{\beta_{cg}}} = C_{\ell_{\beta_w}} + C_{\ell_{\beta_B}} + C_{\ell_{\beta_s}} + C_{\ell_{\beta_t}}$$

where

$$C_{\ell_{\beta_w}} = C'_{\ell_{\beta_w}} + C_{y_{\beta_w}} \frac{(Z_w)}{\beta}$$

Subscripts w, B, s and t denote wing, body, struts and tail respectively. The prime subscript refers to derivative to the wing mid-keel point. All terms are in the stability axes system. X_w and Z_w are defined in the following sketch:

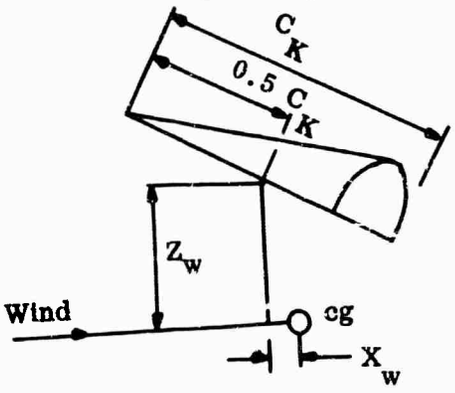

X_w is positive for the mid-keel point forward of center of gravity; Z_w is negative for the wing above center of gravity.

The estimated lateral-directional static stability for the complete glider off-tow is presented in Figure 36, which shows stable values of C_{ℓ_β} and C_{N_β} throughout the usable range of wing angle of attack.

Longitudinal Dynamic Stability

Longitudinal dynamic stability of the TUG in free flight was calculated using an IBM-704 computer to solve the stick-fixed small perturbation equations. The equations used in the program are those developed in Reference 3.

Time and cycles to damp to half amplitude in free flight are shown in Figure 37, which indicates stable longitudinal dynamics throughout the speed range.

Lateral-Directional Dynamic Stability

The methods used to estimate the lateral-directional dynamic stability off-tow were similar to those used for the longitudinal dynamics, i.e., small perturbation equations solved using an IBM-704 computer. The stick-fixed lateral-directional perturbation equations are based on those of Reference 3.

Estimated data are presented in Figure 38 as the inverse of the cycles to damp to half amplitude of the Dutch roll and the inverse of the time to damp to half amplitude of the spiral and roll modes.

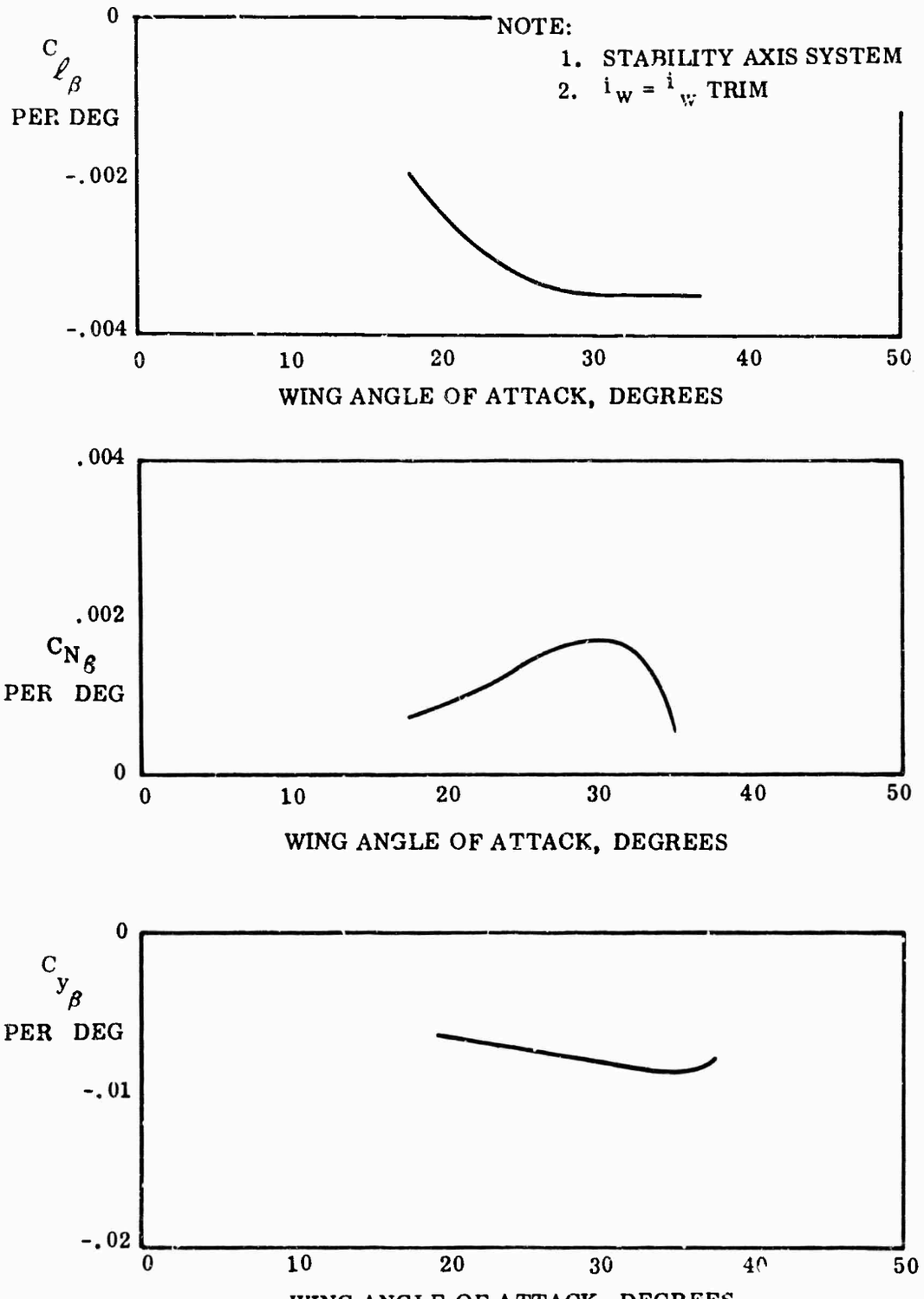

Figure 36. Lateral-Directional Static Stability of Complete Aircraft

NOTE:

1. GROSS WEIGHT = 4200 LB
2. SEA LEVEL STANDARD DAY
3. ——— PHUGOID
   ------ SHORT PERIOD

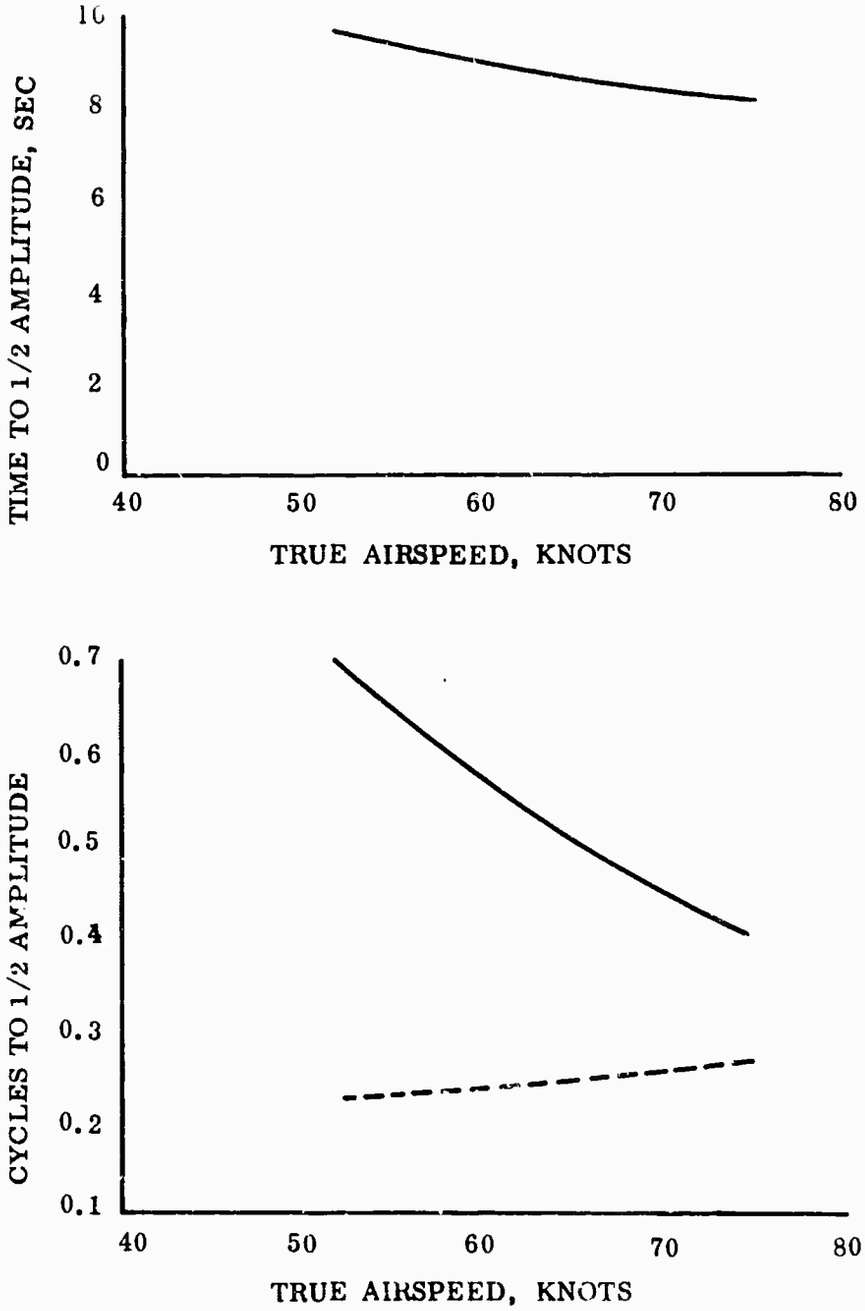

Figure 37. Longitudinal Dynamic Stability

NOTE:

1. GROSS WEIGHT = 4200 LB
2. SEA LEVEL STANDARD DAY
3. 1/TIME AND 1/CYCLE TO 1/2 AMPLITUDE

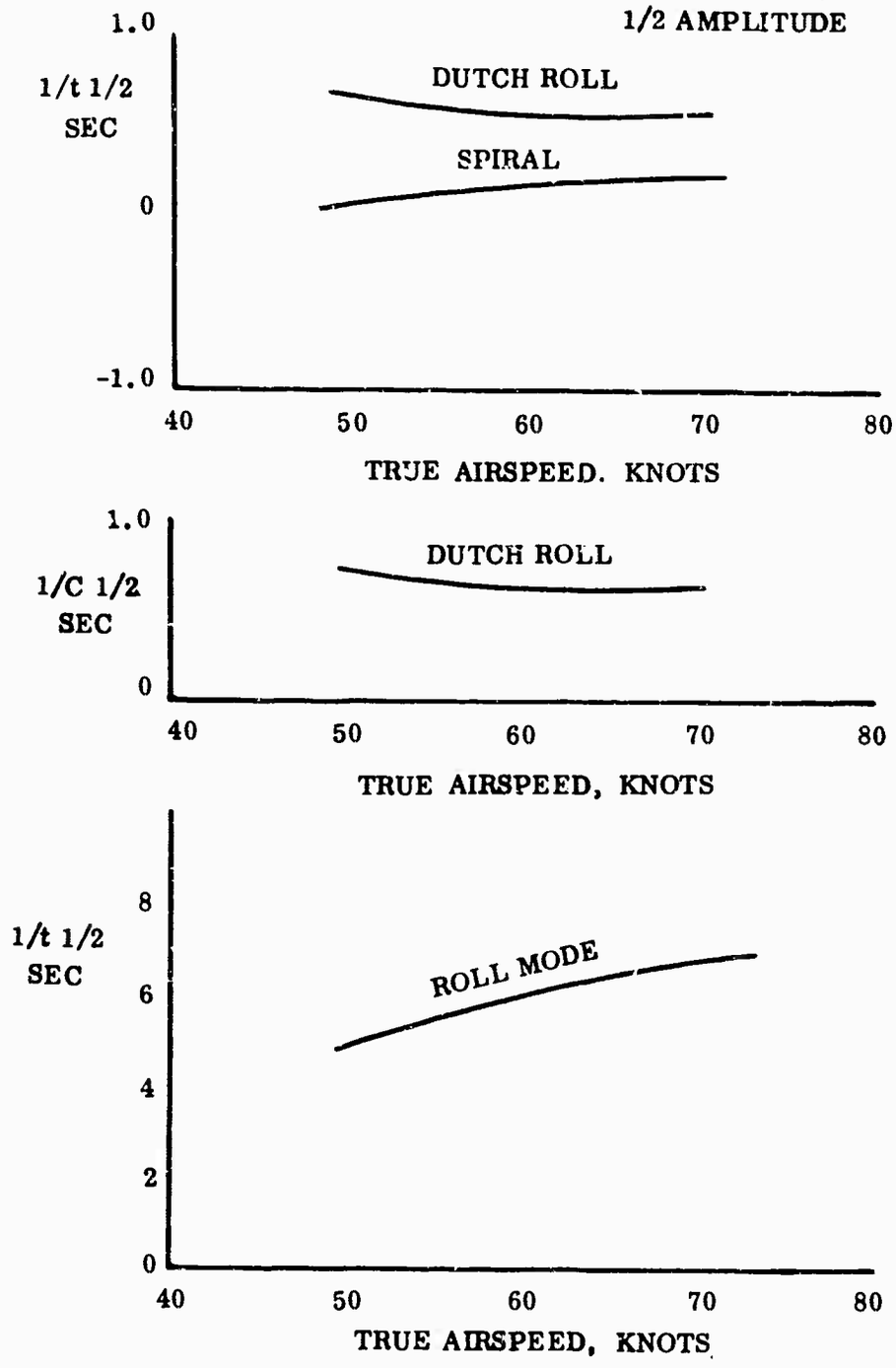

Figure 38. Lateral Dynamic Stability

STRUCTURAL ANALYSIS

GENERAL

The operational Towed Universal Glider has been designed with a philosophy of simplicity and low cost as the most important criterion. This basic design philosophy has necessitated lesser structural efficiency with an accompanying weight penalty imposed on the vehicle. Many design details have been influenced by the results of the Air Cargo Glider System designed, fabricated, and flight-tested by Ryan under Contracts DA 44-177-AMC-868(T) and DA 44-177-AMC-122(T).

DESIGN CRITERIA

The design criteria established for the Towed Universal Glider are based primarily on data obtained from preceding air cargo glider programs. The criteria upon which the original design was predicated have been modified to the extent that data from the TUG flight test program have been incorporated. Loading conditions considered originally which have proven to be insignificant based on flight tests have been deleted. Other conditions which have proved to be significant have been included in the criteria.

GENERAL DATA

1. MATERIAL REFERENCES FOR ALLOWABLE

   a. Metals MIL-HDBK-5

   b. Plastics MIL-HDBK-17

   c. Wood ANC-18

2. DESIGN WEIGHTS

   a. Minimum design gross weight = 1200 lb

   b. Basic design gross weight

      Weight empty = 1200 lb

      Useful load = 4000 lb

   c. Maximum design gross weight = 5200 lb

3. DESIGN ALTITUDE = SEA LEVEL

4. WING SPECIFICATIONS

a. Area S = 554.4 ft^2 (flatplan)

b. Keel length = ℓ_k = 28 ft

c. Wing loading = W/S = 9.39 lb/ft^2

d. Leading edge sweepback = 50° flying
= 45° flatplan

e. Span b = 36 ft

f. Average chord = 14 ft

5. GLIDER VELOCITIES

a. Maximum level speed (S.L.) = 70 knots, gross weight = 5200 lb

b. Stall Speed = 46.8 knots, gross weight = 5200 lb

c. Speed for maximum gust intensity = 64.4 knots, gross weight = 5200 lb

d. Limit Speed, V_L = 105 knots

6. LANDING CONDITIONS

a. Load factors (ultimate)

N_z = 6 G vertical

N_y = 2 G lateral

N_z = 3 G forward

b. Design rate of sink = 10 feet per second

(Assume wing lift = 2/3 gross weight at landing impact)

7. FLOOR DESIGN CRITERIA

   a. Cargo floor to be designed for 250 lb/ft^2 acting locally.

8. GROUND HANDLING

   a. Apply load factor of 1.5 G in all directions.

9. FLIGHT CONDITIONS

   a. Maximum maneuver load factor N_z = 2.5 limit, at 5200 lb (see Figure 39).

   b. For gust load factors, see Figure 39.

LOADS ANALYSIS

Wing pressure data from NACA TN D-983 (Bibliography, Reference 6) have been analyzed to determine the wing airload distribution. The reduced data yielded the load distributions on the wing keel and leading edges for symmetrical flight conditions. The pressure data are presented as plots of pressure coefficient C_p against fraction of local chord projected to the plane of the leading edge and keel at four spanwise locations. A further discussion of the models employed and the data is available in the reference.

The data chosen for analysis in this report are from the model with a 48.6-degree leading-edge sweep. It is felt that this wing, of the three tested, most nearly approximates the wing on the Towed Universal Glider system.

Certain aspects of the model which differ from the actual wing should be pointed out. The pressure data at the lower angles of attack on the rigid model result in negative lift values on the wing. These values, at the lower angle of attack, are somewhat academic and not applicable to flexible wings since the assumed conical shape will not result with negative lift on the membrane. For that matter, the assumed conical shape probably occurs on a flexible wing only at angles of attack near 90 degrees. It is felt, however, that the data for angles of attack larger than about 15 degrees will be fairly representative of the pressures on a flexible wing.

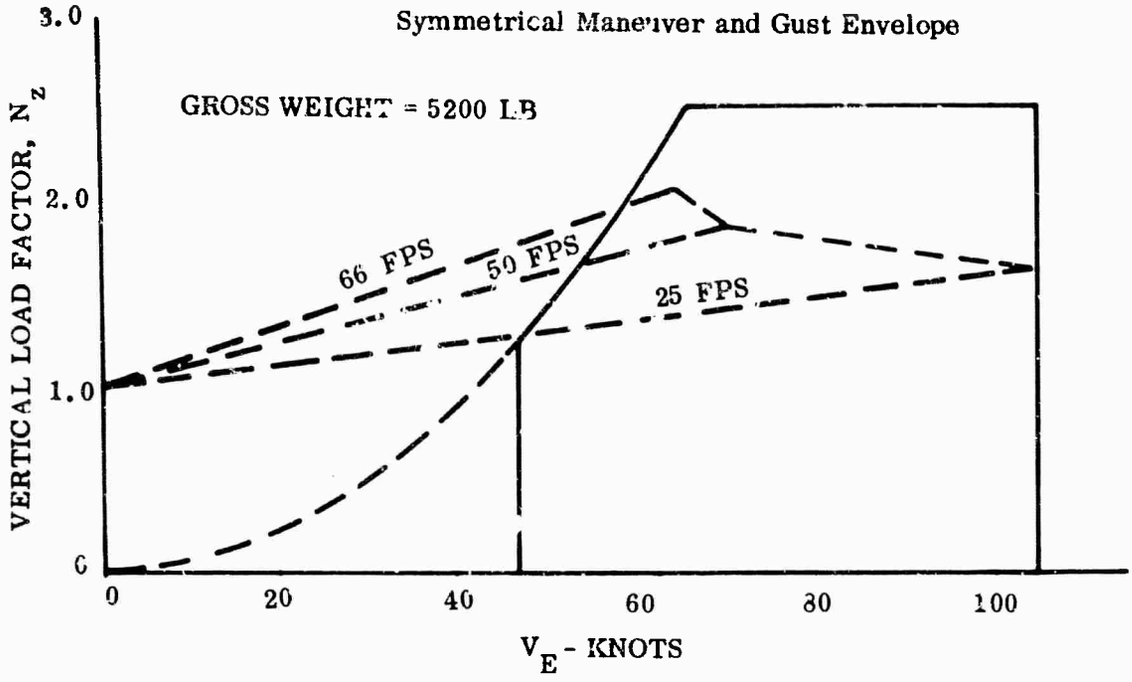

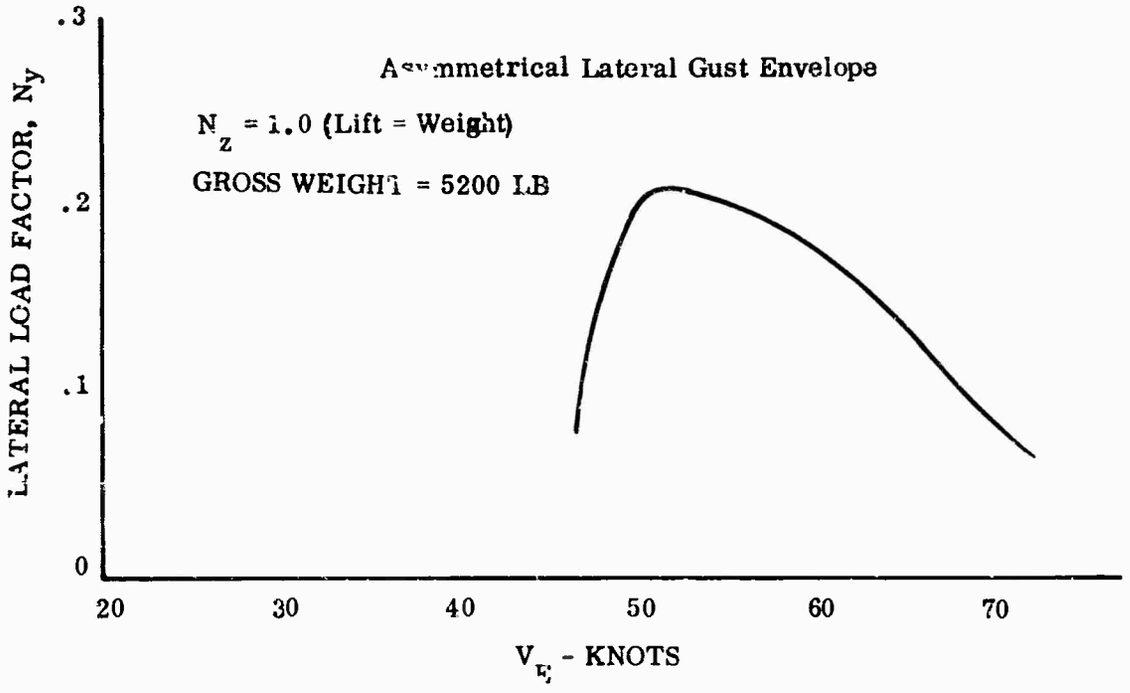

Figure 39. Flight Condition Load Factors

The chordwise pressure data of the reference between 20 and 50 degrees angle of attack have been analyzed. Integration of the chordwise plots yielded points for spanwise loading curves. Representative curves are shown in Figure 40 along with theoretical span loading curves. Integration of the spanwise loading curves from pressure data determined the wing normal force coefficients versus angle of attack.

$$C_N = 2\int_0^1 \frac{c C_n}{(c_{root})} \, d\eta \text{, where } \eta = 2\,y/b$$

Curves of wing normal force coefficient C_N as a function of angle of attack are shown in Figure 41. The curve of force data is from unpublished NASA wind-tunnel data on a flexible wing with geometry approximating the wing on the towed-glider vehicle. Good agreement is shown between the pressure and the force data except at the angles of attack "beyond the stall."

To evaluate the loading on the keel and leading edges, three representative angles of attack were chosen for further analysis. Cross plots of the chordwise data were made at constant percent chord stations (radials from the wing tip). A sufficient number of these cross plots were made to define a three dimensional picture of the loading on a wing semispan. The primary area of uncertainty in this process was due to lack of pressure data at the root chord. A cross plot of these "cross plots" was then made, which resulted in the curves of Figures 42, 43, and 44. These curves essentially give a pictorial representation of the airload distribution on the wing semispan.

The curves of Figures 42, 43, and 44 were integrated to determine their area and centroid. The proportion of airload represented by each curve that is carried by the leading edge was considered to be inversely proportional to the distance between the leading edge and the centroid of each curve. Use of this reasoning resulted in the curves of Figures 45 and 46, which show the distribution of membrane vertical load on the leading edge and keel for angles of attack of 20, 30, and 40 degrees. The dashed curves show estimated load distributions for intermediate angles of attack.

A somewhat further analysis of the data produced the curves of Figure 47 which show longitudinal and lateral center of pressure and the percentage of membrane load on the keel, all as a function of angle of attack. The curves of longitudinal pressure coefficient location show good agreement between the pressure data and the previously mentioned unpublished NACA force data.

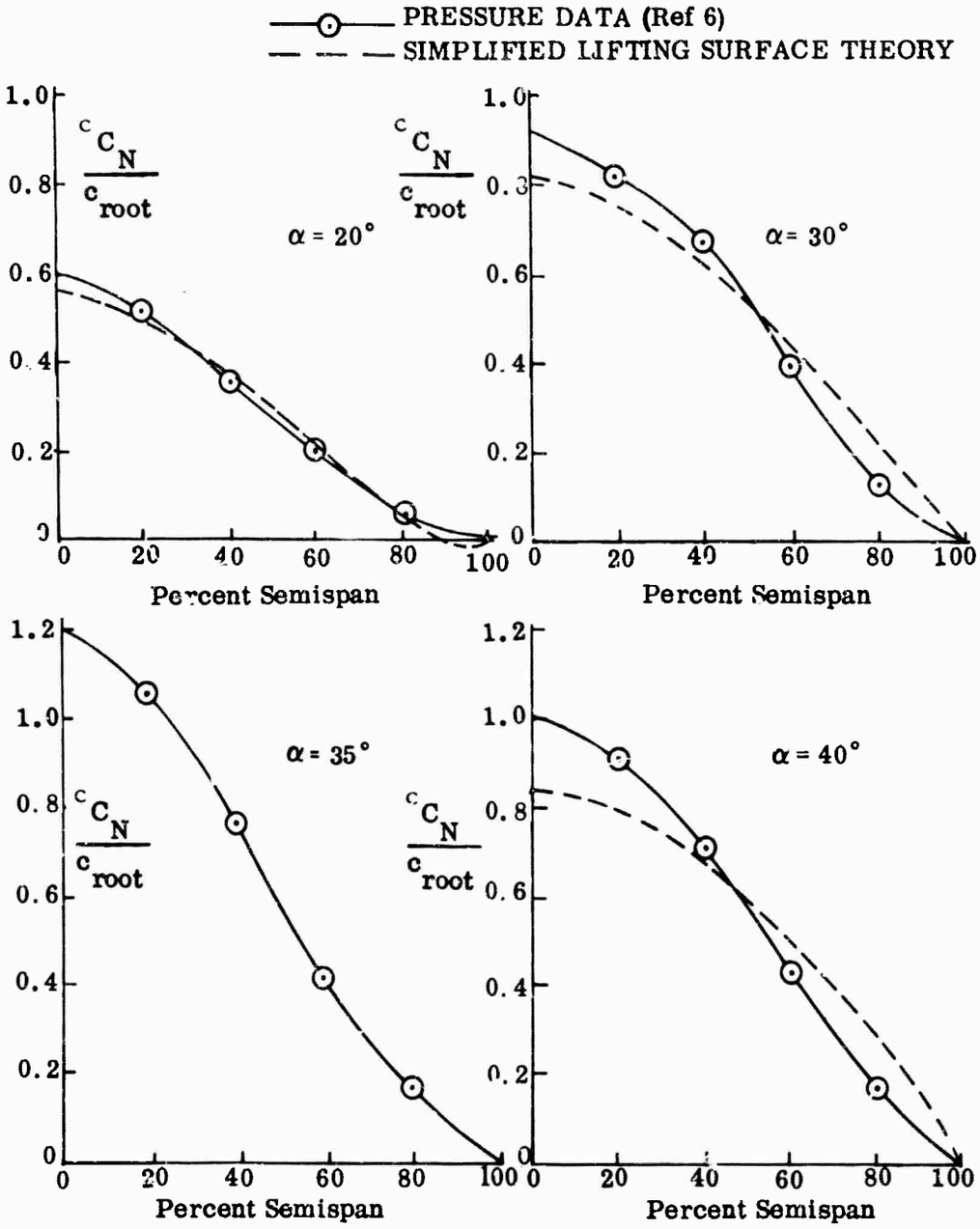

Figure 40. Wing Spanwise Load Distribution

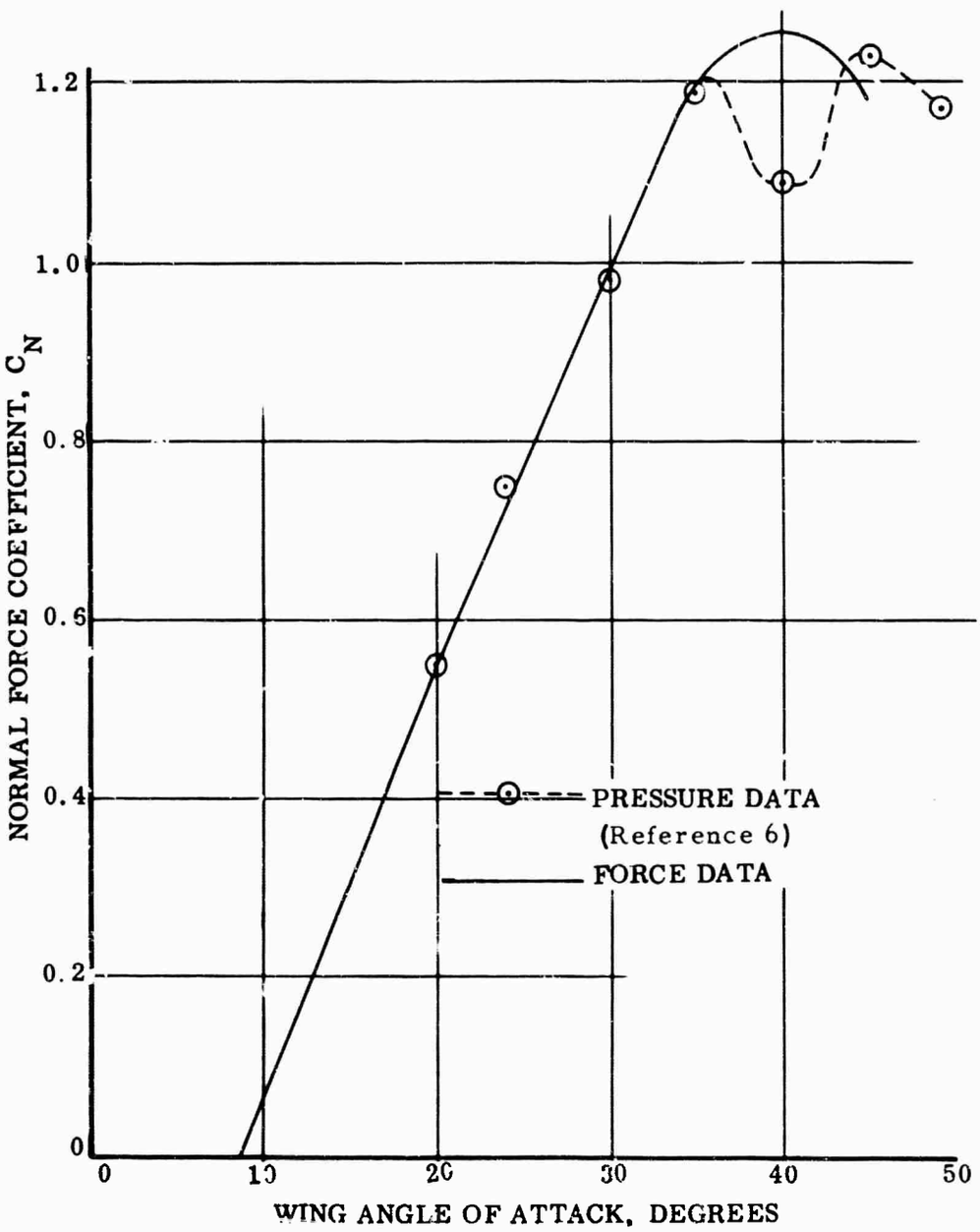

Figure 41. Comparison of Wing-Alone Aerodynamic Characteristics, Force and Pressure Data

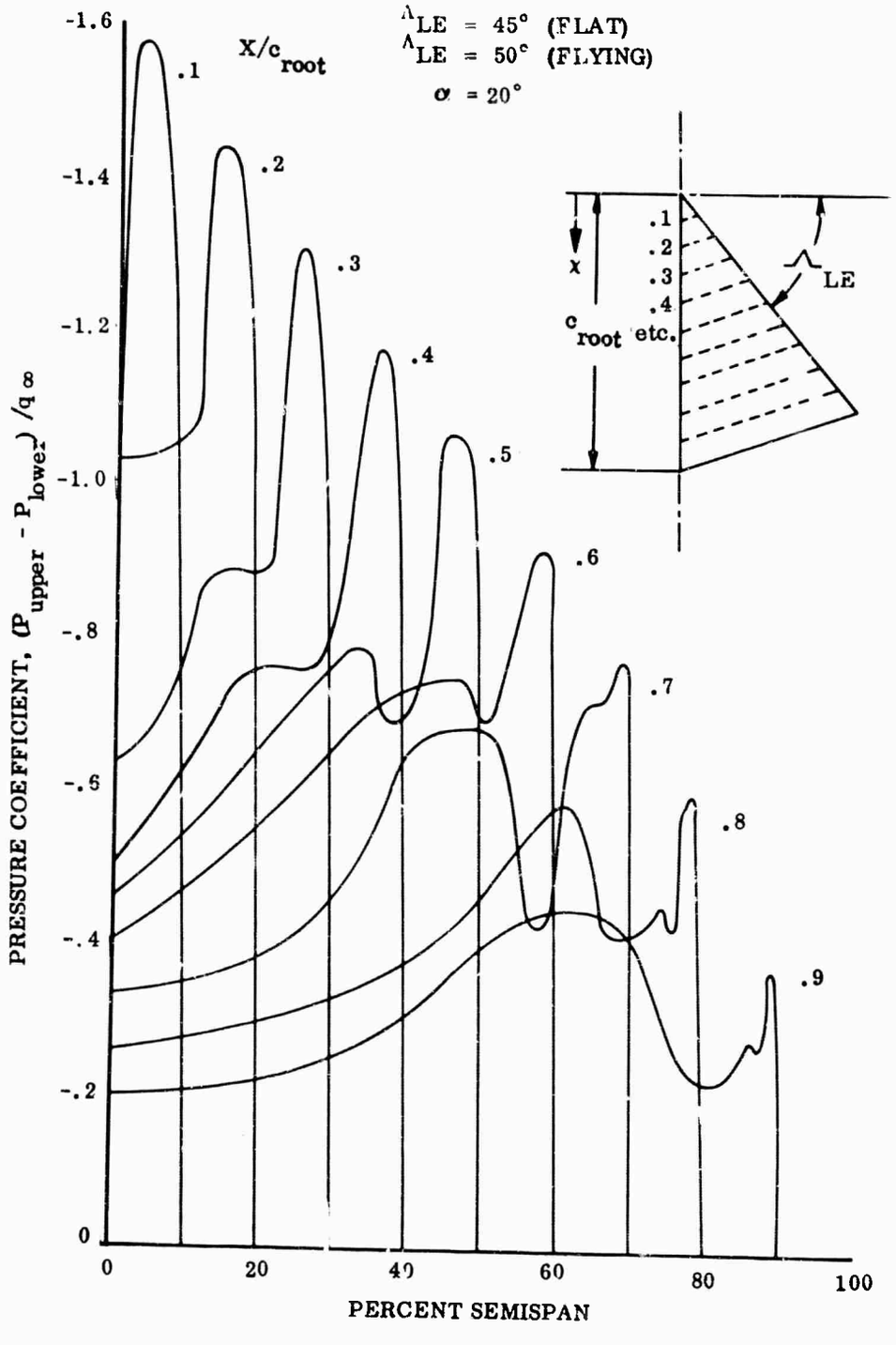

Figure 42. Wing Airload Distribution, 20-Degree Angle of Attack

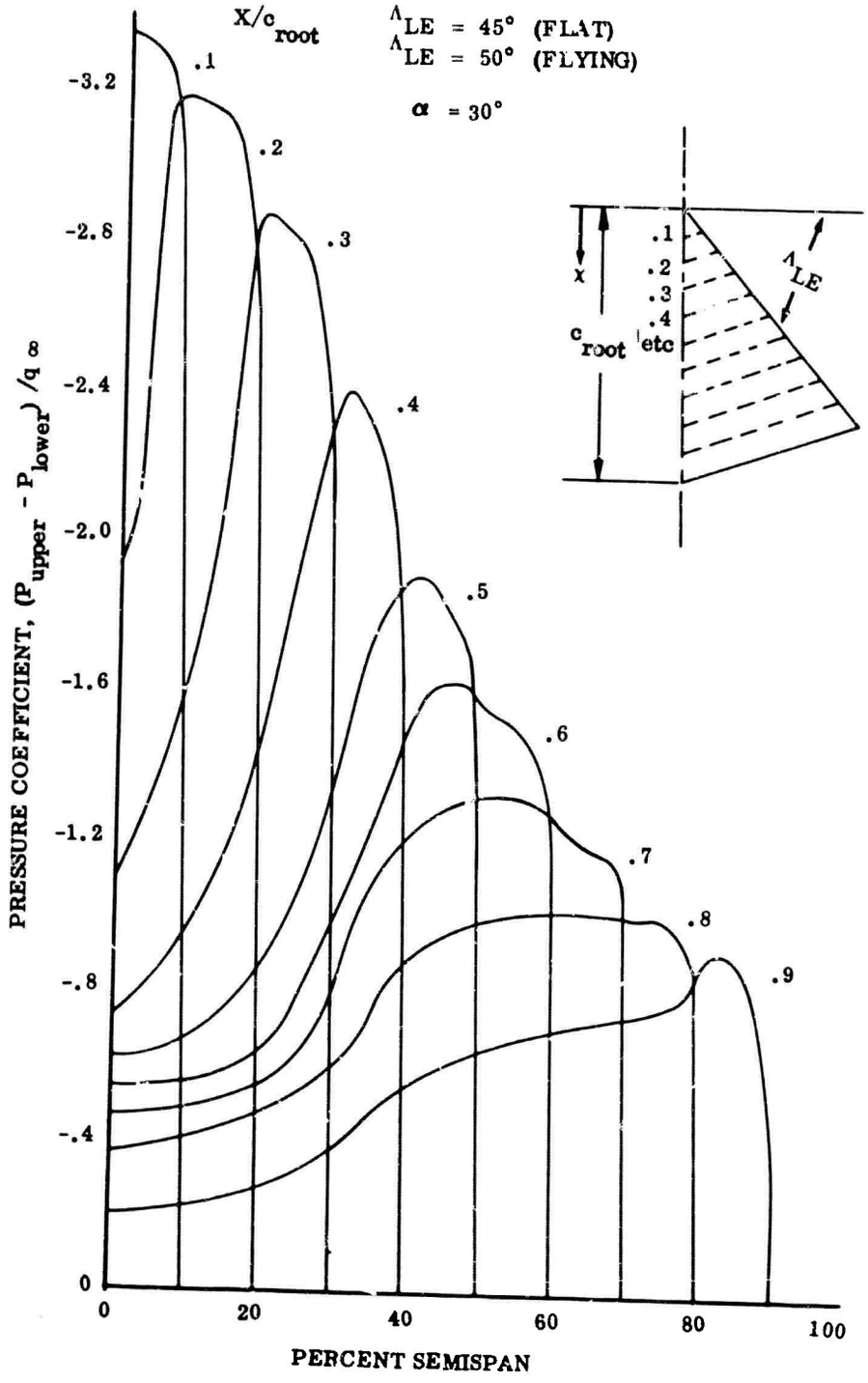

Figure 43. Wing Airload Distribution, 30-Degree Angle of Attack

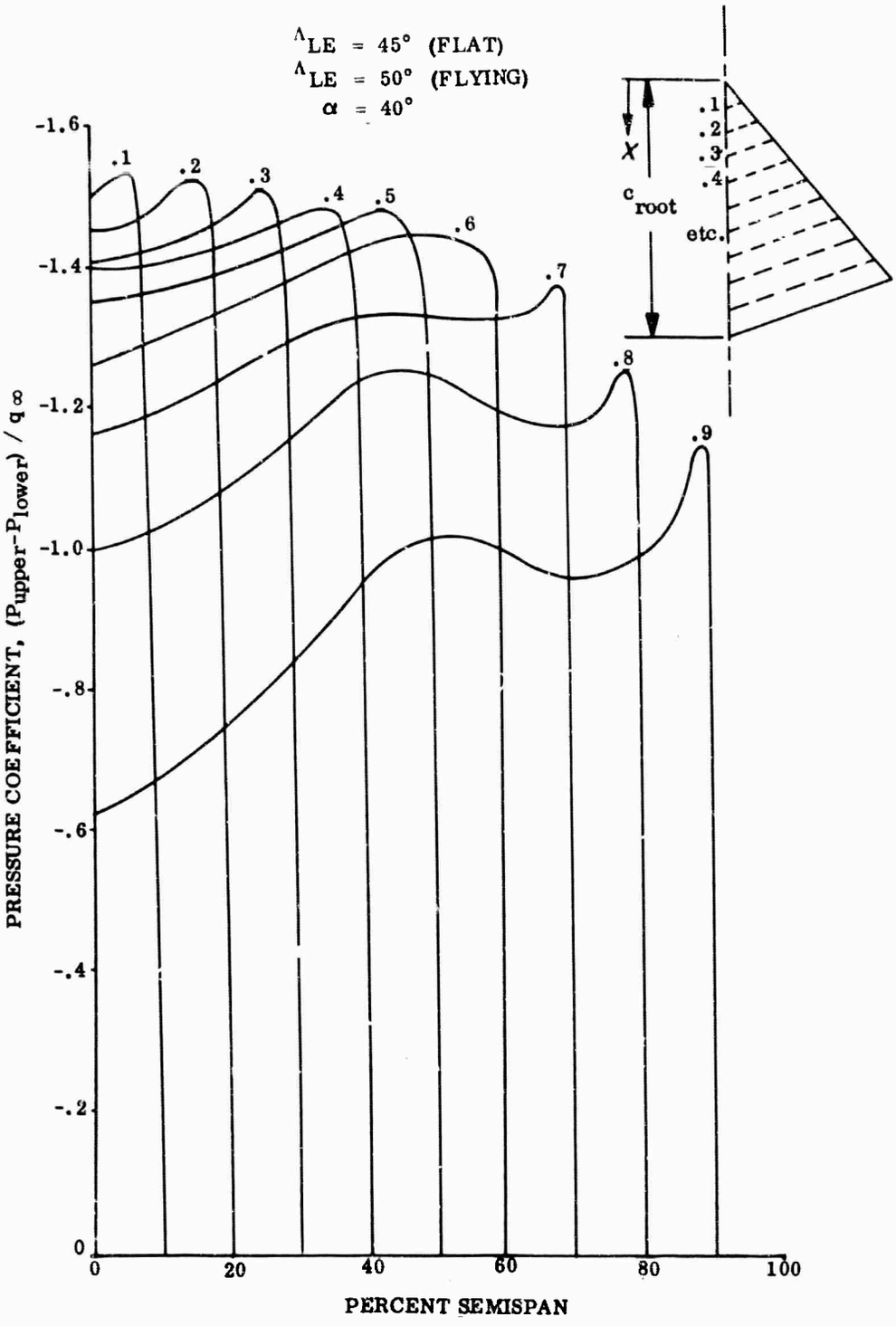

Figure 44. Wing Airload Distribution, 40-Degree Angle of Attack

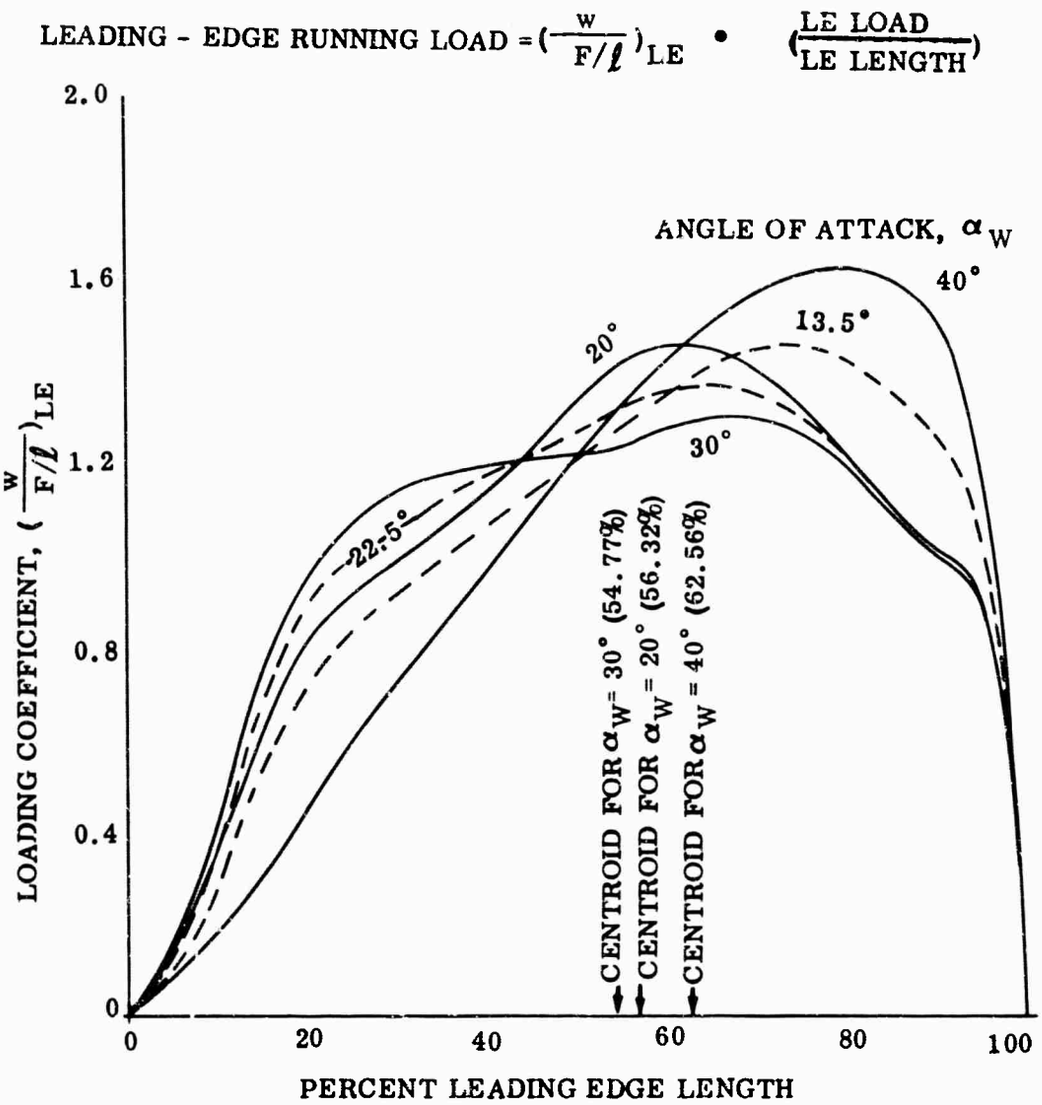

Figure 45. Leading Edge Membrane Load Distribution

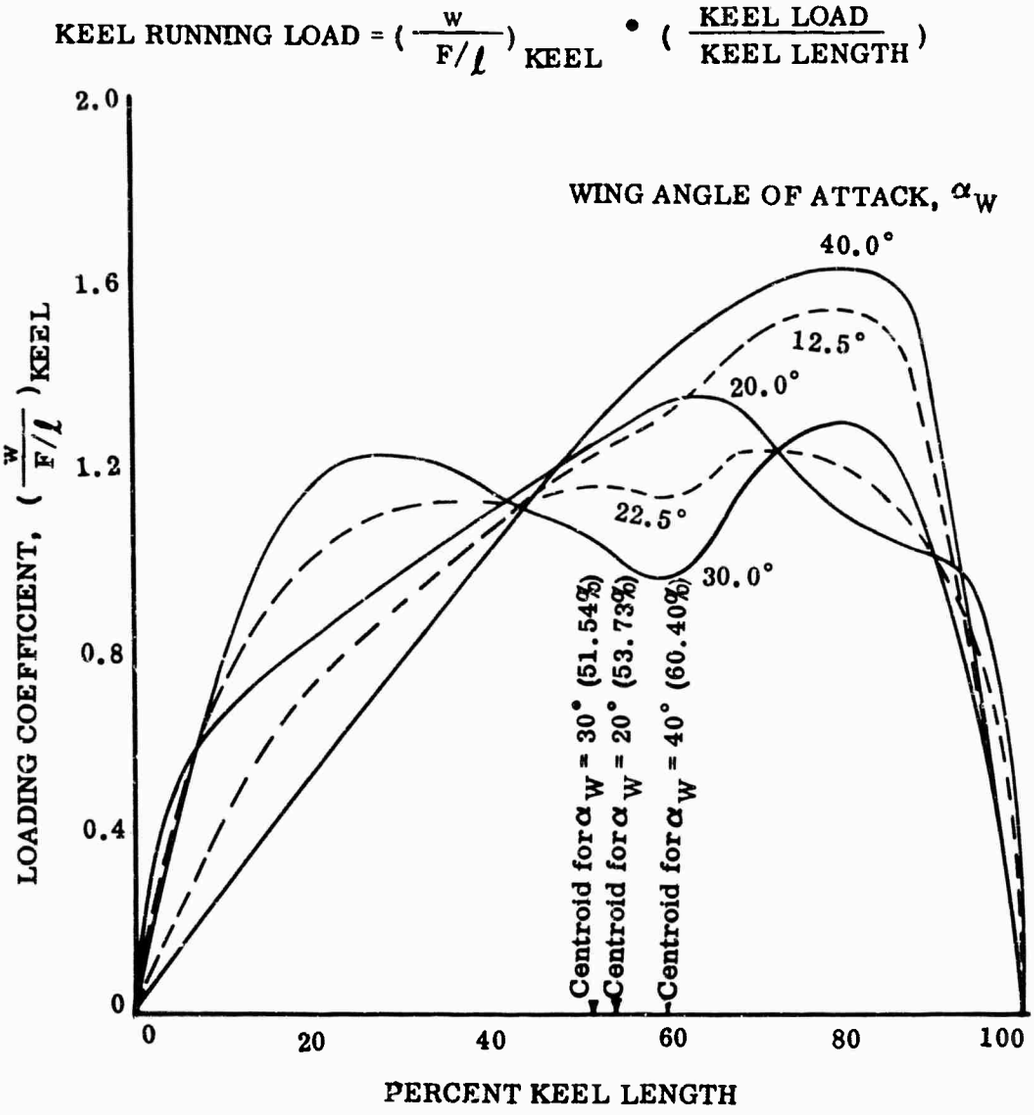

Figure 46. Keel Membrane Load Distribution

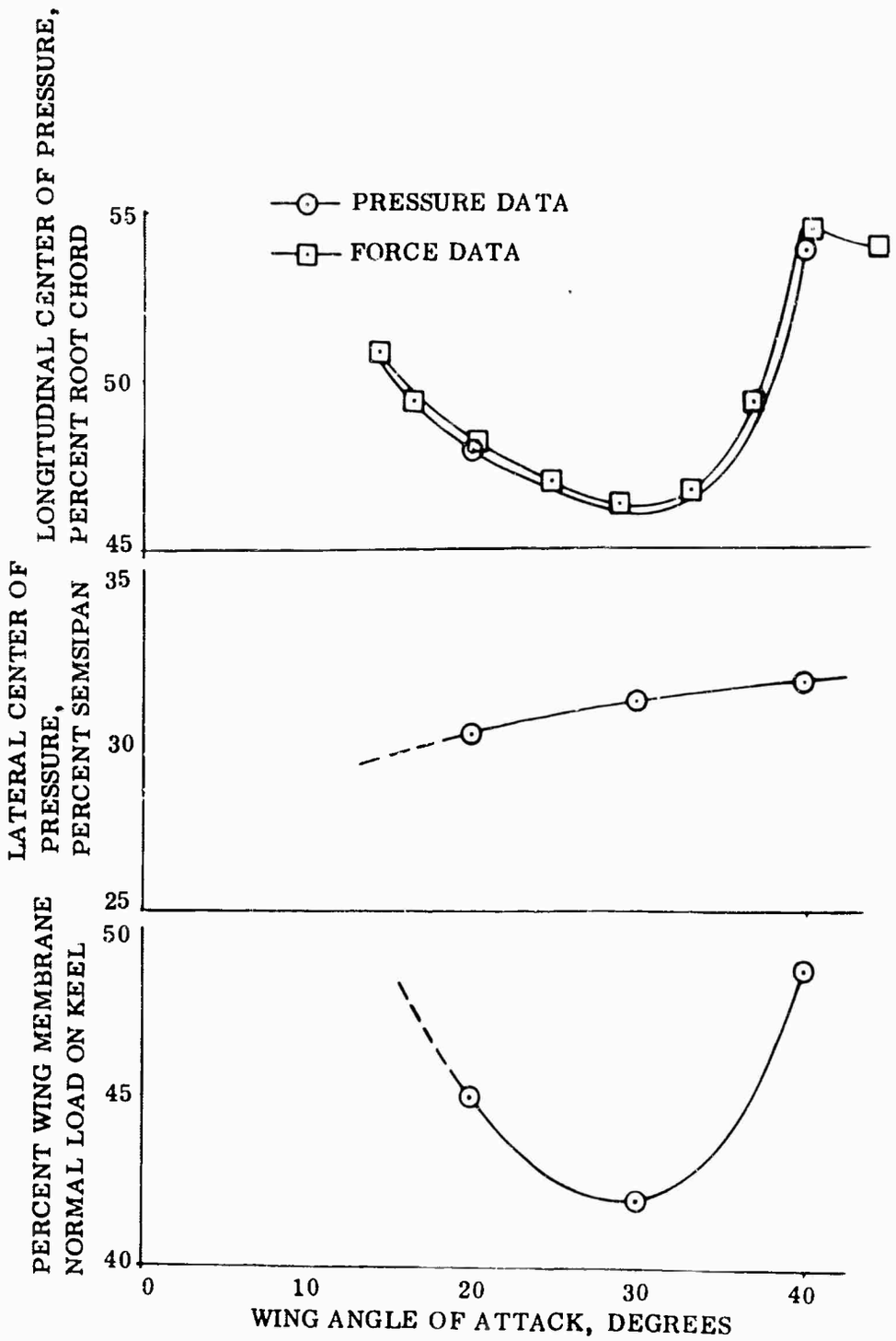

Figure 47. Wing-Alone Airload Characteristics

In order to gain further confidence in the keel and leading edge loading, as determined from the pressure data, a further comparison has been made with force data. The unpublished NASA force test data also give leading edge apex hinge-moment coefficients. These coefficients represent the leading edge moment, at the apex, in the keel/leading-edge plane and normal to this plane. These coefficients are defined as follows:

$$C_{H_H} = (\text{Apex horizontal hinge moment})/qS\,c_{root}$$

$$C_{H_V} = (\text{Apex vertical hinge moment})/qS\,c_{root}$$

If the load distribution on the leading edge in the horizontal (leading edge/keel plane) direction is assumed to be identical to the distribution in the vertical direction, the ratio C_{H_V}/C_{H_H} will represent the ratio of vertical to horizontal load on the leading edge. This assumption is probably valid since by far the largest unreacted load on the leading edge is applied by the membrane.

Figure 48 presents curves of C_{H_V}, C_{H_H}. Also shown on the figure are values of C_{H_V} calculated from the pressure data by means of the following equation:

$$C_{H_V} = \text{Moment}/qS\,c_{root}$$

$$= (C_N\,qS)\ .\ (k)\ .\ (X_{cp})/qS\,c_{root}$$

$$C_{H_V} = C_N\ .\ k\,X_{cp}/c_{root}$$

where

X_{cp} = distance to pressure coefficient of load on leading edge measured along LE (Figure 45)

k = fraction of wing normal force on LE (Figure 47)

Good agreement is shown between the force and pressure data for two of the three angles of attack shown. As with the normal force coefficients, some disagreement at angles of attack beyond the stall is again evident.

NOTES: (1) CURVES ARE FAIRED THROUGH DATA FROM THREE UNPUBLISHED NASA WIND TUNNEL TESTS.
(2) ⊙ ~ CALCULATED FROM PRESSURE DATA, C_{H_V}

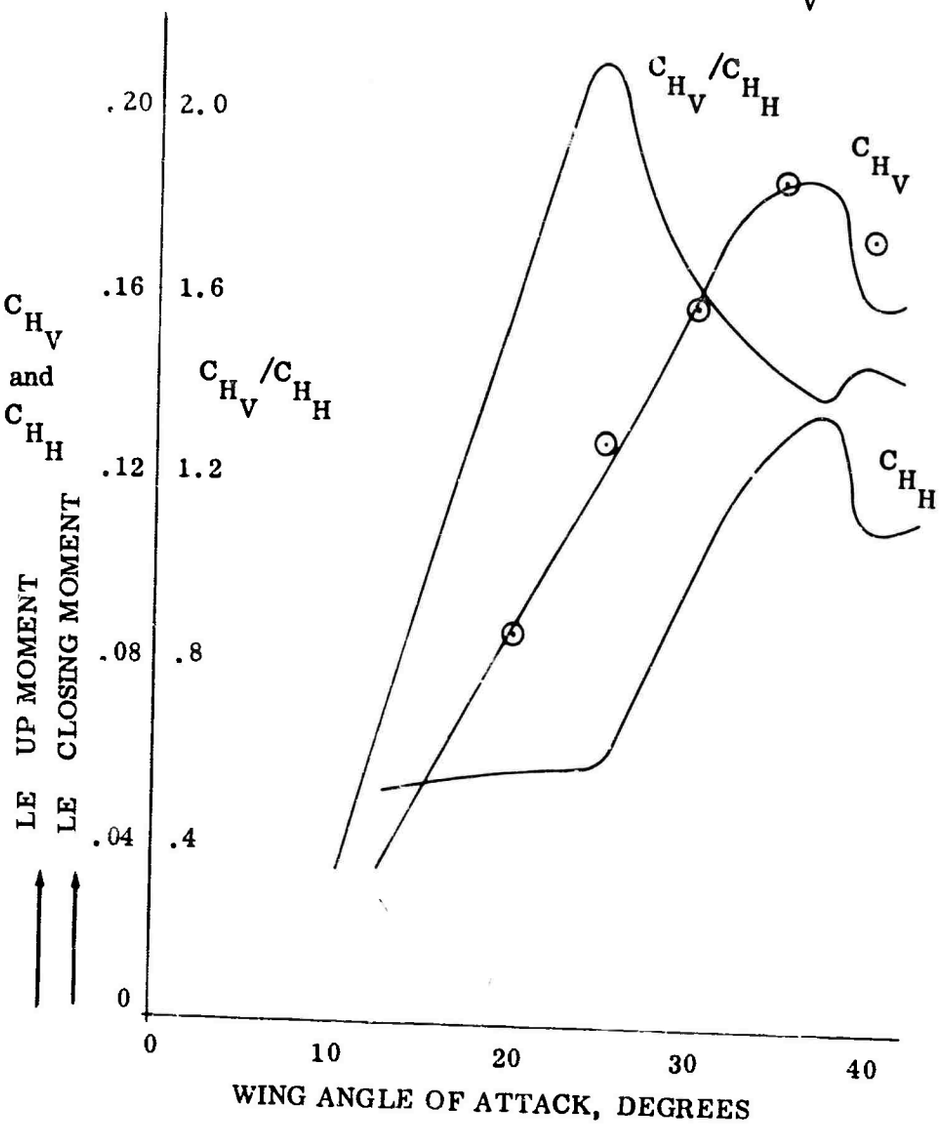

Figure 48. Wing Leading Edge Apex Hinge-Moment Characteristics

With the assumption that the ratio C_{H_V}/C_{H_H} is the ratio of vertical to horizontal load on the leading edge and that the membrane alone applies this load, the average membrane angle at the leading edge can be defined as:

$$\lambda_{LE} = \tan^{-1} (C_{H_V}/C_{H_H})$$

where

λ_{LE} is the angle, measured normal to the leading edge, between the membrane and the LE - keel plane. This angle is shown in Figure 49 as a function of angle of attack. Also shown on the figure is the estimated membrane angle at the keel.

LEADING EDGE AND KEEL SYMMETRICAL FLIGHT LOADS

The preceding analysis has established the airload distribution on the wing, leading edges and keel. The membrane load applied to the leading edge is reacted at two points on the leading edge: at the apex and at the roll trim cable fittings. These fittings are located at about 0.0% and 72.0% of the leading edge respectively.

The data of Figure 45 define the centroid of load acting on the leading edge at five angles of attack. Interpolation of these five values yields load centroid locations for other angles of attack. The wing normal load acting on the leading edge, and the leading edge vertical to horizontal load are shown in Figures 47 and 48. The static balance of the forces on the leading edge resulted in the curves of Figure 50.

The term V_{LE} is the wing normal force (C_{NqS}) multiplied by the fraction of wing normal force on the leading edge from Figure 47. The item V_{LE} defines the leading edge load acting in the wing plans and normal to the leading edge. This was determined by

$$H_{LE} = V_{LE} / (C_{H_V}/C_{H_N})$$

where the ratio of leading edge apex hinge moment coefficients C_{H_V}/C_{H_N} is given in Figure 48. The static balance of the vertical and horizontal forces on the leading edge (forces normal to the leading edge acting parallel and normal to the wing plane) has defined the loads at the apex and spreader-bar fittings; $(V_A)_{LE}$, $(H_A)_{LE}$, $(V_{SB})_{LE}$, and $(H_{SB})_{LE}$.

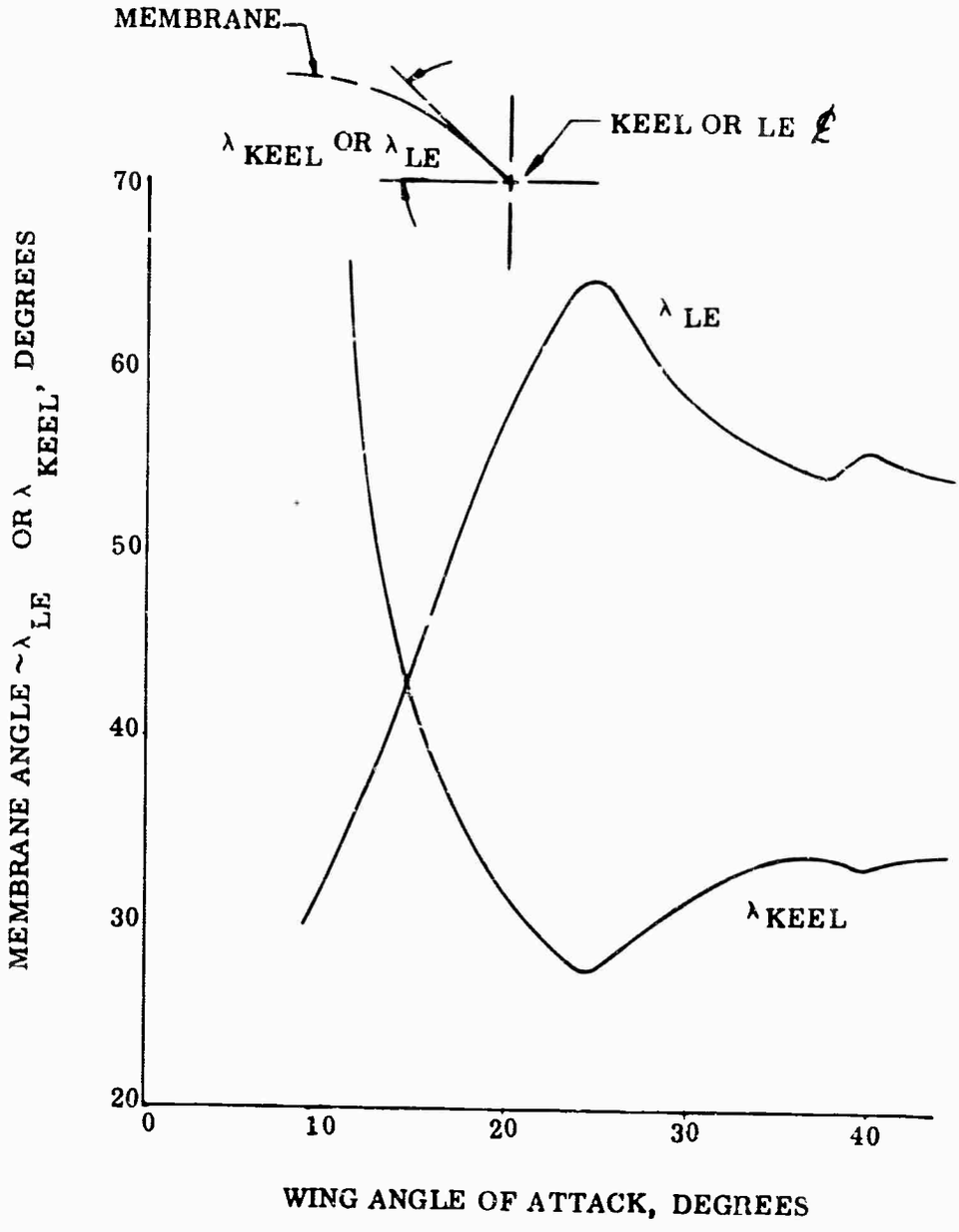

Figure 49. Wing Membrane Angle

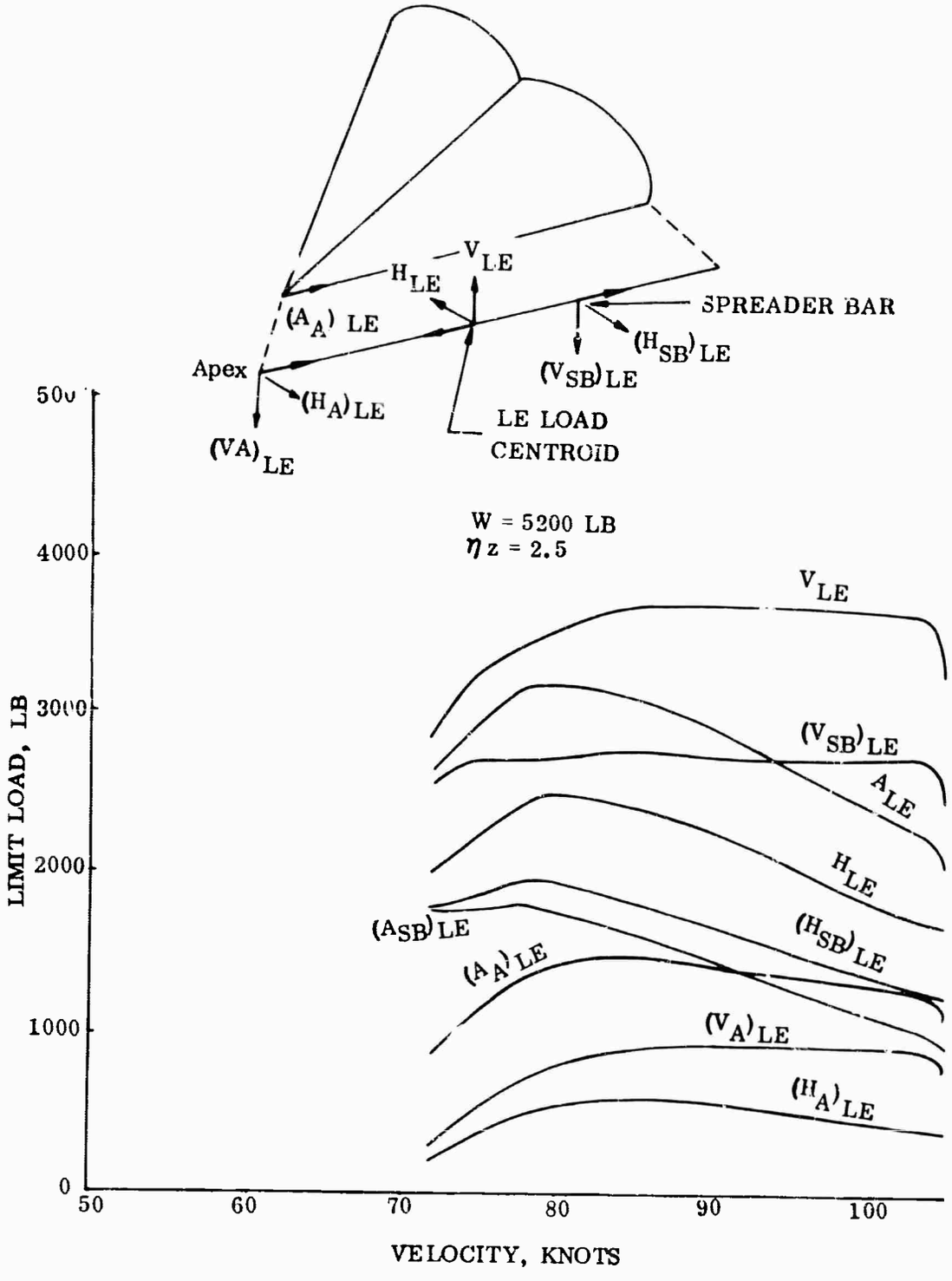

Figure 50. Leading Edge Limit Loads, Symmetrical Flight

The only leading edge loading from the membrane as yet undefined is the load acting along the member. The wing axial force coefficient C_A is considered to be distributed between the keel and leading edges in the same proportion as the normal force (Figure 47).

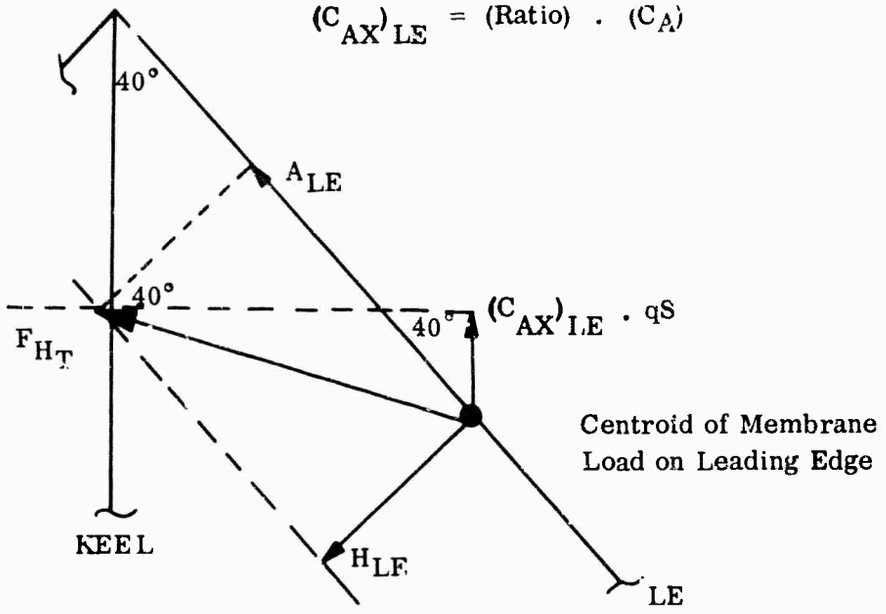

Force vectors $(C_{AX})_{LE}$ qS and H_{LE} are but components of the total horizontal force vector F_{H_T}. Thus, F_{H_T} can be determined. The component of F_{H_T} acting along the leading edge is:

$$A_{LE} = \left[(C_{AX})_{LE} \; qS/\cos 40^\circ\right] + H_{LE} \tan 40^\circ$$

The summation of forces along the leading edge, including the effects of the spreader bar and roll-cable axial load components, gives the axial loads applied to the leading edge at the apex and roll-trim-cable fittings.

The loading on the keel has been determined in a similar manner. For symmetrical flight conditions, only vertical and axial loads are considered on the keel. Vertical loads applied to the keel at the apex (by the leading edges) and by the membrane are reacted by forward and rear keel supports located at about 27.0% and 55.0% of the keel length. A static balance of the vertical loads acting on the keel uses the known values of V_K, $(V_A)_K$, $\left[(V_A)_K = 2(V_A)_{LE}\right]$, and the

locations of the keel membrane load centroid $(X_{EP}/\ell)_k$. The unknown vertical reactions at the two keel supports, $\left(C_{V_F}\right)_K$ and $\left(C_{V_R}\right)_K$, were determined from

$$\begin{bmatrix} 1.0 & 1.0 \\ .27 & .55 \end{bmatrix} \quad \begin{pmatrix} V_F \end{pmatrix}_K \\ \begin{pmatrix} V_R \end{pmatrix}_K = \left\{ \begin{matrix} \left[(V_A)_K + V_K \right] \\ \left[\ell_k \, (X_{cp}/\ell)_K \, (V_K) \right] \end{matrix} \right\}$$

The keel loading for the design load factor is shown in Figure 51.

Examination of the keel loading curves shows that critical loading occurs in flight at velocities of about 70 and 95 knots. The critical loading on the leading edge defined from $\sqrt{V_{LE}^2 + H_{LE}^2}$ occurs at a velocity of about 84 knots. The keel and leading edge load distributions, which have been discussed elsewhere, and the reactions have been used to construct the shear moment and axial loading curves of Figures 52 through 54. The leading edge and keel axial loading resulting from the membrane may be considered as acting along the membrane attachment(s) to the member.

The membrane running load distribution assumes the shape of the curves of Figures 45, 46, and 49 at the keel and leading edges. The peak values of running load as a function of wing angle of attack for the symmetrical load factor envelope are shown in Figure 55.

LEADING EDGE AND KEEL UNSYMMETRICAL FLIGHT LOADS

Unsymmetrical flight loads occur on the wing as a result of a lateral gust. This design condition occurs at a vertical load factor of 1.0.

Wing data for sideslip conditions are somewhat limited. Wing-alone lateral characteristics that are available are side force, rolling moment, and yawing moment derivatives as a function of wing angle of attack. Curves of these derivatives are shown in Figure 56. In addition, leading edge apex vertical (C_{H_V}) and lateral (C_{H_H}) hinge moment coefficients are available for the wing in sideslip at two angles of attack. The data indicate the following:

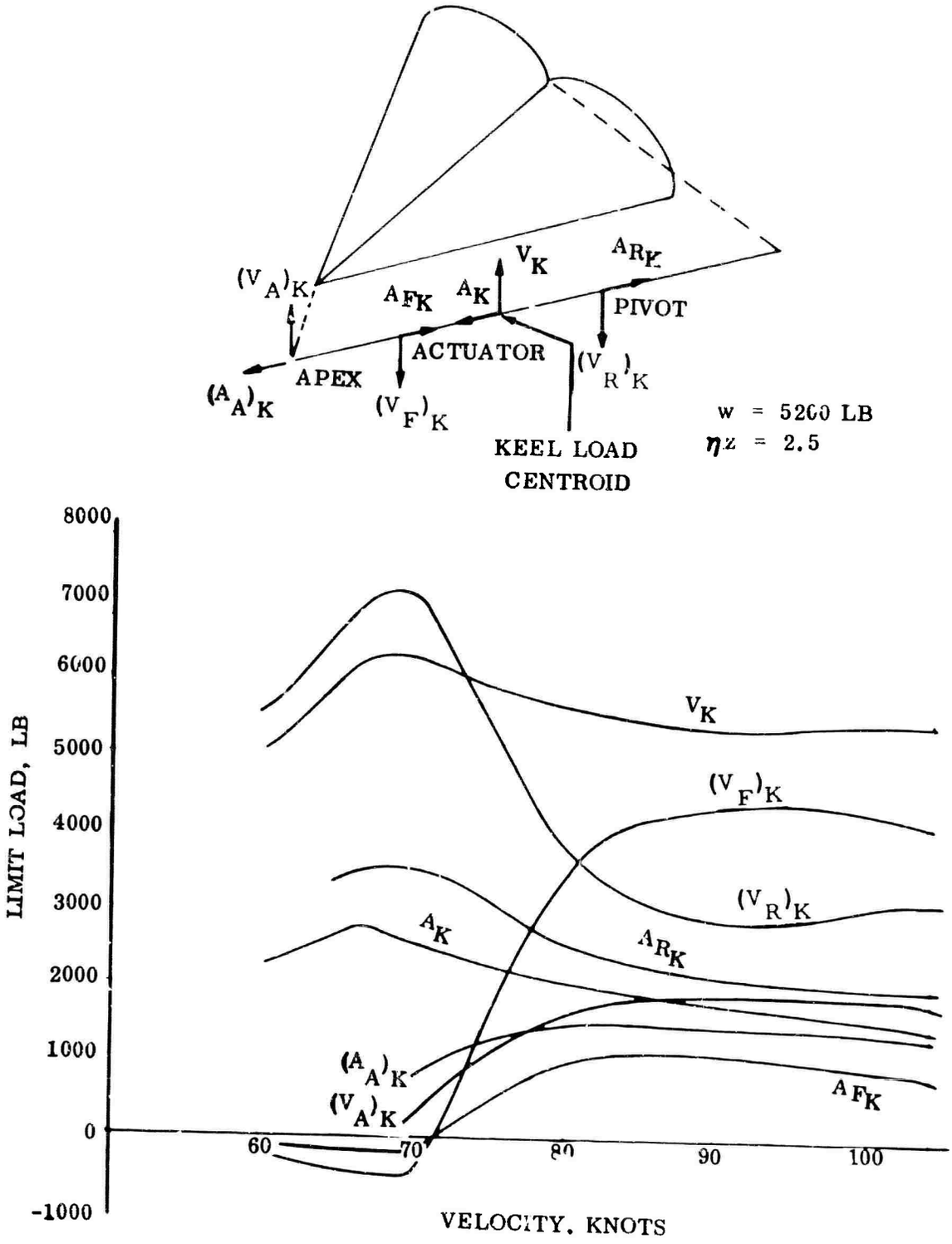

Figure 51. Keel Limit Loads, Symmetrical Flight

ULTIMATE FACTOR OF SAFETY = 1.33

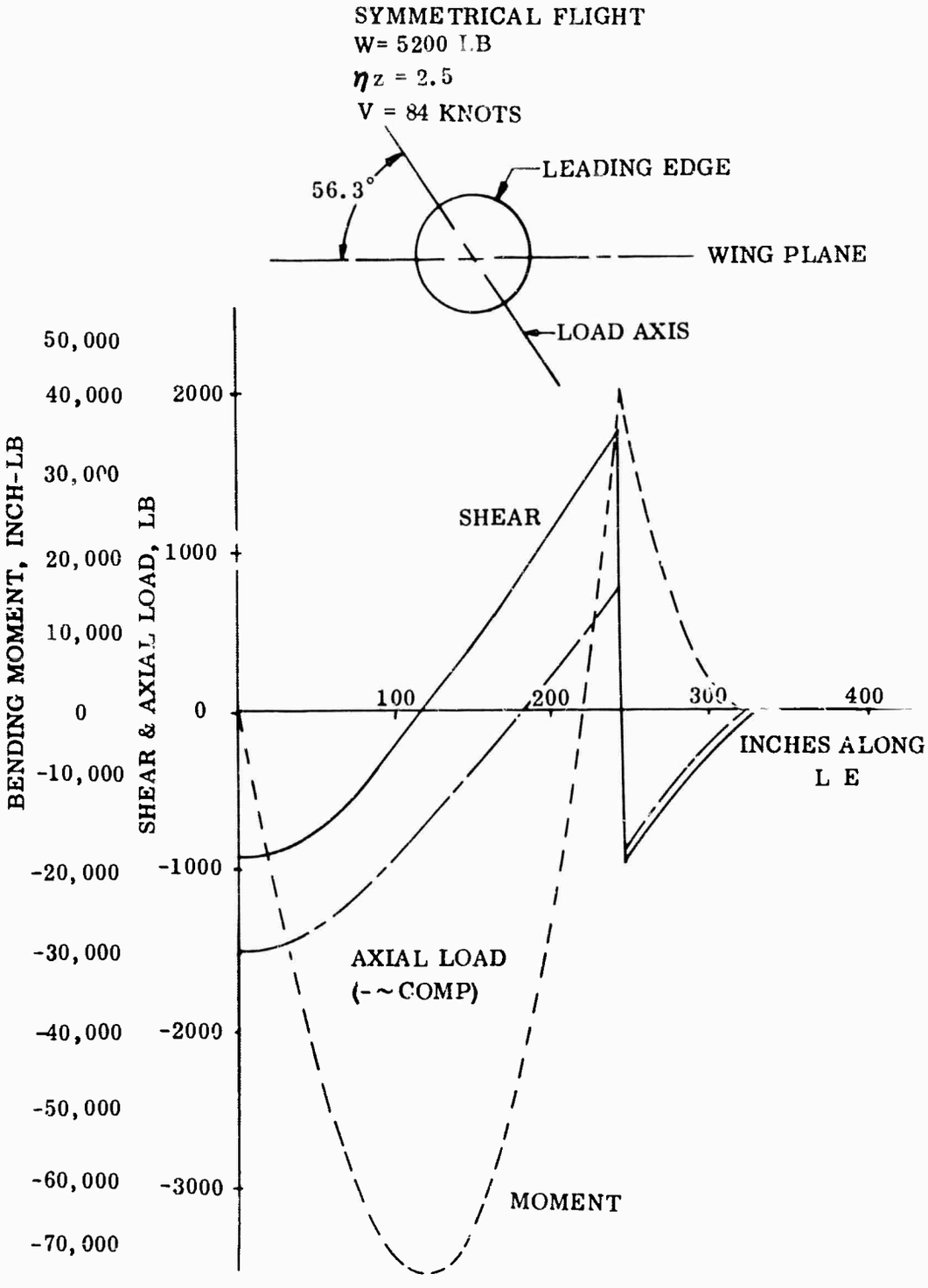

Figure 52. Leading Edge Limit Shear, Moment and Axial Load

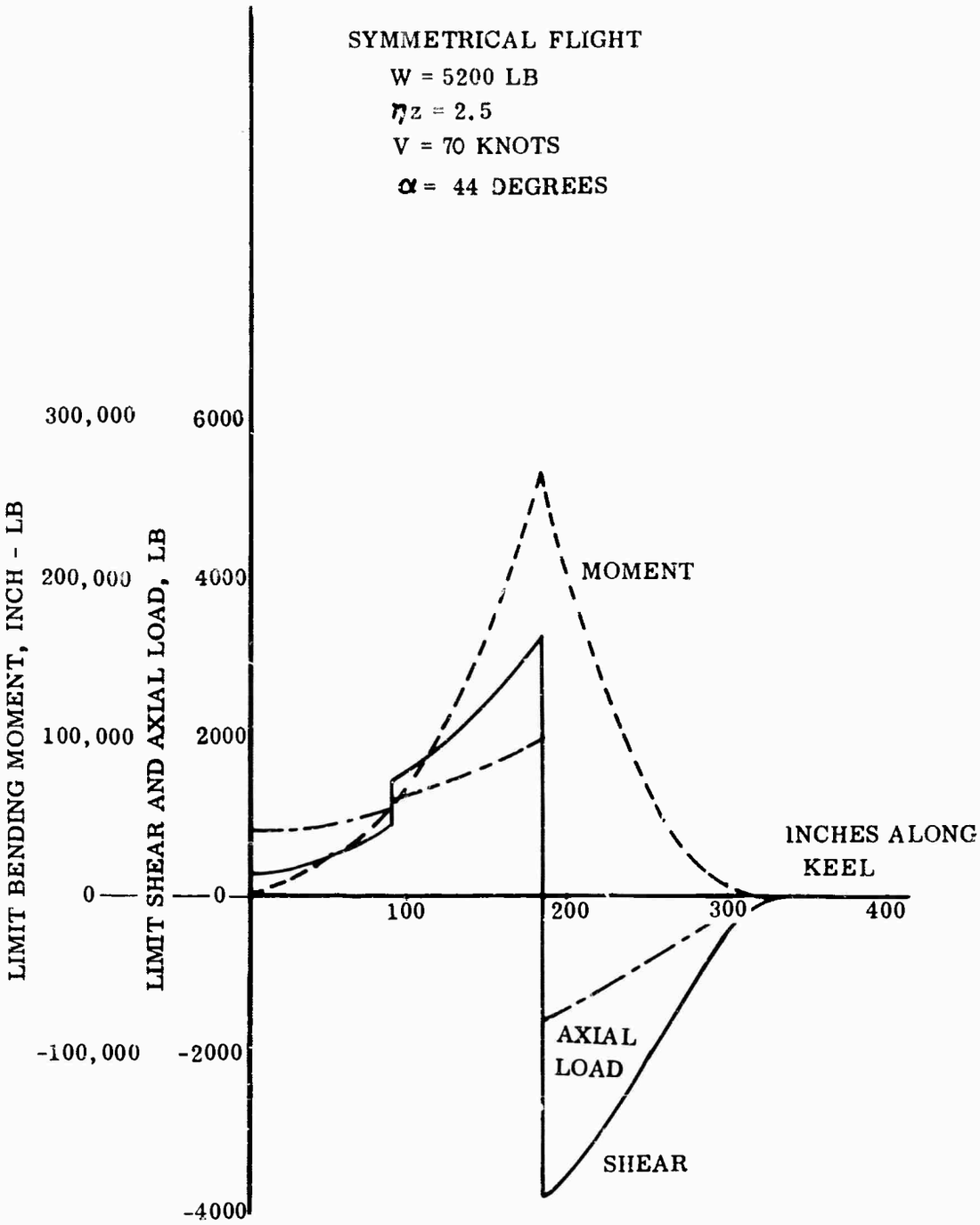

Figure 53. Keel Limit Shear, Moment and Axial Load (70 Knots)

SYMMETRICAL FLIGHT

W = 5200 LB
η_z = 2.5
V = 75 KNOTS
α = 28 DEGREES

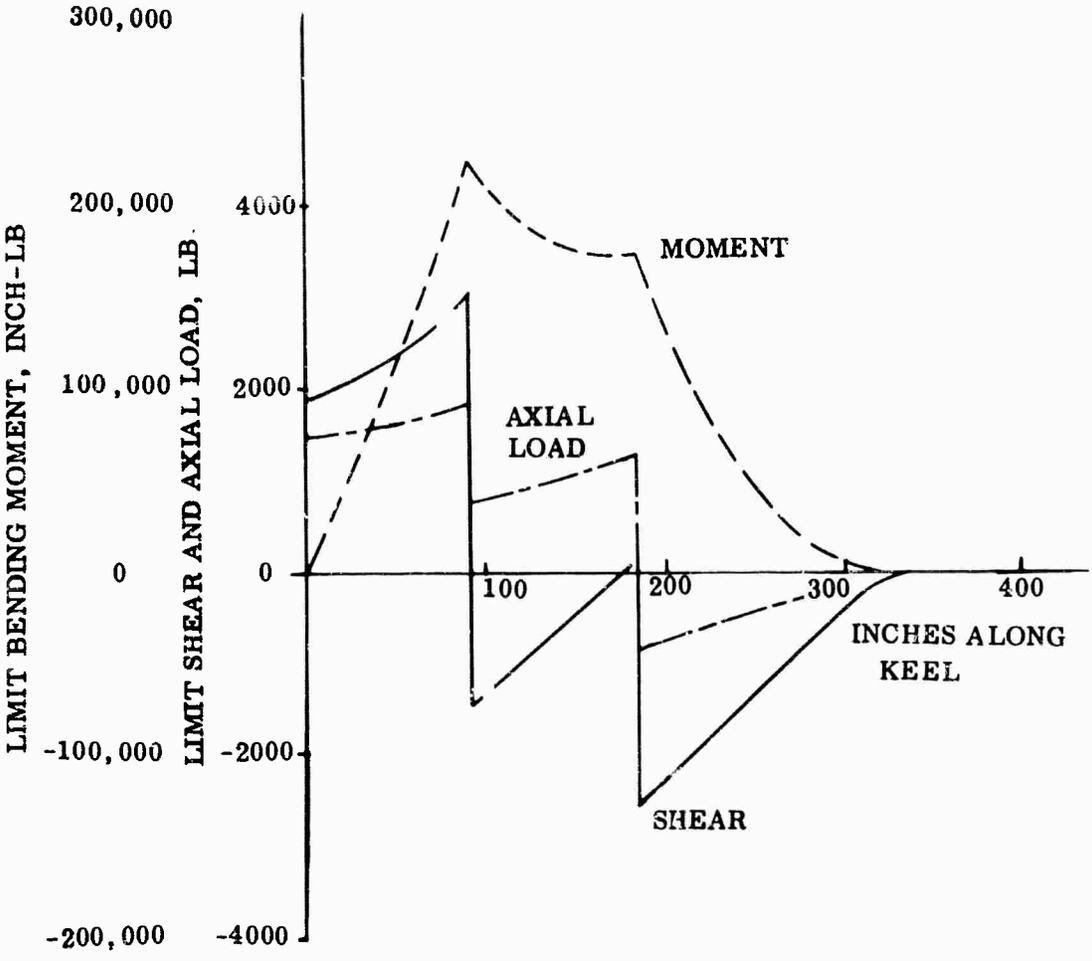

Figure 54. Keel Limit Shear, Moment and Axial Load (75 Knots)

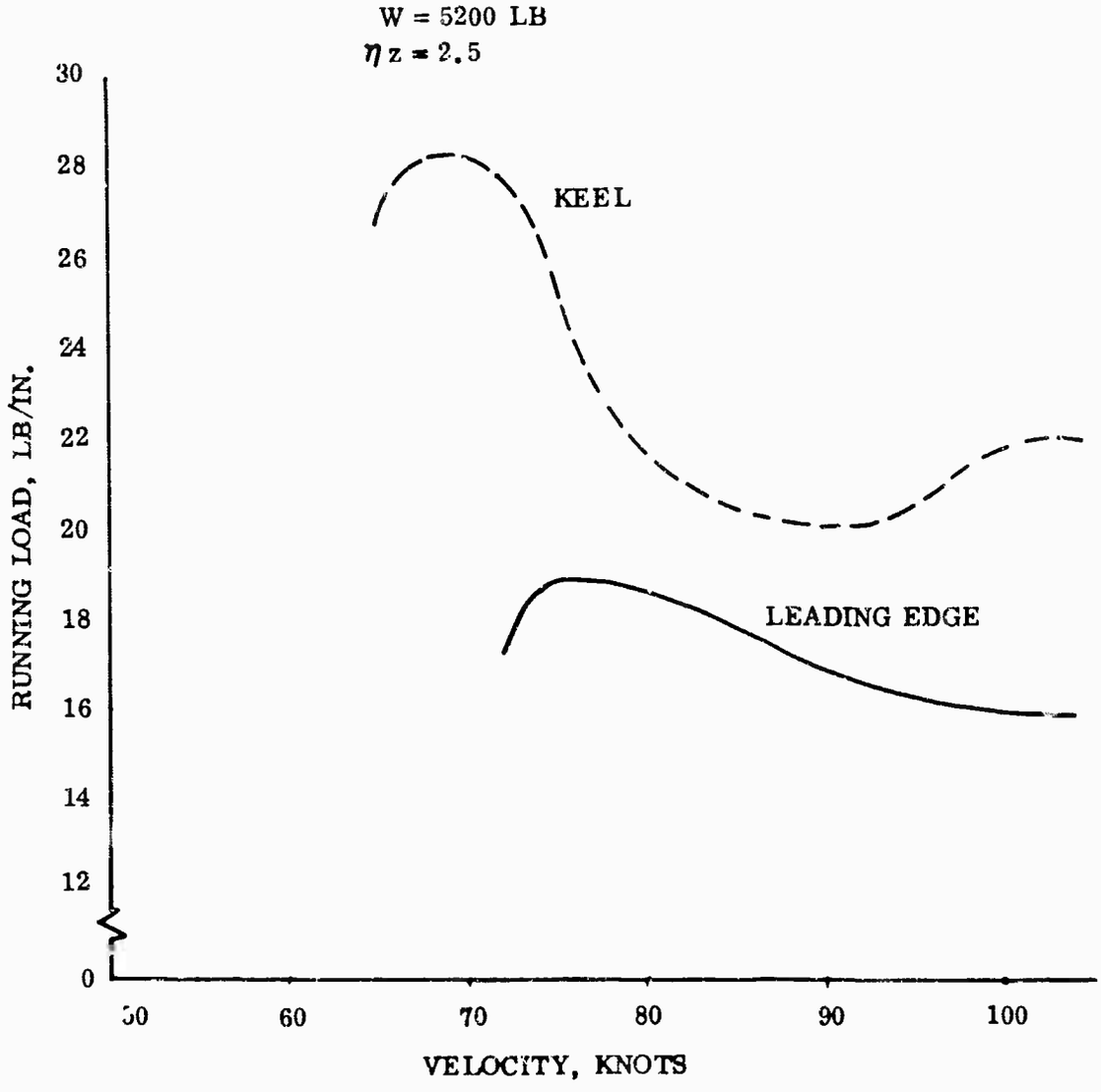

Figure 55. Peak Limit, Membrane Running Load at the Leading Edge and Keel

NOTE:

1. BASED ON FLATPLAN SPAN AND AREA
2. DATA REFERENCED TO KEEL MID-POINT
3. REFERENCED TO WING AXES SYSTEM

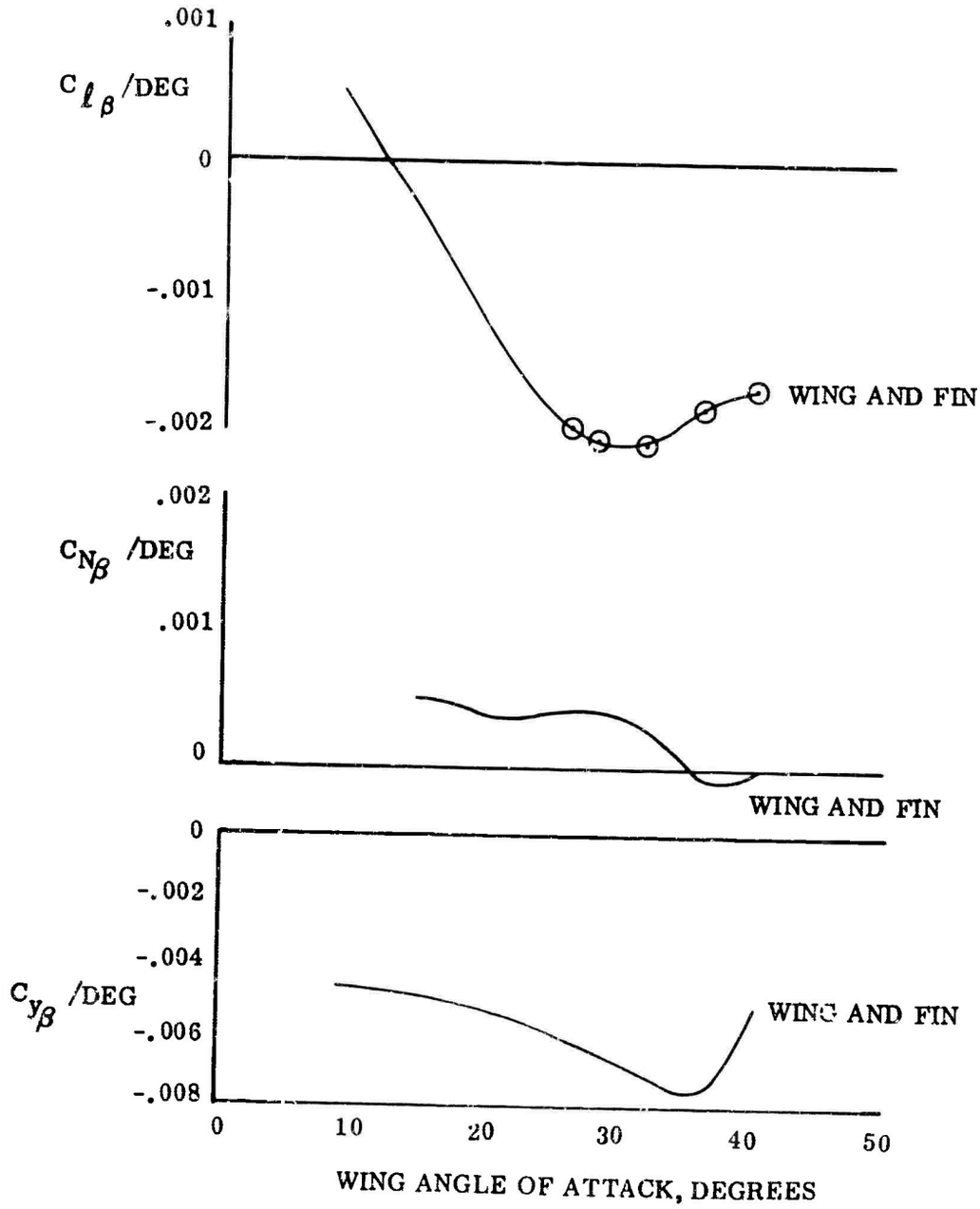

Figure 56. Lateral-Directional Static Stability, Wing Only

α_W	$\partial C_{H_H}/\partial \beta = C_{H_{H_\beta}}$	$\partial C_{H_V}/\partial \beta = C_{H_{V_\beta}}$
18.5°	+ 0.0021 per deg	+ 0.0010 per deg
33.1°	+ 0.0020 per deg	+ 0.00129 per deg

These coefficients act to increase the upward and closing hinge moments on the windward leading edge during sideslip. The opposite effect occurs on the leeward member.

To gain confidence in the above hinge moment data, some further analysis has been made.

The vertical hinge moment derivative $\partial C_{H_V}/\partial \rho$, hereafter referred to as $C_{H_{V_A}}$, has been compared with wing rolling moment data. The comparison has been made by making the following assumptions and then attempting to verify them through comparison of data:

1. The wing rolling moment due to sideslip is due almost entirely to an increase/decrease in vertical membrane loading on the leading edges.

2. The centroid of the incremental vertical load on the leading edges due to sideslip is the same as for symmetrical flight.

$$\text{Rolling moment} = 2C_{V_{LE}}\, y_{cp\,LE}\, qS$$

$$C_{\ell_\beta}\,\beta = \text{Rolling moment}/qS\ell = 2C_{V_{LE}}\,(q_{cp}/\ell)_{LE}$$

$$q_{cp} = (X_{cp}/\ell)_{LE}\ \ell \cos\Lambda_{LE}$$

$$C_{\ell_\beta}\,\beta = 2C_{V_{LE}}\,(X_{cp}/\ell)_{LE}\,\cos\Lambda_{LE}$$

Solving for $C_{V_{LE}}$ we can write

$$C_{V_{LE_\beta}} = \partial C_{V_{LE}}/\partial\beta = 0.5\, C_{\ell_\beta}/(X_{cp}/\ell)_{LE}\cos\Lambda_{LE}$$

Thus, using the above assumptions we can solve for the increment of vertical load on the leading edges due to sideslip $C_{V_{LE_\beta}}$, knowing the wing rolling moment

C_{ℓ_β} and the location of the centroid of load on the leading edge as a fraction of the leading edge length. The derivative $C_{V_{LE_\beta}}$ may also be found as

$$C_{V_{LE_\beta}} = C_{H_{V_\beta}} / (X_{CD}/\ell)_{LE}$$

A comparison of the values of $C_{V_{LE_\beta}}$ calculated from C_{ℓ_β} and $C_{H_{V\beta}}$ is shown in Figure 57. Good agreement is shown. The design limit loading on the leading edges due to lateral gust, however, is not as critical as the symmetrical flight conditions previously shown.

A curve of $\partial C_{H_H} / \partial \rho$ versus angle of attack has been estimated from the available data. This curve permitted calculation of the differential spreader bar compression load due to the lateral gust design conditions. The peak differential load of 1908 pounds limit is reacted by the keel.

ESTIMATED SPREADER BAR LOADING DUE TO GROUND WIND

This analysis of the spreader bar loading due to ground winds can only be considered approximate because of the lack of wing aerodynamic data for the condition under study. With the vehicle resting on the ground, consider a ground wind blowing from the rear. This results in a wing angle of attack of 191° with the wing all the way down. The aerodynamic characteristics at 191° would be identical to those at 169°, were it not for the spreader bar. At 191° the membrane rests on the spreader bar. It is estimated that under identical wind conditions, the force on the wing will be less if the membrane is draped over the spreader bar.

It now remains to determine the aerodynamic characteristics of the wing at 169°, i.e., considering the membrane not contacting the spreader bar. Figure 58 shows the estimated flex-wing lift coefficients in the angle of attack range desired. The curve was estimated considering the data for the 60° delta wing shown on the figure, and the flex-wing geometry.

C_L (@ α_W = 169°) = -0.64

LIFT = -120 lb @ wind speed of 10 knots

LIFT = -431 lb @ wind speed of 20 knots

LIFT = -1080 lb @ wind speed of 30 knots

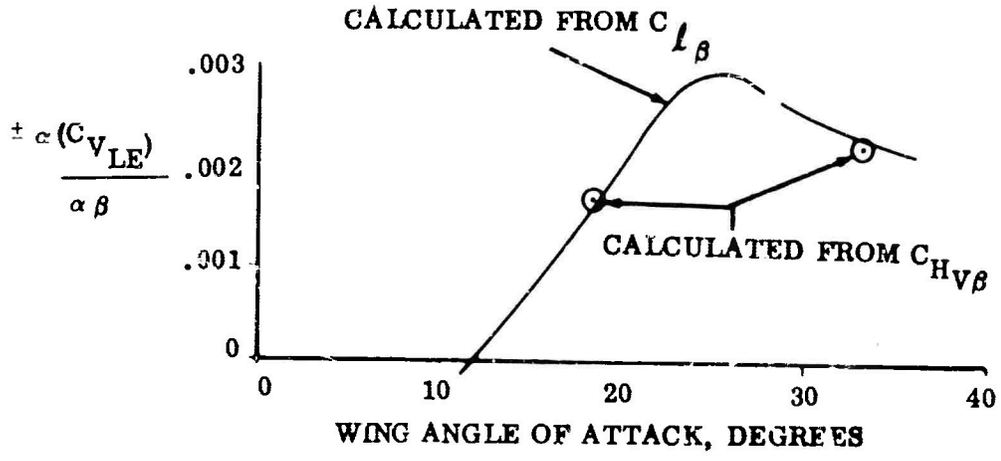

Figure 57. Leading Edge Loading Coefficient

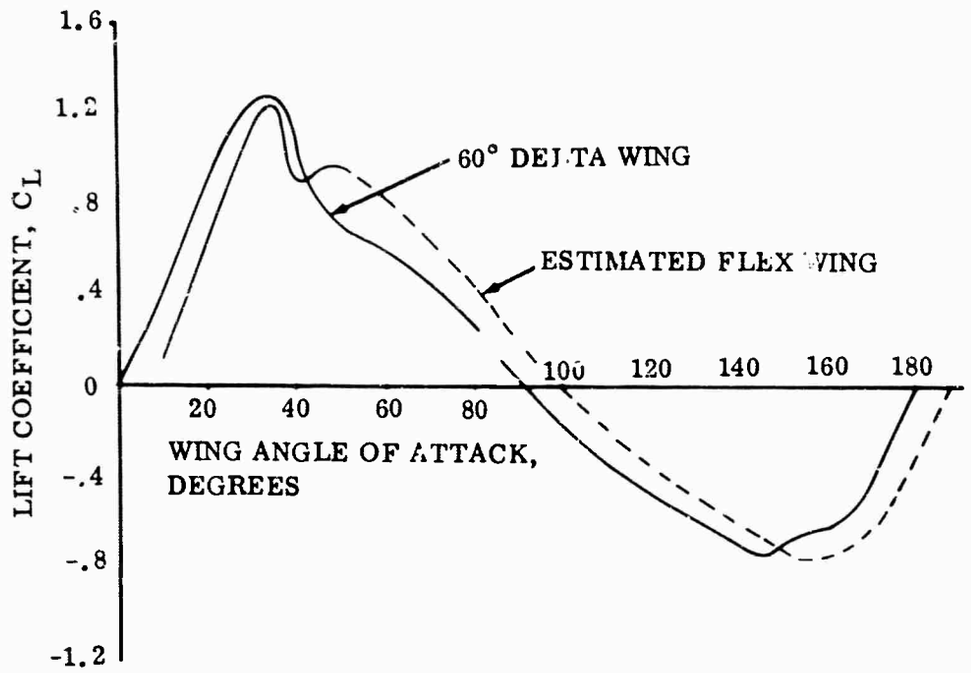

Figure 58. Estimated Flex-Wing Lift Coefficient at High Angles of Attack

The lift on semispan can be considered acting at 40% of the semispan and reacted by bending in the spreader bar. The root bending moment in the spreader bar is

$$M = (0.5)\ (\ell)\ (0.4)\ (b/2)$$

M = 5180 in-lb @ windspeed of 10 knots

M = 20800 in-lb @ windspeed of 20 knots

M = 46650 in-lb @ windspeed of 30 knots

The bending moment due to weight is 7260 inch-pounds. Plotting the maximum spreader bar bending moment versus wind speed (Figure 59) shows that the wing is capable of sustaining a wind of 17.5 knots.

WING SUPPORT LOADS, FLIGHT CONDITIONS

The loads upon the wing under the design conditions have been discussed in the preceding section. The wing is joined to the body by means of six struts and two cables. The leads in these members were determined considering the vehicle geometry and the loads upon the wing.

Two support struts are attached to the keel at approximately 27.0% of its length. Vertical loads at this location are reacted by the pitch control struts. These struts also react side loads.

The leading edge vertical up loads are reacted by the roll trim cables. These cables are attached to the leading edge/spreader bar fitting. Because of the geometry of the roll control system, tension in these cables introduces additional loading in the leading edge and spreader bar members. Leading edge down loading is reacted by bending in the spreader bar.

The keel is supported at 55% of its length by four struts which form two A-frames.

The loading coefficients for the wing supporting members have been evaluated. The limit loads in the members for the symmetrical flight load factor envelope are shown on Figure 60. These loads are a result of airloads only and do not include weight-inertia effects.

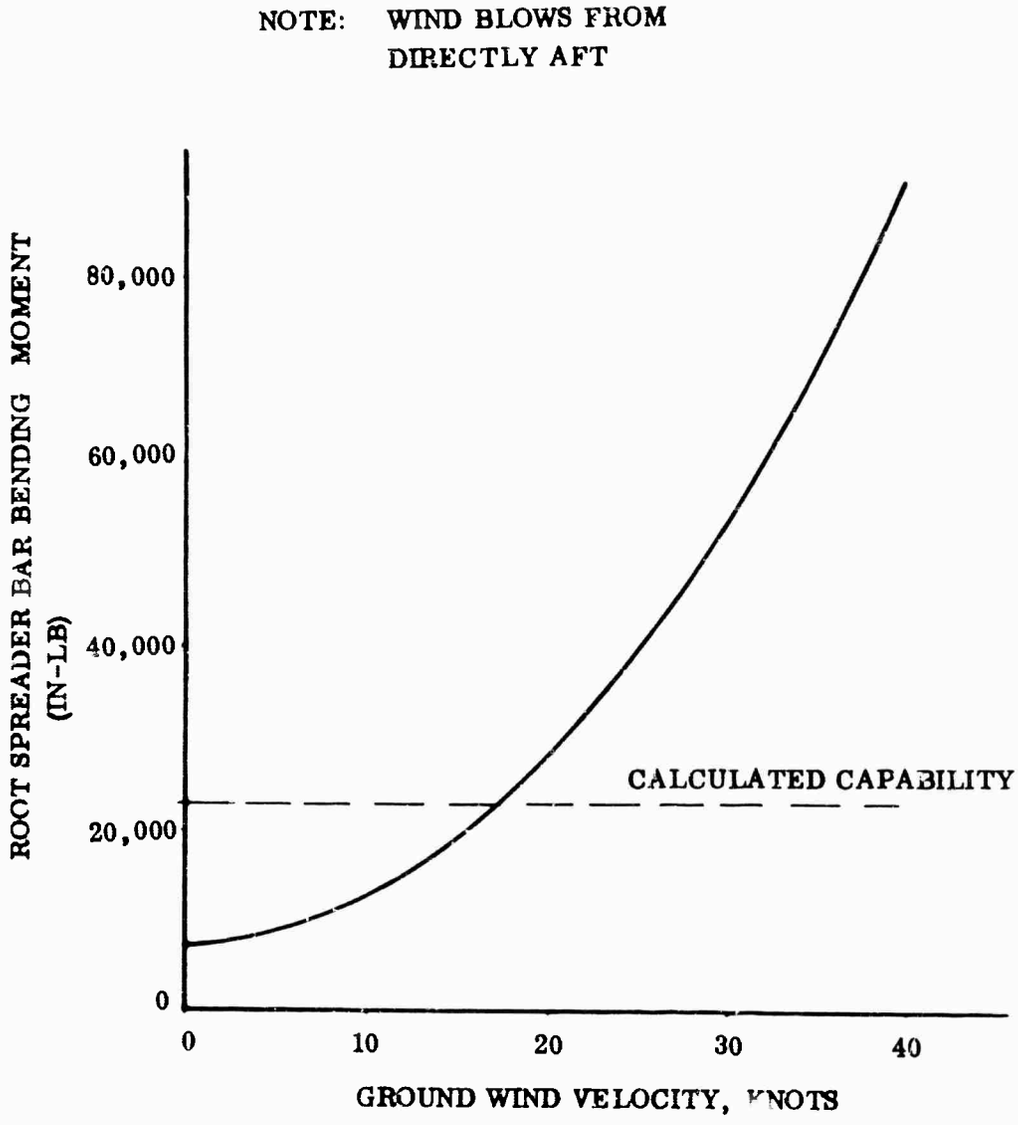

Figure 59. Estimated Spreader Bar Loading Due to Ground Winds

W = 5200 LB
$\eta z = 2.5$

TENSION IN ONE UPPER TOW BRIDGE CABLE = 800 LB
TENSION IN ONE LOWER TOW BRIDGE CABLE = 1000 LB
TENSION IN ONE AFT TOW BRIDGE CABLE
AXIAL LOAD OF -300 LB (COMPRESSION) IS APPLIED TO
CENTER STRUT BY TOW BRIDGE CABLE IN ADDITION TO LOADS BELOW
TOW BRIDGE CABLE LOAD OF 270 LB ACTS INWARD NORMAL
TO CENTER STRUT

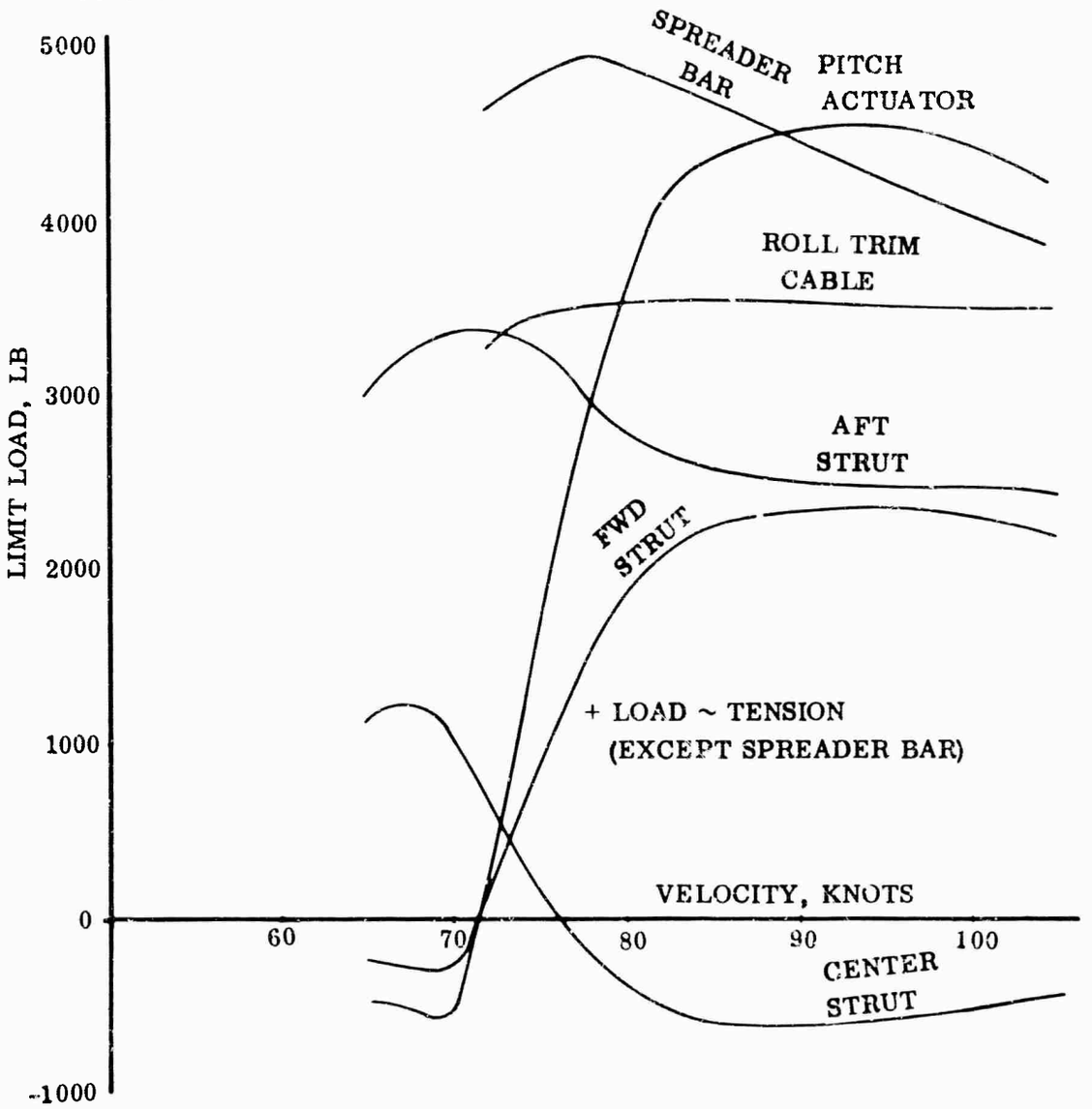

Figure 60. Limit Wing Loads, Symmetrical Flight

The loading in the wing support members resulting from the design lateral gust conditions has also been evaluated. The only loads that may prove to be critical are compression loads in the aft and center A-frame members. The maximum compression load in a member of the aft A-frame is 243 pounds.

The maximum compression load acting in a member of the center A-frame is 1463 pounds. In addition, a 145-pound limit load acts downward as a result of the bridle cable. A load of 131 pounds acting inward normal to the strut is also applied at the bridle cable fitting.

LANDING LOADS

The design criteria stipulate that the structure shall be designed for landings on the skids which result in the following landing load factors acting separately but in conjunction with wing lift equal to 2/3 weight:

N_z vertical skid load factor = 6.0 down

N_y lateral skid load factor = 2.0

N_x longitudinal skid load factor = 3.0 forward

The design landing gross weight is 5200 pounds.

For the 6 g vertical load factor, the load shall be evenly distributed between the two skids. The distribution along the skids shall be as shown in the following sketches:

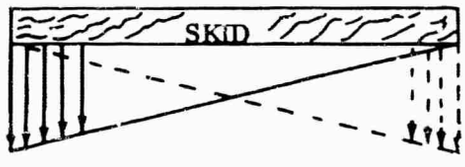

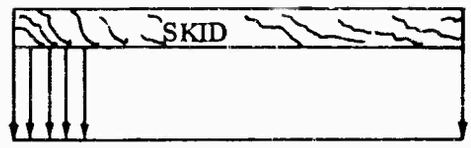

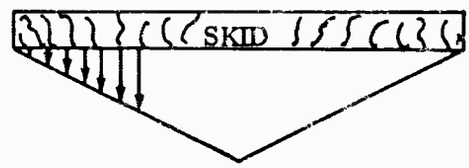

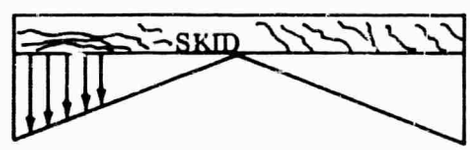

The treadwise distribution shall be considered as follows:

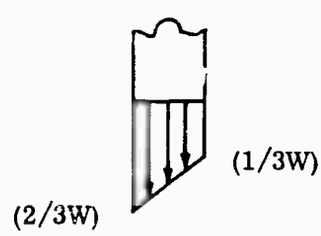

Unbalanced pitching moments shall be considered reacted by rotational inertia.

For the 2.0 g lateral condition, the distribution of load along the skids shall be as considered above and shall be distributed between the skids in the following manner:

60% of N_y . W acting inward on one skid acting simultaneous with
40% N_y . W ultimate acting outward on the other skid.

For the 3.0 g forward load factor condition, the load shall be considered to be evenly distributed along and between the skids.

The landing gear are designed such that the skids contact the ground whenever a 2.0 g ground landing load factor is exceeded.

LANDING GEAR

The forward spring-mounted gear is assumed to have the following characteristics:

$F_v = R\delta$

Vertical Force = F_v

Deflection = δ

When F_v = 5200 (2) (0.25) = 2600 pounds

δ = 0.833 ft

$R = F_v/\delta = 3120$ lb/ft

$F_v = 3120\ \delta$

m = proportionate vehicle mass on one wheel

= 40.4 slugs

$$\frac{\alpha^2\delta}{\alpha t^2} = 77.3\ \delta$$

Solution yields

$$\delta = C_1 \cos \sqrt{77.3}\, t + C_2 \sin \sqrt{77.3}\, t$$

$$\delta = C_1 \cos 8.79\, t + C_2 \sin 8.79\, t$$

$$\dot{\delta} = 8.79\, C_1 \sin 8.79t + 8.79\, C_2 \cos 8.79t$$

When

$t = O$

$\delta = O$

$\dot{\delta}$ = vertical velocity = V_v

$C_1 = O$, $C_2 = V_v/8.79 = 0.114\, V_v$

$$\delta = 0.114\, V_v \sin 8.79\, t$$

But

$$\delta = F_v/3120$$

$$F_v = 356\, V_v \sin 8.79\, t$$

The spin-up loads developed upon landing can be determined as follows:

Wheel torque = $T_w = I_w \dfrac{d^2\theta}{dt^2} = r f F_v$

θ = wheel angular velocity, rad/sec

I_w = wheel moment of inertia

= 1.7 slug - FT^2

r = tire rolling radius = 14.1" ≥ 1.18 ft.

f = Coefficient of sliding friction between tire and ground = 0.55

$$F_v = 356\, V_v \sin 8.79\, t$$

Solution results in

$$\dot{\theta} = 1.55\, V_v \left[1 - \cos 8.79\, t\right] \text{ (radians)}$$

For a landing at (1.25) (stall speed) = 100 FPS

$$\dot{\theta}_{max} = V/r = 100/1.18 = 84.7 \text{ rad/sec}$$

$$\dot{\theta} = 84.7 = 15.5\, V_V \left[1 - \cos 8.79t\right]$$

For V_V = 10 FPS

$$\cos 8.79t = 0.45$$

$$8.79 = 1.10 \quad t = 0.125$$

Thus, the wheel will be fully spun-up at t = 0.125 second; the vertical force at this time acting at the ground is:

$$F_V = (356)\,(10) \sin (8.79)\,(0.125) = 3168 \text{ lb}$$

But the wheel is designed to rebound out of the way at a load of 2600 pounds; thus the peak spin-up load acting at the ground is:

$$F_{SU} = K_{SU}\, 0.55\, F_V = (1.4)\,(0.55)\,(2600) \text{ lb} = 2000 \text{ lb}$$

In combination with a vertical load, F_V = 2600 lb

Considering the requirements of MIL-A-8862, the spring-back load acting at the axle is:

F_{SB} = 1788 lb in combination with

F_V = 2600 lb

An unsymmetrical vertical loading on the gear, in combination with spin-up and spring-back loads shall be considered wherein the total load acting on the forward or aft pair of wheels shall be distributed between the pair in the ratio 60/40, except that the maximum vertical load on one wheel need not exceed 2600 pounds (2.0 g s). This condition results in the following limit loading:

Acting Simultaneously:

F_V = 2600 lb on one wheel with 1733 lb on other

F_{SU} = 2000 lb on one wheel with 1333 lb on other

Acting Simultaneously:

F_V = 2600 lb on one wheel with 1733 lb on other

F_{SB} = 1788 lb on one wheel with 1192 lb on other

For a side drift landing, the following limit loading condition shall be considered acting at the ground:

F_V = 1300 lb acting on each wheel in conjunction

with F_{SIDE} = 1040 lb acting inward on one wheel and

F_{SIDE} = 780 lb acting outward on other wheel

STRESS ANALYSIS

Critical loads for each component of the TUG were taken from the preceding section, and stress analyses were performed, using the same methods developed and applied in Reference 2. Positive margins of safety were found for all components.

FLIGHT TEST PROGRAM

SUMMARY

The flight test program was concluded after two periods of testing. The first period of nine weeks began on 21 September 1964, and the second of six weeks began on 27 September 1965. Twenty-eight test operations were conducted during these two periods, including twenty-four towed glider flights. (Refer to Appendix I.)

A U.S. Army H-34 helicopter was used for all tow missions except for one tow of a zero-payload glider by a UH-1D helicopter. A glider gross weight of 4646 pounds with 2840 pounds payload was the maximum load flown. No POL or odd-geometry type cargo was towed in the glider by the three pilots who accomplished the various missions. (Refer to Appendix II.)

Several glider modifications were accomplished in the field as a result of the test program. Flying techniques and flight envelopes were determined for weights that were attained. Some distances were measured, but no attempt was made to optimize takeoff and landing performance. Extensive instrumentation was not required because sufficient information could be obtained from flight observations for qualitative evaluation. (Refer to Appendix III.)

TEST PROCEDURES

Previous experience with similar towed vehicles resulted in the early establishment of checkout procedures and methods of operation. Necessary ground operations with the test vehicles preceded the first helicopter towed flights. Roadability aspects of the vehicle were checked throughout the program during transport to and from flight operations. Flight operations were primarily centered around weight buildup and flight envelope expansion.

This program was broken into two test periods one year apart, so some repetition of flight preparatory work was required. Also, two different flight crews were used, for which training periods were required.

CONTROLS & INSTRUMENTATION

The tow cable was 3/16-inch steel, encased with multiple conductor electrical wiring in a rubber sheath. Length varied from 400 feet to 485 feet. A cargo hook at the glider end of the cable was attached to a D-ring on the

TUG tow bridle. The other end of the cable terminated in a D-ring for attachment to the helicopter tow harness hook. A 3,000-pound weak link was inserted in the helicopter end of the cable, as was a strain link to measure tow tension.

The glider wing incidence angle could be controlled from the helicopter to any position over the full range of 11 through 21 degrees. Appropriate limit lights and a dial reading position monitor were part of the test equipment. A glider power switch and indicator light were provided to conserve glider battery power. The cable hook at the glider could be released electrically from two positions in the helicopter: by the pilot through a panel switch, or by the airborne glider controller through a control panel button. The hook at the helicopter could be opened to release the tow cable, by the pilot through a stick switch and by the airborne controller through a parallel control panel switch. In addition, the pilot could release the cable by mechanical means through a foot pedal and release wire to the helicopter hook.

A tow cable tension readout was available at the glider controller's station. Standard helicopter flight instruments were used for airspeed, altitude, free air temperature, rate-of-climb/descent and engine power data. Chase aircraft and ground controller comments were also recorded, especially with regard to helicopter-glider altitude differentials and glider body angles. Altitude separation and tow cable angle estimates were also made by the airborne controller.

Ground and airborne photo chase film coverage was obtained. Ground observers measured takeoff and landing distances, although there was no attempt to obtain maximum performance. An impactograph was installed on a few flights but no conclusive data were obtained. Weather information was obtained from base facilities.

GROUND TOW TESTS

Prior to the start of helicopter towed flights, several test vehicle preparatory operations were conducted. The gliders were towed by truck to burn in the brakes and check tracking. The effect of the tow cable input to the brake release handle was closely observed; operation appeared smooth in action even over rough surfaces. Tow bridle and hook movement as well as release operation were checked under load. The Fiberglas spring-axle characteristics were determined over various surfaces and at speeds up to 50 MPH. Wheel centering, tow bar adequacy, and glider turn radius were checked. Radio and other support equipment was checked out, and runway inspection and operating procedures were reviewed.

HELICOPTER PRE-TOW CHECKS

Prior to the start of helicopter tow missions, several operations were conducted with the helicopter, crew, and equipment. Practice takeoff profiles and landing pattern letdowns were flown. Power requirements and techniques to attain specified takeoff windows were determined. Waveoff and emergency procedures were included in crew training. Takeoff, tow and release operations were made with the tow cable only. The airborne gear was checked out and all release modes were operated under load. Runway procedures were reviewed, but no low speed tow/taxi tests with the helicopter-cable-glider combination were made. Experience had shown that the potential hazards and disadvantages far outweighed any benefits that might be gained, especially after adequate pretesting of the separate components of the system.

FLIGHT TEST OPERATIONS.

Procedures were established for complete system checkout. The glider was towed from the hangar to the vicinity of the takeoff area, where the wings were spread and a hookup was made to the helicopter. A complete check of all helicopter release and glider control operations was made. After successful completion of these checks, the system was unhooked and all elements moved to the takeoff area. The cable was stretched out; the helicopter and glider were rehooked ready for takeoff.

A ground controller made general behavior observations from a jeep during the takeoff roll; then he moved to the landing area to provide a landing pattern advisory commentary.

Normally the glider was towed to a test altitude for determination of the level flight envelope. After determination of the envelope of the configuration under test, a descent was followed by a traffic pattern letdown and landing with a ground control advisory. Some turnaround operations were accomplished from the drop zone landing terrain in order to take maximum advantage of limited test range availability.

The flight envelope was established by either holding a constant airspeed and varying the wing angle, or by holding a wing setting and varying airspeed to limiting conditions. One boundary was set by a minimum altitude separation limit between the helicopter and glider. Minimum altitude separation is that altitude difference between the glider with its tow cable and the helicopter tail rotor, which was established for the purpose of flight safety. The other limit was determined by the glider depression angle below the helicopter, established at 60 degrees. The maximum depression angle is the maximum angle of the tow cable from the horizontal to the towed glider. At angles greater than 60 degrees the glider was not lifting itself, much of its weight being carried by the helicopter. Data were taken at each flight condition, including pilot and chase aircraft observer comments.

Initial flight operations were made with zero payload. Based on the results of the previous flight, weight buildup and flight parameters were determined for the next operation. Approximately 500-pound increments were used to build up the payload/gross weight.

Landing waveoffs/flybys were made as required for determination of body angles using the intended landing parameters. The landings were accomplished on a cut signal given by the ground controller with the glider 3 to 5 feet above the terrain. The glider release was activated and followed in 2 to 3 seconds by a release of the tow cable at the helicopter.

TEST CREWS

The test crews were comprised of U.S. Army and Ryan personnel. Army pilots flew the tow and chase helicopters, with Ryan personnel as ground and airborne glider controllers. The aircraft were maintained by Army crews, and the gliders by Ryan. Bell helicopter personnel were on station, but no UH-1D certification for TUG tow was accomplished.

BASE SUPPORT

Yuma Proving Ground provided material, shop and operations support. Hangar space, office space and equipment, normal utilities and base personnel services were provided. Photographic services, chase aircraft, communications equipment and vehicles were used. Range scheduling, weather data, aircraft servicing, and crash and fire equipment were made available. The cooperation and support of base personnel were significant contributions to the program.

TEST RESULTS

A total of 77 work days were spent in the two test periods. The following represents the areas of effort expended as percentages of the total.

Setup/Preparation		22%
Test Operations		34%
Time Lost Due to:		
Range Support	1%	
Weather	5%	
Repairs/Modifications	18%	
Tow Support	20%	
TOTAL LOST		44%
		100%

A total of 24 towed flights out of 28 test operations were performed for a total of 11 hours 34 minutes of flight time. Operations were divided as follows:

TEST PERIOD	FTO's	H-34 TOW	UH-1D TOW	TRUCK TOW	UH-1D CABLE ONLY	H-34 PATTERN PRACTICE
1	16	14	0	2	0	0
2	12	9	1	0	1	1
	28	23	1	2	1	1

The maximum gross weight towed was 4646 pounds, including 2840 pounds payload. Maximum airspeed attained was 80 KIAS; minimum flight speed was 40 KIAS.

SYSTEM MODIFICATIONS

Several minor modifications were incorporated as a result of the test program, especially in the early stages. Included were additions of strut lowering brackets for height clearance, battery tie-down revision to obviate shorts, fin root metal trim to prevent wing tears, and eyebolt for ease of wing removal; modification of wheel centering system; reinforcement of rear spring axle well structure; and installation of spring axle rub angles and guards and protective mitt guard to the tow cable hook.

Major changes were: installation of an improved keel pivot fitting, relocation of upper tow bridle attaching point, bonded and stitched reinforcement of wing trailing edge, and modification of the landing gear skid installation. This last change resulted in a complete revision to the forward body for structural clearance and beef-up to minimize impact damage. This revision added approximately 100 pounds to the glider weight empty, and moved the basic center of gravity forward approximately 4 inches.

LEVEL FLIGHT ENVELOPES (Figure 61)

The majority of flight time was spent on level flight envelope limit investigations as payload and gross weight were increased. Upper airspeed limits were defined by an acceptable helicopter/glider altitude separation, i.e., 75 to 100 feet. The minimum airspeed limit produced an altitude separation in the order of 300 feet. The tow cable depression angle range for these altitude separations was approximately 15 to 60 degrees.

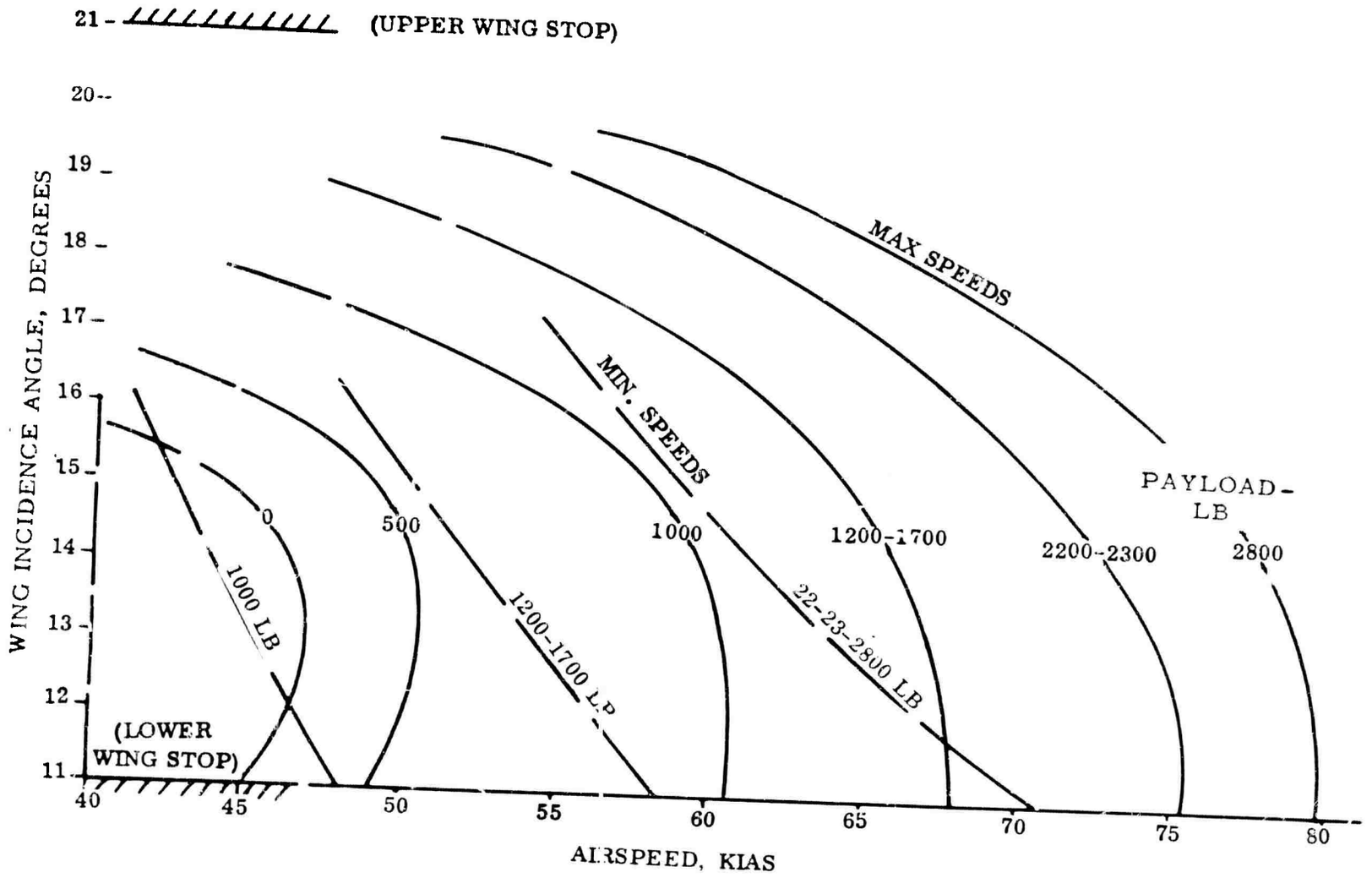

Figure 61. Level Flight Envelopes

The minimum required and maximum allowable airspeeds both increased with weight similar to the stall speed on a free-flight vehicle. The speed spread in some portions of the envelope was less than 10 KIAS for a given wing angle and gross weight. This small speed differential was sufficient to change the glider altitude by over 200 feet, and is an indication of the rather rigorous observance of a speed schedule that was required.

An additional upper velocity limit was encountered at 75 and 80 knots in the form of wing fabric trailing edge high-frequency flutter. This flutter caused trailing edge tearing which resulted in asymmetric towed flight, and in one case complete loss of control, and crash. The course of the flight test program did not permit evaluation of remedial designs of the wing fabric.

An operational flight envelope would fall within the limits of the indicated allowable envelope. However, further definition of some random glider characteristics would be required; c.g., lateral oscillation and fabric flutter at high speed, pitch oscillations at low speed, and spontaneous movement in turbulence.

REPRESENTATIVE FLIGHT DATA

Figure 62 presents the plotted data from flight test operations (FTO) 27 and 28. These two operations were at the same gross weight and were the last flights flown in the test program.

A notation of the estimated tow cable depression angle is made at each level flight point. Takeoff, climb, descent and landing points are identified. All fall within the scope of the level flight envelope.

TOW CABLE TENSION

Tow cable tension (Figure 63) was measured by recording the output of a strain link attached to the helicopter harness and the tow cable. Figure 63 shows the magnitude and relative tow cable loads for takeoff, climb, and cruise conditions. Descent and landing loads were equivalent or less than the given level flight values.

TAKEOFF & LANDING DISTANCES

Some takeoff and landing distance measurements were taken (Figure 64), although no attempt was made to optimize performance. Figure 64 indicates trends and shows order of magnitude of the uncorrected data.

The variations in takeoff points are probably due to the different techniques of two different crews. Takeoff profile and the amount and rate of helicopter power application are some of the variables. The spread in the landing curves can be attributed to the difference in braking pressures.

AIRSPEED CORRECTION

The level flight airspeed correction for the CH-34 helicopter is shown in Figure 65. This helicopter performed all tow missions except one. This curve includes both instrument and position error corrections.

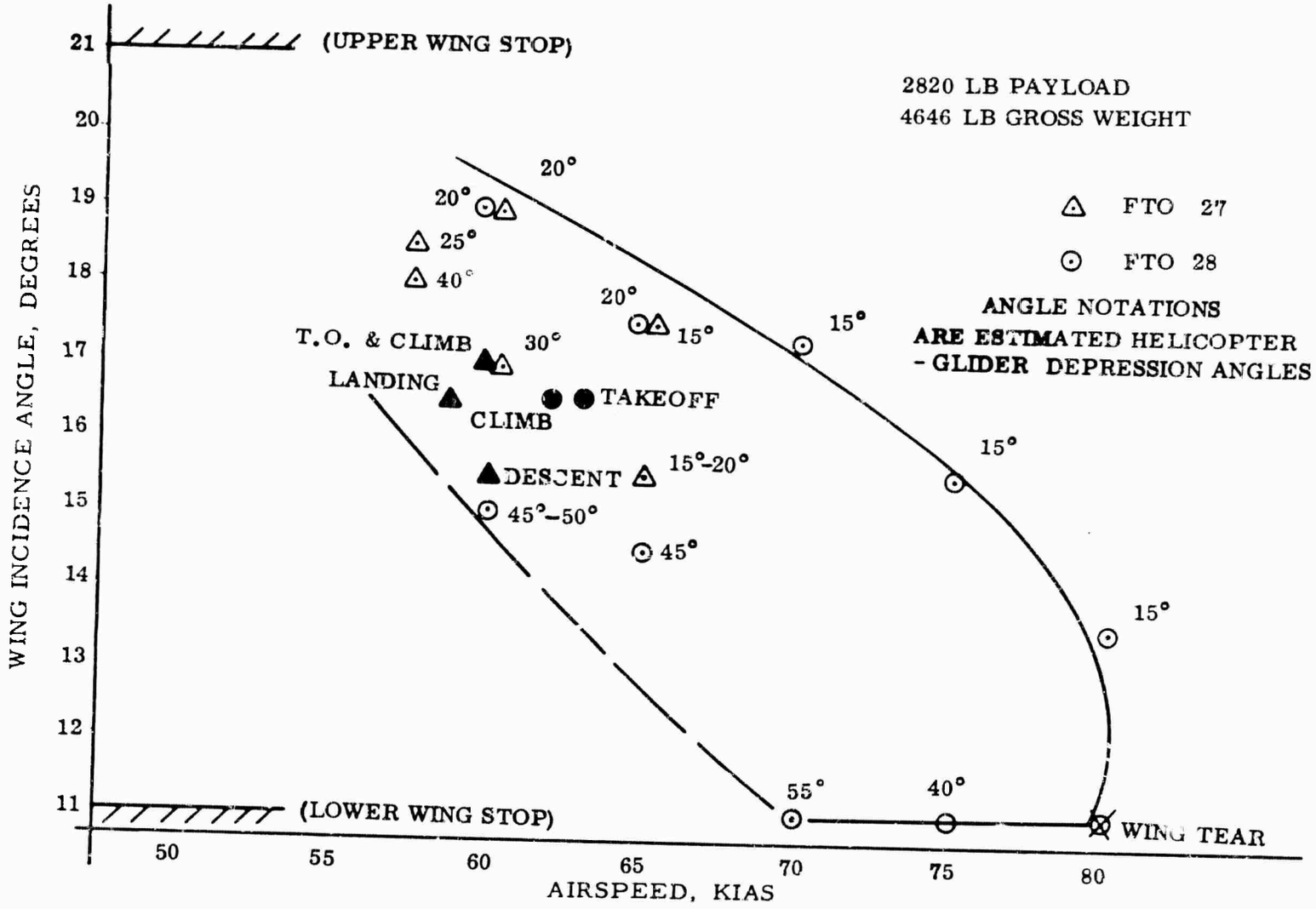

Figure 62. Representative Flight Data

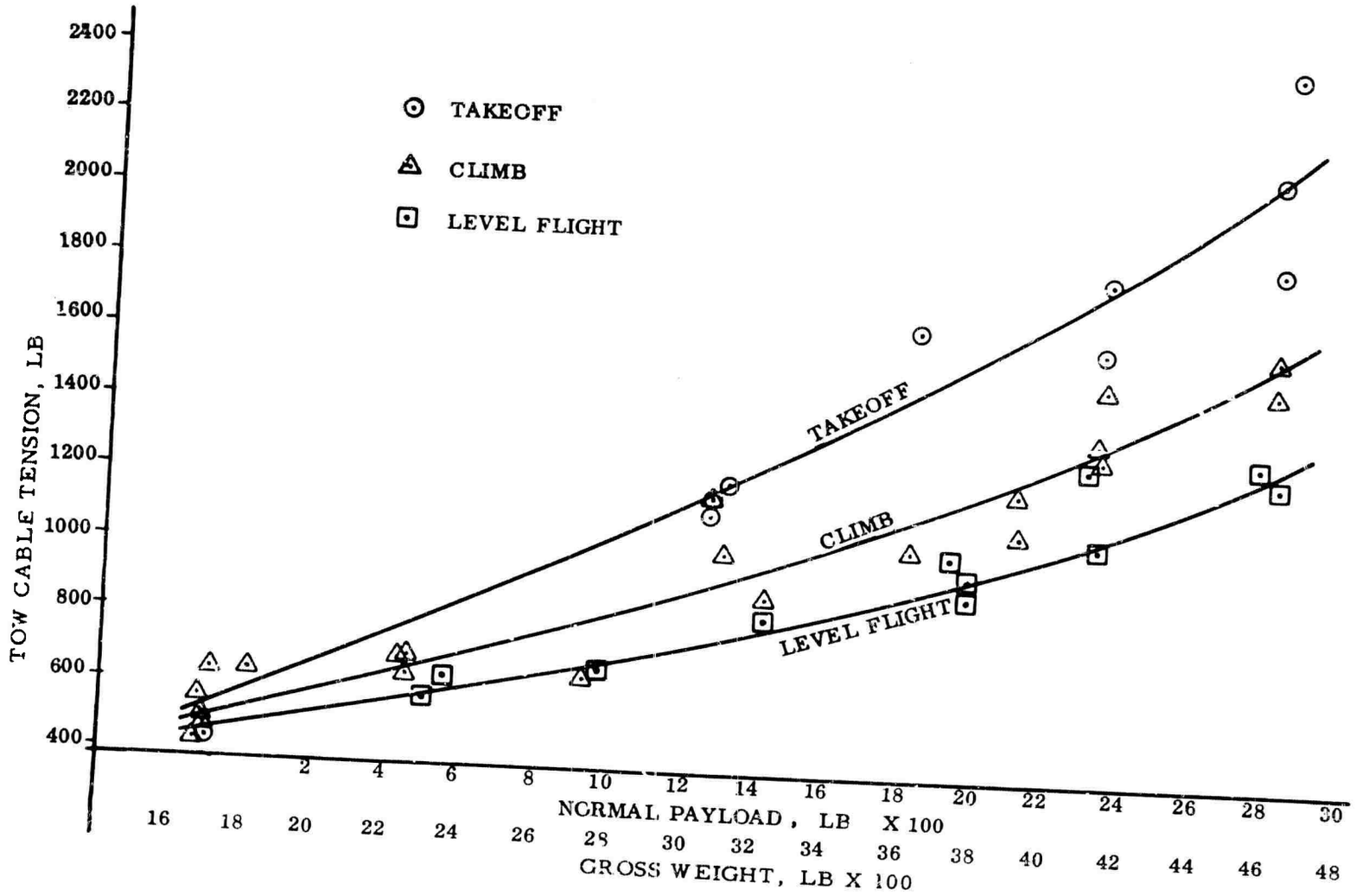

Figure 63. Tow Cable Tension

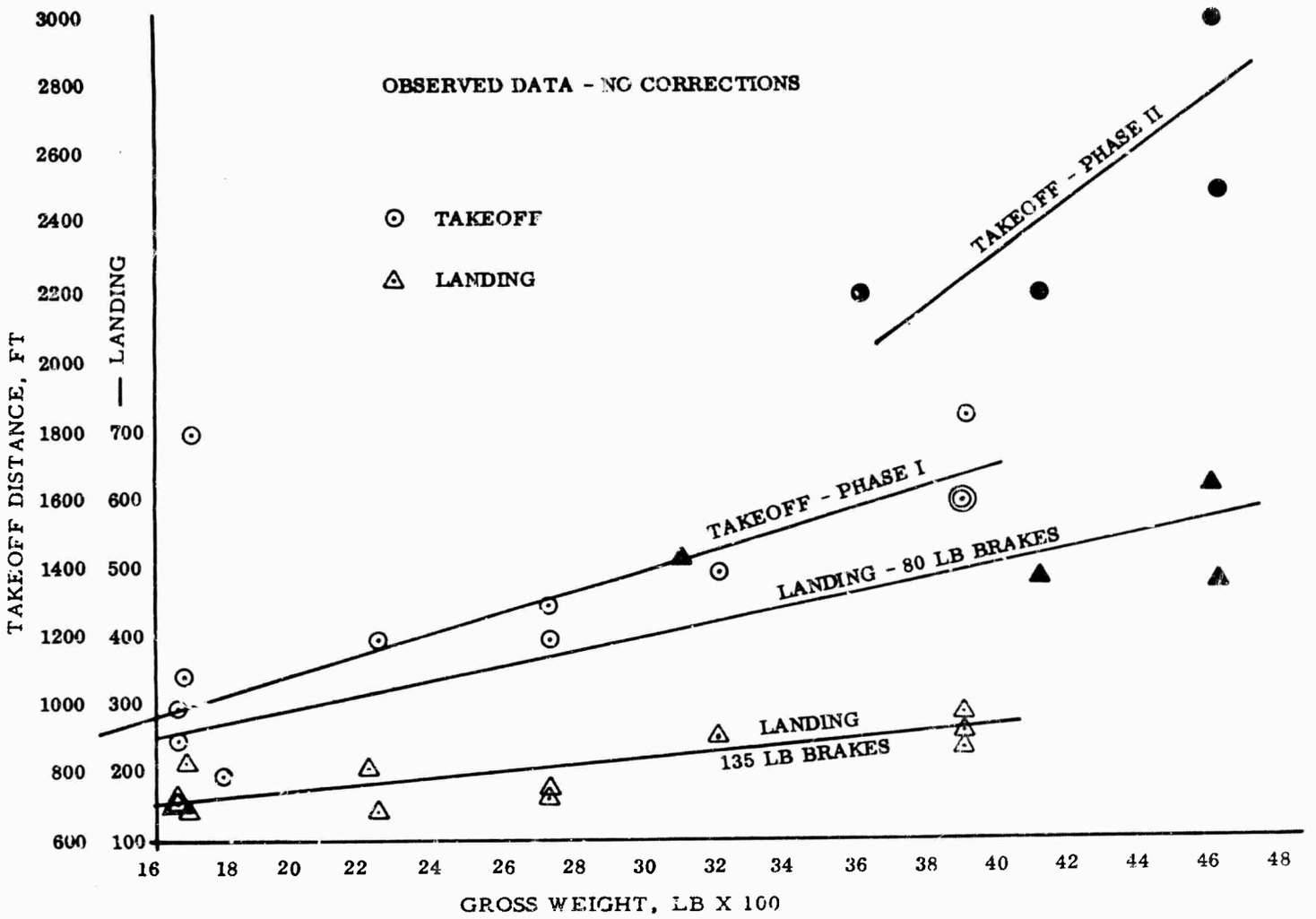

Figure 64. Takeoff and Landing Distances

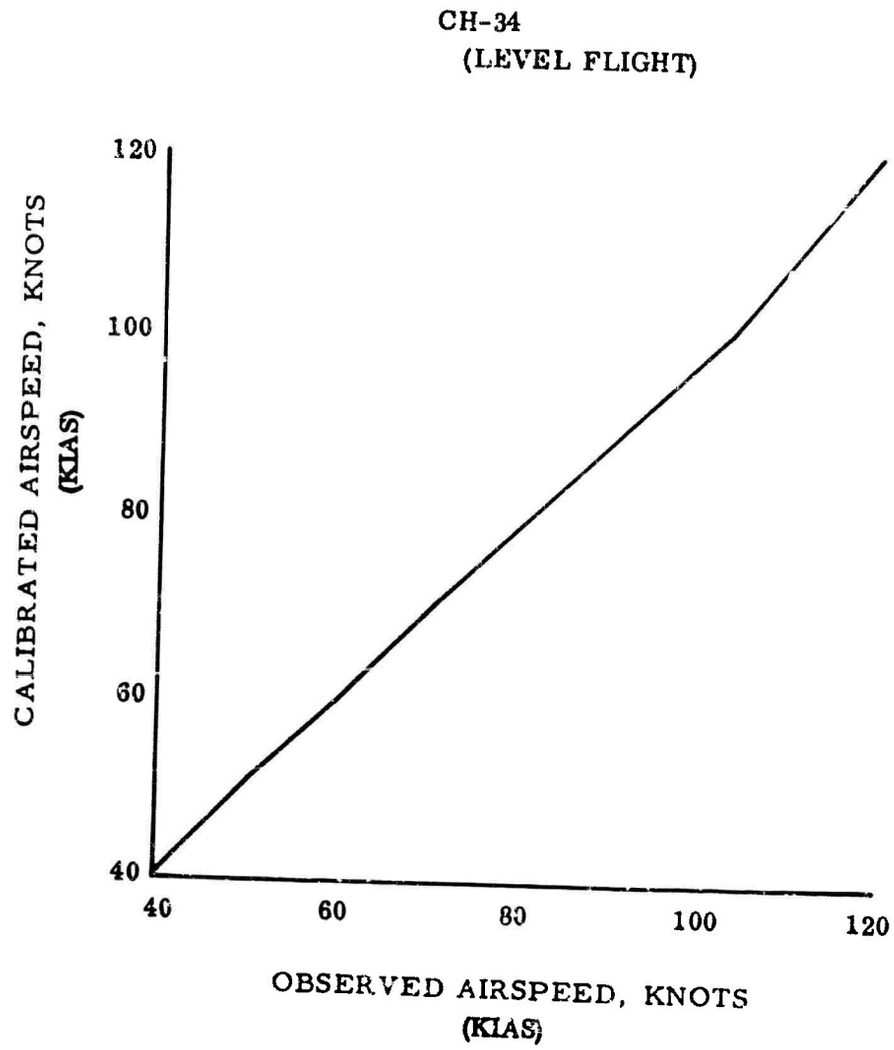

Figure 65. Airspeed Correction

CONCLUSIONS

The results of the flight test program have demonstrated the feasibility of the TUG system.

The flight performance characteristics satisfied all expectations for towed missions. Takeoff and landing maneuvers on tow with the H-34 helicopter did not present any serious problems and were highly successful. Towed flight operations were conducted with payloads up to 2840 pounds. The velocity envelope over the weight range extended from 40 knots indicated airspeed for an empty glider to 80 knots for a glider gross weight of 4646 pounds (2820-pound payload).

At 75- and 80-knot speeds, the trailing edge of the flexible wing set up a destructive high-frequency flutter which resulted in wing fabric tearing. The addition of fabric doublers did not help this problem, and a wing configuration with battens and boltropes had not been flight tested when the test program was concluded due to vehicle damage. This damage consisted mostly of torn wing membranes and delaminated running gear springs.

It was concluded that:

- The TUG vehicle was practicable.
- An operating limit speed of 70 knots due to wing trailing edge flutter exists with the present configuration.
- Forces felt by the towing helicopter through the tow cable were 1/3 to 1/2 of the TUG gross weight in all flight regimes.
- Rehabilitation of the test vehicles and further flight testing and testing of wing design improvements is required if the 70-knot limit noted above is to be raised.
- Rehabilitation of the test vehicles and resumption of flight testing are required to confirm operating weights above the 2840-pound payload thus far reached.

REFERENCES

1. Gessow, Alfred, and Tapscott, Robert J.: Charts for Estimating Performance of High Performance Helicopters. NACA Technical Report No. 1266, 1956

2. Gessow, Alfred, and Crim, Almer D.: An Extension of Lifting Rotor Theory to Cover Operation at Large Angles of Attack and High Inflow Conditions. NACA Technical Note 2665, 1952

3. Northrop Aircraft, Inc.: Dynamics of the Airframe. BUAER Report No. AE-6-4II, 1952

4. Merkle, E.U.: Substantiating Data for the Standard Aircraft Characteristics Charts for the UH-1B Helicopter, Bell Helicopter Company, Report No. 204-099-763, June 1961

5. Ryan Aeronautical Co., Flexible Wing Air Cargo Delivery System, Final Program Report, Ryan Report 63B109, 31 October 1963

6 NACA TN D-983, Low Subsonic Pressure Distribution on Three Rigid Wings Simulating Paragliders with Varied Canopy Curvature and Leading-Edge Sweep, Unpublished

APPENDIX I

OPERATIONS LOG - TUG

FTO 179-	DATE	VEHICLE		FLIGHT TIME		WEIGHT - LB		C G		PERTINI CONFIGURA ITEMS
		BODY	WING	FTO	ACCUM	GROSS	PAYLOAD	STA	W. L.	
1(T)	10-7-64	1	1	0	0	1724	0	168.2	48.0	Basic TUG - Wi
2	8	1	1	:18	:18	1724	0	168.2	48.0	LUG type fwd w
3(T)	9	2	2	0	:18	1710	0	168.6	47.3	All mods incorp
4	13	2	2	:25	:43	1710	0	168.6	47.3	---
5	14	2	2	:22	1:05	1710	0	168.6	47.3	Keel - S/B shin
6	15	2	2	:24	1:29	2260	573	169.5	45.0	Back to Std. bra
7	21	3	3	:35	2:04	1687	0	168.7	46.8	Tow bridle up 1
8	22	3	3	:27	2:31	1687	0	168.7	46.8	Tow bridle up 2
9	23	3	3	:21	2:52	2232	567	169.4	45.7	Tow bridle up 2
10	11-5-64	3	3	:44	3:36	2744	1079	169.5	43.3	Bridle up 10 inc
11	5	3	3	:09	3:45	2744	1079	169.5	43.3	---
12	6	3	3	:20	4:05	3230	1565	169.3	43.5	---
13	9	3	3	:20	4:25	3926	2261	169.5	35.4	---
14	9	3	3	:09	4:34	3926	2261	169.5	35.4	Removed tow ba
15	11	3	3	:19	4:53	3926	2261	164.2	35.4	L. G. fwd. 5.3 i
16	20	1	1	:21	5:14	1824	0	164.7	44 4	Fwd fuselage &
PROGRAM SUSPENDED										
17	10-4-65	-	-	0	5:14	-	-	-	-	Helo & cable on
18	6	-	-	0	5:14	-	-	-	-	Helo only - no c
19	7	1	1	0	5:14	1815	0	164.7	44.4	Repeat of 179-1
20	8	2	2	:32	5:46	1821	0	166.3	44.4	UH-1D Tow
21	15	1	3	:48	6:34	3078	1247	170.0	36.4	Wing/Body chan
22	19	1	1	:40	7:14	3119	1247	169.0	36.4	---
23	20	1	1	:50	8:04	3631	1759	170.7	33.9	---
24	21	1	1	:50	8:54	4150	2319	170.5	39.6	---
25	26	2	3	1:00	9:54	4140	2334	169.5	33.8	Doubler on wing
26	27	2	4	:10	10:04	4646	2840	170.0	37.9	New wing - no d
27	28	2	4	:55	10:59	4626	2820	169.9	35.7	Rerigged RT wi
28	11-2-65	2	4	:35	11:34	4626	2820	169.9	35.7	Bonded doubler
END PROGRAM										

C G		PERTINENT CONFIGURATION ITEMS	FLIGHT SUMMARY
STA	W. L.		
168.2	48.0	Basic TUG - Wings folded	Truck Tow - 4 Runs
168.2	48.0	LUG type fwd wing pivot	11-15-17°, 40-50 KIAS H-34 Fire-Jettison
168.6	47.3	All mods incorp	Truck Tow - 4 Runs
168.6	47.3	---	No Data-Turbulence and out of trim - DZ LDG, OK
168.6	47.3	Keel - S/B shim decr break	11-13-15-17°, 40-50 KIAS DZ LDG. OK
169.5	45.0	Back to Std. brake press	11-13-15-17°, 40-50 KIAS DZ Hard LDG
168.7	46.8	Tow bridle up 10 inches	Lateral Osc - Turbulence - LDG OK
168.7	46.8	Tow bridle up 20 inches	15-13-11°, 40-50 KIAS 17°, 40 KIAS LDG OK
169.4	45.7	Tow bridle up 20 inches	15-13-11°, 45-55 KIAS 17°, 50 KIAS DZ LDG OK
169.5	43.3	Bridle up 10 inches here and on	15-13-11°, 45-60 KIAS 17°, 45 KIAS LDG OK
169.5	43.3	---	Turnaround Flt DZ - T.O., Pattern and LDG OK
169.3	43.5	---	11 thru 17°, 50-65 KIAS DZ OK
169.5	35.4	---	11 thru 17°, 55-75 KIAS DZ Bowed "A"
169.5	35.4	Removed tow bars	Turnaround Flt - DZ T.O./Pattern/LDG 17° OK
164.2	35.4	L.G. fwd. 5.3 inches	15 thru 21° - Small Envelope—DZ LDG–Crack Struts
164.7	44.4	Fwd fuselage & skid mod	11° only reliable data - NG pitch monitor
-	-	Helo & cable only	UH-1D Towing cable only
-	-	Helo only - no cable	CH-34 Practice landing patterns
164.7	44.4	Repeat of 179-16	Lat. Osc. On T.O. -50' Jettison - Struts Folded
166.3	44.4	UH-1D Tow	Poor T.O. -Small Envelope-Wing Torn - LDG Damage
170.0	36.4	Wing/Body change	CH-34 Tow 11-20°, 45-65 KIAS No damage LDG.
169.0	36.4	---	11 thru 17°, 55-70 KIAS Light damage LDG
170.7	33.9	---	11 thru 16°, 50-68 KIAS No damage LDG
170.5	39.6	---	Wing Torn - Weak Link Broke - Crash LDG
169.5	33.8	Doubler on wing T. E.	11 thru 18° 50-80 KIAS Light damage LDG.
170.0	37.9	New wing - no doubler	Lost down-wing control after T.O. DZ LDG
169.9	35.7	Rerigged RT wing dn	Excessive T.B. Flutter - small envelope DX LDG
169.9	35.7	Bonded doubler on T. E.	11 thru 19°, 60-80 KIAS, Wing Torn, jettison crack

APPENDIX II
TUG CONFIGURATION AND PERFORMANCE SUMMARY

FTO		TOW HELO.		VEHICLE		WEIGHT LB GROSS PAYLOAD	C G HORIZ VERTICAL	TOW BRIDLE	LANDING GEAR	BRAKES	BODY STRUCTURE	WING-KEEL SPREADER BAR
NO. 179-	DATE	TYPE S/N	PILOT	BODY	WING							
1(T)	10-7-64	N/A	N/A	1	1	1724 0	168.2 48.0	Original	Modified to Std Configuration	Modified to Standard Configuration	Modified to Std Configuration	Modified to Std. Configuration
2	10-8-64	CH-34 030	BERRY	1	1	1724 0	168.2 48.0	Original	Instl spring guards	Modified to Standard Configuration	Modified to Std Configuration	Keel ball joint replaced with lug type block pivot assembly
3(T)	10-9-64	N/A	N/A	2	2	1710 0	168.6 47.3	Original	Instl spring guards	Modified to Standard Configuration	Modified to Std Configuration	Keel ball joint replaced with lug type block pivot assembly
4	10-13-64	CH-34 030	BERRY	2	2	1710 0	168.6 47.3	Original	Instl spring guards	Modified to Standard Configuration	Modified to Std Configuration	Keel ball joint replaced with lug type block pivot assembly
5	10-14-64	CH-34 030	BERRY	2	2	1710 0	168.6 47.3	Original	Instl spring guards	Lever pressure reduced 135 to 80 lb	Instl rubber angle on rear spring well area	Instl shim S/E to keel
6	10-15-64	CH-34 030	BERRY	2	2	2260 573	189.5 45.0	Original	Instl spring guards	Changed back to Std. 80 to 135 lb (Std.)	Instl rubber angle on rear spring well area	Install shim S/E to keel
7	10-21-64	CH-34 030	BERRY	3	3	1687 0	168.7 46.8	Up 10" alan' Ht. of Fwd. A-Frame from orig	Instl spring guards	Changed back to Std. 80 to 135 lb (Std.)	Instl reinf doublers rear spring well area	Std (Incl previous modifications)
8	10-22-64	CH-34 030	BERRY	3	3	1687 0	168.7 46.8	Up 20" (Upper cable sleeves) from orig	Instl spring guards	Changed back to Std. 80 to 135 lb (Std.)	Instl. reinf. doublers rear spring well area	Std (Incl previous modifications)
9	10-23-64	CH-34 030	BERRY	3	3	2232 567	169.4 45.7	Up 20" (Upper cable sleeves) from orig	Instl spring guards	Changed back to Std. 80 to 135 lb (Std.)	Instl reinf doublers rear spring well area	Std (Incl previous modifications)
10	11-5-64	CH-34 030	BERRY	3	3	2744 1079	169.5 43.3	Lowered 10" Now 10" up from orig	Instl spring guards	Changed back to Std. 80 to 135 lb (Std.)	Instl reinf doublers rear spring well area	Std. (Incl previous modifications)
11	11-5-64	CH-34 030	BERRY	3	3	2744 1079	169.5 43.3	Lowered 10" Now 10" up from orig	Instl spring guards	Changed back to Std. 80 to 135 lb (Std.)	Instl reinf doublers rear spring well area	Std (Incl previous modifications)
12	11-6-64	CH-34 030	BERRY	3	3	3230 1565	169.3 43.5	10" up frem orig	Std + guards	Std	Std	Std (Including block pivot assy)
13	11-9-64	CH-34	BERRY	3	3	3926 2261	169.5 35.4	10" up from orig	Std + guards	Std	Std	Std (including block pivot assy)
14	11-9-64	CH-34 030	BERRY	3	3	3926 2261	169.5 35.4	10" up from orig	Std + guards	Std	Removed tow bars	Std (including block pivot assy)
15	11-11-64	CH-34 030	BERRY	3	3	3926 2261	164.2 35.4	10" up from orig	Std + guards	Std	Removed tow bars	Std (including block pivot assy)
16	11-20-64	CH-34	BERRY	1	1	1824 0	164.7 44.4	10" up from orig	Instl fwd skid mod	Std	Front end cutout for repairs	Modified to Std

	ELECTRICAL SYSTEM	INSTRUMENTATION	TAKEOFF			LANDING			REMARKS
			WING ∠ KIAS	DISTANCE SURFACE DIRECTION	WIND-VEL. KNOTS DIRECTION	WING ∠ KIAS	DISTANCE SURFACE DIRECTION	WIND-VEL. KNOTS DIRECTION	
	Mod battery tie-down with insulation material	Modified pitch monitor system to Std. Configuration	N/A	N/A	N/A	N/A	N/A	N/A	Truck tow only
	Mod. battery tie-down with insulation material	Modified pitch monitor system to Std Configuration	15° 50	1800' Runway 350°	Calm	Jettison 1500' terrain 11° - 40	110' Rough 30°	Calm	First tug flight cockpit fire 1500' jettison - boondock LDG - Moderate damage
	Mod. battery tie-down with insulation material	Modified pitch monitor system to Std Configuration	N/A	N/A	N/A	N/A	N/A	N/A	Truck tow only
	Mod. battery tie-down with insulation material	Modified pitch monitor system to Std Configuration	15° 42	700' Runway 170°	7 150°	11° 40	150' DZ 70°	4 90°	Atmospheric turbulence
	Mod. battery tie-down with insulation material	Modified pitch monitor system to Std Configuration	16° 40	1100' Runway 350°	Calm	11° 36	220' DZ 70°	Calm	Small flight envelope
	Reran 3 wires from hook to terminal board in helo.	Modified pitch monitor system to Std Configuration	16° 42	1200' Runway 350°	3 350°	13° 45	150' DZ 70°	Calm	Hard landing
18)	Reran 3 wires from hook to terminal board in helo.	Modified pitch monitor system to Std Configuration	15° 50	1000' Runway 350°	3 090°	11° 40	160' DZ 70°	Calm	Atmospheric turbulence
18)	Reran 3 wires from hook to terminal board in helo.	Impactograph Sta. 130	15° 50	900' Runway 350°	4 090°	11° 40	160' DZ 70°	Calm	No impactograph data
	Reran 3 wires from hook to terminal board in helo.	Impactograph Sta. 200	16° 50	2090' Runway 170°	6-8 150-160°	15° 45	210' DZ 100°	4 120°	
	Reran 3 wires from hook to terminal board in helo.	Impactograph Sta. 200	16° 45	1200' Runway 350°	3 0-45°	15° 45	180' DZ 70°	Calm	
	Reran 3 wires from hook to terminal board in helo.	Impactograph Sta. 200	15° 45	1300' DZ 070°	Calm	15° 45	170' DZ 70°	Calm	Turnaround flight on DZ
	Std and previous mods	Impactograph Sta. 200	16° 60	1400' Runway 350°	2 030°	15° 52	260' DZ 070°	Calm	—
	Std and previous mods	Impactograph Sta. 230	17° 45	1600' Runway 350°	Calm	15° 55	270' DZ 70°	Calm	4-wheel touchdown on LDG - light damage
	Std and previous mods	Impactograph Sta. 230	17° 55	1600' DZ 070°	Calm	17° 55-45	290' DZ 70°	Calm	Turnaround flight on DZ
	Std and previous mods	Impactograph Sta. 230	19° 55	1850' Runway 350°	7 270°	19° 55-45	240' DZ 70°	Calm	CG forward 5.3"
	Std mods	Impactograph Sta. 170	17° 50	800' Runway 350°	3 360°	11° 42	140' DZ 270°	6-9 300°	Skid mod CG forward 3.5"

APPENDIX II
TUG CONFIGURATION AND PERFORMANCE SUMMARY
(CONTINUED)

FTO		TOW HELO.		VEHICLE		WEIGHT ~LB GROSS PAYLOAD	C G HORIZ VERTICAL	TOW BRIDLE	LANDIN
NO. 179-	DATE	TYPE S/N	PILOT	BODY	WING				
17	10-4-65	UH-1D 032	HARTWIG	N/A	N/A	N/A	N/A	N/A	N/A
18	10-6-65	CH-34 030	WOMACK	N/A	N/A	N/A	N/A	N/A	N/A
19	10-7-65	CH-34	WOMACK	1	1	1815 0	164.7 44.4	10" up from orig	Instl fwd skid mod
20	10-8-65	UH-1D 032	HARTWIG	2	2	1821 0	166.3 44.4	10" up from orig	Instl fwd skid mod
21	10-15-65	CH-34 030	WOMACK	1	3	3078 1247	170.0 36.4	10" up from orig	Instl fwd skid mod
22	10-19-65	CH-34 030	WOMACK	1	1	3119 1247	169.0 38.4	10" up from orig	Instl fwd skid mod
23	10-20-65	CH-34 030	WOMACK	1	1	3631 1247	170.7 36.4	10" up from orig	Instl fwd skid mod
24	10-21-65	CH-34 030	WOMACK	1	1	4150 2319	170.1 39.6	10" up from orig	Instl fwd skid mod
25	10-26-65	CH-34 030	WOMACK	2	3	4140 2334	169.5 33.8	10" up from orig	Instl fwd skid mod
26	10-27-65	CH-34 030	WOMACK	2	4	4646 2840	170.0 37.9	10" up from orig	Instl fwd skid mod
27	10-28-66	CH-34	WOMACK	2	4	4626 2820	169.9 35.7	Mod to Std	Mod to Std
28	11-2-65	CH-34	WOMACK	2	4	4626 2820	169.9 35.7	Mod to Std	Mod to Std

NDING GEAR	BRAKES	BODY STRUCTURE	WING-KEEL SPREADER BAR	ELECTRICAL SYSTEM	INSTRUMENTATION	T.	
						WING ∡ KIAS	DIS SUI DIR
	N/A	N/A	N/A	N/A	N/A	N/A	
	N/A	N/A	N/A	N/A	N/A	N/A	
l fwd mod	80 lb lever pressure	Mod to Std	Mod to Std	Mod to Std	None	17° 50	
fwd mod	80 lb lever pressure	Mod to Std	Mod to Std	Mod to Std	None	17° 50	
fwd mod	80 lb lever pressure	Mod to Std	Mod to Std	Mod to Std	None	16° 55	
fwd mod	90 lb lever pressure	Mod to Std	Mod to Std	Mod to Std	None	16° 60	
fwd mod	80 lb lever pressure	Mod to Std	Mod to Std	Mod to Std	None	16° 60	
fwd mod	80 lb lever pressure	Mod Std	Mod to Std	Mod to Std	None	17° 60	
fwd mod	80 lb lever pressure	Mod to Std	Added 2-1/2 inch doubler to wing T. E.	Mod to Std	None	17° 48	
fwd mod	90 lb lever pressure	Mod to Std	Std (new wing) w/o doubler)	Mod to Std	None	18° 60	
o	80 lb lever pressure	Mod to Std	R/H wing rigged down 4 turnbuckle turns	Mod to Std	None	17° 60	
o	80 lb lever pressure	Mod to Std	Instl bonded doubler on wing T.E. and new fin	Mod to Std	None	16.5° 63	

TION	TAKEOFF			LANDING			REMARKS
	WING ∡ KIAS	DISTANCE SURFACE DIRECTION	WIND-VEL. KNOTS DIRECTION O.A.T.	WING ∡ KIAS	DISTANCE SURFACE DIRECTION	WIND-VEL. KNOTS DIRECTION O.A.T.	
	N/A	N/A	—	N/A	N/A	—	Helicopter with cable tow only.
	N/A	N/A	—	N/A	N/A	—	Helicopter only practice landing passes on DZ.
	17° 50	— Runway 350°	2.3 K 60°	—	—	—	Jettison just after T.O. due to oscillations
	17° 50	— Runway 350°	Calm 22°C	11° 45	— DZ —	Calm — — —	Wing T.E. tear noted in flight hard DZ LDG
	16° 55	— Runway 60°	Calm — 22°C	15° 45	— DZ 90°	Calm — —	No damage landing
	16° 60	2100' Runway 60°	4 K 40° 18°C	15° 45	537' DZ 90°	Calm — —	Min. damage LDG
	16° 60	2200' Runway 60°	Lt -Var — 20°C	14° 50	— DZ 300°	4-6 K 300° —	No damage LDG
	17° 60	— Runway 60°	Calm — 26°C	— — —	— — —	— — —	Wing tore - later the weak link broke - crash & vehicle expended
	17° 48	2200' Runway 60°	Calm — 22.5°C	16° 55	490' DZ 270°	Calm — 25°C	T.E. Doubler partially torn loose during flight
	18° 60	25-2600' Runway 60°	4 KT 80° 24°	16° 55	480' DZ 270°	Calm — 24°C	Lost down wing control after T.O. DZ LDG w/chase control
	17° 60	3000' Runway 60°	Calm — —	16.5° 57-60	625' DZ 270°	Calm — 25°C	T.E. flutter small envelope
	16.5° 63	— Runway 60°	2-4 KT 90° 18°	— — —	— — —	— — —	Wing torn - crash - expended

FTO 179-	FLT COND	i_w DEG	KIAS	LB TOW TENSION	ϕ D DEG	Δh FT	MAP "HG	OAT °C	REMARKS
1(T)		TRUCK TOW ONLY - NO FLIGHT DATA -							
2	Grd	15	15				45	28	Wing fill
	T.O.	15	50				45	28	
	Climb	15	50	640	15	100	35	28	
	Level	15	45	500	40	200	31	29	
	Level	15	40	420	45	200	30	29	
	Grd	15	50	560	10	50	31	29	High
	T.O.	11	50	580	10	75	31	29	
	Climb	11	45	420	15	100	30	29	
	Level	11	40	460	60	300	30	29	
	Turn	11	40					29	Turn OK
	Level	17	40	400	10	50	30	29	
	Prior Descent	11	40	— FIRE - JETTISONED GLIDER AND THEN TOW CABLE —					
3(T)		— TRUCK TOW ONLY — NO FLIGHT DATA —							
4	Grd	15	18				45	28	Wing fill
	T.O.	15	42	440			45	28	Too high in turn
	Climb	15	50				33	28	
	"	13	45						OK turn
	Level	15	50			150 50			Spontaneous

FTO 179-	FLT COND	i_w DEG	KIAS	LB TOW TENSION	ϕ D DEG	ΔL LT	MAP "HG	OAT °C	REMARKS
4	Level	11	40	300	20	150			
Cont	Ldg pass	11	40	460					2-3° nose up
	Ldg	11	40						
ATMOSPHERIC TURBULENCE & TRIM CONDITION CANCELLED FURTHER TESTING									
5	Grd	16	15				45	25	
	T.O.	16	40				45	25	
	Climb	15	45	480	35	200	35	25	
	Climb	15	50	500	15	100	35	25	
	Level	15	40	320	15	100	30	25	
	Level	15	50	400	5	25	30	25	Too high
	Level	13	40	540	60	300	30	25	
	Level	13	50	400	10	75	30	25	
	Level	11	50	440	15	100	30	25	
	Level	11	40	420	60	300	30	25	
	Level	17	40	400	10	100	30	25	
	Descent	11	43	400	10	100	31	25	2-300 fpm
	Ldg	11	38				29	25	
6	Grd	16	20				45	25	
	T.O.	16	42				45	25	
	Climb	11	55	640	20	150	34	25	
	Climb	11	60	680	15	100	34	25	
	Level	15	50	560	15	100	32	25	

FTO 179-	FLT COND	i_w DEG	KIAS	LB TOW TENSION	γ D DEG	Δh FT	MAP "Hg	OAT °C	REMARKS
6	Level	15	40	480	25	250	30	25	±100' Rise and Fall
Cont	Level	13	40	560	30	200	30	25	
	Level	13	50	540	10	50	30	25	
	Level	11	55	520	5	25	30	25	Too high
	Level	11	40	560	60	350	30	25	Lt. pitch osc.
	Level	17	40	520	15	100	30	25	
	Ldg	13	45				30	25	
7	Grd	15	15				46	23	Wing fill
	T.O.	15	50				46	23	
	Climb	15	50	440	20	150	35	23	
	Level	15	50	— LATERAL OSCILLATION —					
	Level	11	40	340	20	150	30	23	
	Ldg	11	40	440	30	200	29	23	
ATMOSPHERIC TURBULENCE CANCELLED FURTHER TESTING									
8	Grd	15	15				49	21	
	T.O.	15	50				49	21	
	Climb	15	50	560	30	200	35	24-27	
	Level	15	50	400	5	50	30	26	Too high
	Level	15	40	360	15	150	29	26	
	Level	13	40	460	30	250	30	26	
	Level	13	50	500	5	25	30	26	Too high
	Level	11	50	420	10	100	30	26	OK
	Level	11	40	440	45	300	30	26	
	Level	17	40	340	10	100	30	26	
	Ldg	11	40						

FTO 179-	FLT COND	i_w DEG	KIAS	LB TOW TENSION	ϕ D DEG	Δh FT	MAP "HG	OAT °C	REMARKS
9	Grd	16	12				47	27	Wing fill
	T.O.	16	50				47	27	
	Climb	16	55	680	15	150	35	27	
	Level	15	55	600	20	150	32	26	±100' rise & fall
	Level	15	45	4-500	45	250	30	25	Lt. pitch osc.
	Level	13	55	560	10	75	30	25	
	Level	13	45	680-700	30	300	30	25	Pitch Osc.
	Level	11	50	560			31	25	Lt. pitch osc.
	Level	11	55	600	10	75	31	25	
	Level	17	50	480	15	150	30	25	
	Ldg	15	45						
10	T.O.	16	45				46	18	
	Climb	15	60	640	25	200	37	20	
	Level	15	60	620	10	75	35	22	
	Level	15	45	640	50	300	31.5	22	Pitch Osc.
	Level	13	45	540	50	250	29.5	20.5	Pitch Osc.
	Level	13	60	540	20	150	31.5	21.5	
	Level	11	60	600	20	150	31.5	22	
	Level	11	50	580	60	300	30.5	21.5	
	Level	17	45	500	30	150	30	22	
	Ldg	15	45				29	20	
11	(NO DATA)								
	TURNAROUND FLIGHT ON DZ								

FTO 179-	FLT COND	iw DEG	KIAS	LB TOW TENSION	◁ D DEG	Δ h FT.	MAP "HG	OAT °C	REMARKS
12	T.O.	16	60			200	4[illegible]		
	Climb	15	60	880	15	100	37.5	21	
	Level	15	65	760	10	75	33.5		
	Level	15	50	760	60	350	31.0		
	Level	13	55	760	50	300	31.5		Lt. p[illegible]ch osc.
	Level	13	65	760	15	100	33.0		
	Level	11	65	780	5	50	33.0		
	Level	11	55	840	60	300	32.0		Lt. pitch osc.
	Level	17	60	740	10	100	33.0		
	Level	17	50	720	60	250	31.5		Dutch roll
	Ldg	15	52						
13	Grd	17	20				49	14	
	T.O.	17	45				49	14	Helo nose dov.
	Climb	17	60	1080	45	200	42	14	attitude limit
	Lev	17	55	960	50	300	35	16	
	Level	17	65	820	10	75	35	16	
	Level	15	70	820	10	50	35	16	
	Level	15	55	900	45/50	200/300	33	18	
	Level	13	55	900	60	350	33	18	
	Level	13	70	880	15	100	36	18	
	Level	11	75	960	10	75	35	18	
	Level	11	60	880/920	50	300	37	[illegible]	Lt. pitch osc.
	Ldg	15	55				33	18	

FTO 179-	FLT COND	i_w DEG	KIAS	LB TOW TENSION	$\dot{q}$ D DEG	Δh FT	MAP "HG	OAT °C	REMARKS
TURNAROUND FLIGHT ON DZ									
14	T.O.	17	60						
	Pattern	17	55	880	50	300			Lt. pitch osc.
	Ldg.	17	55						
15	Grd	19	20			49	14		Wing fill
	T.O.	19	55			49	14		
	Climb	19	60	1200	30	200	42	12	
	Level	19	65	860	10	75	40	12	
	Level	17	67	920	15	100	35	12	Helo nose dwn attitude limit
	Level	15	67			300	35	12	Helo nose down & pitch osc.
	Level	17	60	900	50	250	33	12	
	Level	17	55	860			33	10	Too low
	Level	19	55	920	50	250	33	10	
	Level	21	55	780	10	75	31	10	
	Level	21	45	900	50	300	30	10	
	Ldg	19	55-45				31	12	
16	Grd	17	18				49	8	Wing fill
	T.O.	17	50				49	8	
	Climb	15*	55	640	20	150			*Questionable wing angles due to erratic pitch monitor
	Level	15	50	480	15	100	32		
	Level	15	40	400	30	200	31		
	Level	13	40	480	60	350	31		
	Level	13	55	520	10	50	32		
	Level	11	55	480	15	100	32		
	Level	11	40	440	30	200	30.5		
	Ldg	11	42				28		

FTO 179-	FLT COND	i_w DEG	KIAS	LB TOW TENSION	ψ D DEG	Δh FT	MAP "HG	OAT °C	REMARKS
17	— UH-1D CABLE TOW ONLY TO 85-90 KTS. - NO DATA								
18	— CH-34 ONLY - PRACTICE LANDING PASSES - NO DATA								
19	JETTISON AFTER LIFTOFF DUE TO OSCILLATIONS — NO DATA —								
20	T.O.	17					30	22	
	Climb	15	55				42		
	Level	15	44	700	30			29	
	Level	15	43	600	30				Stable
	Level	15	45	590	20				
	Level	15	48						Lat. Osc.
	Level	15	38	550	45				
	Level	13	42	600	25				Turn
	Level	13	47	600	0				Co-Alt.
	Level	11	45	600	0				Co-Alt.
	Level	11	40						
	Level	11		500	30				
	Descent	11	45	300					
	Landing	11	45						
21	T.O.	16	50	1100	50		44	22	
	Climb	15	55	1150	45		38	20	
	Level	15.5	65	1150	20		33	18	
	Level	11	65	1025	50		34	18	

FTO 179-	FLT COND	i_w DEG	KIAS	LB TOW TENSION	ϕ D DEG	Δh FT	MAP "HG	OAT °C	REMARKS
21	Level	11	60	1000	45		31.5	18	
Cont	Level	16.5	60	825	20		32	18	
	Level	18	55	700			30	18	
	Level	12	55	675			31.5	18	
	Level	12.5	50	800			31	18	
	Level	20.5	50	1000			31	18	
	Level	19.5	45	1000			33	18	
	Level	15	45	700			30	18	
	Descent	15	45	500			27	19	
	Ldg	15	45						
22	T.O.	16	60	1200	30	200	45	18	
	Climb	15	60	1000	25	150	38	20	
	Level	17	60	750			31	21	
	Level	11	60	700			31	21	
	Level	11	65	850		100	32.5	21	
	Level	12	65	800			32.5	21	
	Level	11	70	900		50-75	35	21	
	Level	11	65	800			32.5	21	
	Level	12	65	800			32.5	21	
	Level	11	55	725			30	21	
	Level	16.5	55	750			30	21	
	Descent	15	45	500			26.5	21	300 FPM
	Ldg	14.5	45						

FTO 179-	FLT COND	i_w DEG	KIAS	LB TOW TENSION	ϕ D DEG	Δh FT	MAP "HG	OAT °C	REMARKS
23	Grd	16	10				44	20	Wing fill
	T.O.	16	60	1650	40		45	22	
	Climb	15	60	1025	30	150	38	24	
	Level	15.5	60	800	20	75	33	24	
	Level	11	60	800	35	200	33	24	
	Level	11	65	1000	30	100	34	24	
	Level	15	65	900	15-20	50-75	33.5	24	
	Level	11	68	950	20	75-100	34	24	
	Level	13	55	800	50	300	31.5	24	
	Level	16	55	700	35	150	32	24	
	Level	15.5	50	1000			31.5	24	Pitch/roll
	Descent	15	55	600	30	100	29	24	
	Ldg	14	50	500					
24	Grd	17	10				45		Wing fill
	T.O.	17	60	1800	40	200	48	26	
	Climb	17	60	1500	50	300	40	26	
	Climb	17	60	1300	20	150	40	25	
	Cruise	16.5	60	1100	30	125	34	25	Roll
	Cruise	11	65	1200	20	100	34	23	
	Cruise	13	65	1100	10-15	75	33	23	
	Cruise	11	70	1200	10-15	75	34	23	
	Cruise								

FTO 179-	FLT COND	i_w DEG	KIAS	I.B TOW TENSION	ϕ D DEG	Δh FT	MAP "HG	OAT °C	REMARKS
24 Cont	Cruise	12.5	70	1200	20	75	35	23	
	Cruise	11	75	1200			38	23	
	Cruise	11	78	1300	25	125	40	23	Roll
	Descent	11	55	600			26	24	200 FPM R/D
	Descent	14.5	55						
	Go-around	14	50-55	2400 & rising	70				Crash - weak link broke
25	Grd	17	0				44	22.5	Wing fill
	T.O.	17	48	1600	40	200	48	24	
	Climb	17	60	1350	35	150	41		500 FPM R/C
	Level	18.5	60	900	30	150	33	28	
	Level	16	60	1000	40	200	34	27.5	
	Level	17	65	1050	20	100	35	28	
	Level	14	65	1050	35-40	200	35	28	
	Level	13	70	1125	45	300	26	28	
	Level	15.5	70	1000	25	125	35	28	
	Level	14.5	75	1100	20	100	37.5	28	
	Level	11	75	1100	35	175	37.5	28	
	Level	21	55	1000	30	150	33	27.5	
	Level	14.5	55	1050	55	325	33	28	(Reverse cable
	Level	15	50	1100			33	28	bow at 14° wing)
	Level	19.25	50	1025	45	225	33	28	
	Level	11	80	1275			42	28	Tens. 1250-1300
	Level	16.5	45						wing stall
	Descent	15	55	1000	30	150	32	28	
	Ldg	16	55					25	

FTO 179-	FLT COND	i_w DEG	KIAS	LB TOW TENSION	γ D DEG	Δh FT	MAP "HG	OAT °C	REMARKS
26	T.O.	18	60	2400			48	24	
	Climb	18	60						(Lost down win
	Ldg.	18	55	1200	20		33	24	control)
27	T.O.	17	60	2100	40	200	48		
	Climb	17	60	1600	30	150	44	27	
	Level	19	60	1300	20	100	35	28	
	Level	17	60	1200	30	150	34	28	
	Level	17.5	65	1100	15	75-100	35	28	
	Level	15.5	65	1225	15-20	100-125	35	28	
	Level	18.5	55	1250	25	150	33.5	28	
	Level	18	55	1200	40	200	33.5	28	
	Descent	15.5	60	1100			33	28	200 FPM R/D
	Wave-off	17	60						
	Wave-off	16	60						
	Wave-off	17	57-60						
	Ldg	16.5	57-60	1000			32	25	
28	T.O.	16.5	63	1850	40	200	44	18	
	Climb	16.5	62	1500	40	200	42	20	
	Level	19	60	1200	20	100	35	20	12° helo nose down

FTO 179-	FLT COND	i_w DEG	KIAS	LB TOW TENSION	ϕ D DEG	Δh FT	MAP "HG	OAT °C	REMARKS
28	Leve'	15	60	1300	45-50	300	34	20	
Cont	Level	14.5	65	1450	45	250-275	36	20	15° helo nose down
	Level	17.5	65	1200	20	100	35	22	
	Level	17.25	70	1200	15	75	36	22	Wing Flutter
	Level	11	70	1350	55	300	36.5	22	17° helo nose down
	Level	11	75	1400	40	250-275	39	22	2?° helo nose down
	Level	15.5	75	1250	15	75	38	22	
	Level	13.5	80	1400	15	75	43	22	30° helo nose down
	Level	11	80				42	22	Wing tear, jettison, crash

UNCLASSIFIED
Security Classification

DOCUMENT CONTROL DATA - R & D

(Security classification of title, body of abstract and indexing annotation must be entered when the overall report is classified)

1. ORIGINATING ACTIVITY (Corporate author)	2a. REPORT SECURITY CLASSIFICATION
Ryan Aeronautical Company San Diego, California	UNCLASSIFIED 2b. GROUP

3. REPORT TITLE

Flexible Wing Towed Universal Glider

4. DESCRIPTIVE NOTES (Type of report and inclusive dates)

Final Report 7 October - 20 November 1964 and 4 October - 2 November 1965

5. AUTHOR(S) (First name, middle initial, last name)

6. REPORT DATE	7a. TOTAL NO. OF PAGES	7b. NO. OF REFS
October 1967	150	6

8a. CONTRACT OR GRANT NO.	9a. ORIGINATOR'S REPORT NUMBER(S)
DA 44-177-AMC-179(T) b. PROJECT NO. c. Task No. 1F121401A14172 d.	USAAVLABS Technical Report 67-57 9b. OTHER REPORT NO(S) (Any other numbers that may be assigned this report) 29267-1

10. DISTRIBUTION STATEMENT

This document has been approved for public release and sale; its distribution is unlimited.

11. SUPPLEMENTARY NOTES	12. SPONSORING MILITARY ACTIVITY
	U.S. Army Aviation Materiel Laboratories Fort Eustis, Virginia 23604

13. ABSTRACT

This report is the final report on the Design, Fabrication, and Test of a Flexible Wing Towed Universal Glider. The purpose of the glider design was to develop an unpowered, roadable, winged vehicle which could carry up to 4000 pounds of payload on an open bed which would put minimum restrictions on cargo volume and shape.

The vehicle towed by a helicopter would extend the normal helicopter internal load and slingload capacity as well as place hazardous cargo remote from the helicopter and crew.

DD FORM 1 NOV 68 1473 REPLACES DD FORM 1473, 1 JAN 64, WHICH IS OBSOLETE FOR ARMY USE.

UNCLASSIFIED
Security Classification

UNCLASSIFIED

Security Classification

14. KEY WORDS	LINK A		LINK B		LINK C	
	ROLE	WT	ROLE	WT	ROLE	WT
Model 179 (Ryan) TUG Glider Flex-Wing Glider						

UNCLASSIFIED

Security Classification